

# Investigation of Dinoflagellate Plastid Protein Transport using Heterologous and Homologous *in vivo* Systems



Dissertation zur Erlangung des Doktorgrades  
der Naturwissenschaften  
(Dr. rer. nat.)

Vorgelegt dem Fachbereich Biologie  
der Philipps-Universität Marburg

von

**Andrew Scott Bozarth**

aus Columbia, Maryland, USA

Marburg/Lahn 2010

---

Vom Fachbereich Biologie der Philipps-Universität  
als Dissertation angenommen am 26.07.2010 angenommen.

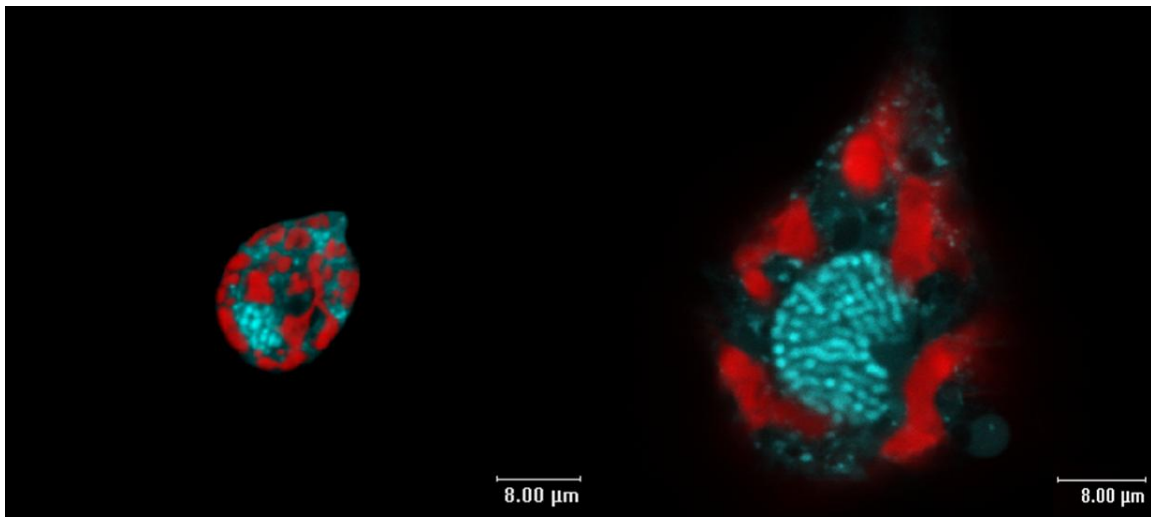
Erstgutachter: Prof. Dr. Uwe-G. Maier

Zweitgutachter: Prof. Dr. Klaus Lingelbach

Prof. Dr. Andreas Brune

Prof. Dr. Renate Renkawitz-Pohl

Tag der Disputation am: 11.10.2010



Results! Why, man, I have gotten a lot of results.

I know several thousand things that won't work!

-Thomas A. Edison

---

## Publications

**Bozarth A**, Susanne Lieske, Christine Weber, Sven Gould, and Stefan Zauner (2010) Transfection with Dinoflagellate Transit Peptides (in progress).

Bolte K, Bullmann L, Hempel F, **Bozarth A**, Zauner S, Maier UG (2009) Protein Targeting into Secondary Plastids. *J. Eukaryot. Microbiol.* 56, 9–15.

**Bozarth A**, Maier UG, Zauner S (2009) Diatoms in biotechnology: modern tools and applications. *Appl. Microbiol. Biotechnol.* 82, 195-201.

Maier UG, **Bozarth A**, Funk HT, Zauner S, Rensing SA, Schmitz-Linneweber C, Börner T, Tillich M (2008) Complex chloroplast RNA metabolism: just debugging the genetic programme? *BMC Biol.* 6, 36.

Hempel F, **Bozarth A**, Sommer MS, Zauner S, Przyborski JM, Maier UG. (2007) Transport of nuclear-encoded proteins into secondarily evolved plastids. *Biol Chem.* 388, 899-906.

**TABLE OF CONTENTS**

<b>1</b>	<b>INTRODUCTION.....</b>	<b>1</b>
1.1	THE EVOLUTION OF PHOTOSYNTHETIC EUKARYOTES.....	1
1.1.1	Primary Endosymbiosis.....	1
1.1.2	Protein Targeting to Primary Plastids.....	3
1.2	SECONDARY ENDOSYMBIOSIS AND THE CHROMALVEOLATE HYPOTHESIS.....	5
1.3	CONSEQUENCES OF HARBORING EUKARYOTIC ENDOSYMBIONTS.....	8
1.3.1	Genomic Reorganization.....	8
1.3.2	Protein Transport into Chromist Plastids.....	9
1.4	INFRAKINGDOM ALVEOLATA.....	11
1.4.1	Alveolates as Such.....	11
1.4.2	Protein Transport into Apicomplexan Plastids.....	12
1.5	DINOFLLAGELLATES.....	14
1.5.1	Features of Dinoflagellate.....	14
1.5.2	Ecological Impetus.....	16
1.5.3	Genomic Arrangement of Dinoflagellates.....	17
1.5.4	Protein Targeting in Dinoflagellates.....	19
1.5.5	<i>Ceratium horridum</i> .....	23
1.5.6	<i>Amphidinium carterae</i> .....	23
<b>2</b>	<b>AIMS.....</b>	<b>25</b>
<b>3</b>	<b>RESULTS.....</b>	<b>26</b>
3.1	ANALYSIS OF SYNTHESIZED CERATIUM HORRIDUM ESTS.....	26
3.1.1	Analysis of <i>Ceratium horridum</i> cDNA Library.....	26
3.1.2	<i>C. horridum</i> EST Sequence Homologies.....	27
3.1.3	<i>C. horridum</i> EST Sequence Functions.....	30
3.1.4	Determination of <i>Ceratium horridum</i> Plastid-Targeted Proteins.....	32
3.1.5	<i>Ceratium horridum</i> Transit Peptide Classification.....	34
3.1.6	<i>Ceratium horridum</i> Transit Peptide Variations between Isoforms.....	36
3.1.7	Comparison of <i>Ceratium horridum</i> Transit Peptides with Those of Other Phototrophs.....	37
3.1.8	Statistical Comparative Analysis of Dinoflagellate Transit Peptides.....	40
3.2	HETEROLOGOUS IN VIVO IMPORT STUDIES.....	43
3.2.1	Heterologous in vivo Import into the <i>Pisum sativum</i> Chloroplasts using <i>Amphidinium carterae</i> PsbO and Prk Transit Peptides.....	44
3.2.2	Heterologous in vivo Import into the <i>Pisum sativum</i> Chloroplasts using Chromalveolate PsbO and Prk Transit Peptides.....	47
3.3	HETEROLOGOUS IN VIVO PROTEIN IMPORT INTO THE PLASTIDS OF PHAEODACTYLUM TRICORNUTUM USING AMPHIDINIUM CARTERAE PSBO AND PRK TARGETING SIGNALS.....	48
3.3.1	HETEROLOGOUS IN VIVO PROTEIN IMPORT IN PHAEODACTYLUM TRICORNUTUM USING AMPHIDINIUM CARTERAE PSBO AND PRK SIGNAL PEPTIDES.....	48
3.3.2	HETEROLOGOUS IN VIVO PROTEIN IMPORT IN PHAEODACTYLUM TRICORNUTUM USING AMPHIDINIUM CARTERAE PSBO AND PRK SIGNAL, TRANSIT, AND THYLAKOID TARGETING PEPTIDES.....	49
3.4	TRACKING HOMOLOGOUS PROTEIN TARGETING IN AMPHIDINIUM CARTERAE.....	52
3.4.1	SUCROSE FRACTIONATION OF AMPHIDINIUM CARTERAE.....	52
3.4.2	EFFECTS OF BREFELDIN A ON PROTEIN MOBILITY IN SUCROSE GRADIENT FRACTIONATIONS OF AMPHIDINIUM CARTERAE.....	55
3.4.3	ELECTRON MICROSCOPIC EXAMINATION OF THE EFFECTS OF BREFELDIN A ON PROTEIN LOCALIZATION IN AMPHIDINIUM CARTERAE.....	59
3.4.3.1	IMMUNOGOLD LABELING WITH A-PSBO IN AMPHIDINIUM CARTERAE CELLS TREATED WITH BREFELDIN A.....	61
3.4.3.2	IMMUNOGOLD LABELING WITH A-RbCL IN AMPHIDINIUM CARTERAE CELLS TREATED WITH BREFELDIN A.....	63
<b>4</b>	<b>DISCUSSION.....</b>	<b>66</b>

4.1	CERATIUM HORRIDUM EST LIBRARY .....	66
4.1.1	General Features .....	66
4.1.2	Gene Transfers .....	67
4.1.3	Plastid Targeting Signals .....	69
4.2	HETEROLOGOUS IN VIVO IMPORT ASSAYS USING DINOFLAGELLATE TARGETING SIGNALS .....	72
4.2.1	<i>In vivo</i> transfection of <i>Pisum sativum</i> with <i>Amphidinium carterae</i> <i>PsbO</i> and <i>Prk</i> Transit Peptides 73	
4.2.2	Heterologous <i>in vivo</i> Transfections of <i>Phaeodactylum tricornutum</i> .....	74
4.2.2.1	Heterologous <i>in vivo</i> Transfections of <i>Phaeodactylum tricornutum</i> with <i>Amphidinium carterae</i> Signal Peptides .....	75
4.2.2.2	Heterologous <i>in vivo</i> Transfections of <i>Phaeodactylum tricornutum</i> with <i>Amphidinium carterae</i> <i>BTSs</i> .....	75
4.2.3	Implications of <i>in vivo</i> Transfections.....	78
4.3	BFA-SENSITIVE AND BFA-INSENSITIVE PROTEIN TRANSPORT IN AMPHIDIUM CARTERAE.....	79
4.4	CONCLUSIONS.....	83
<b>5</b>	<b>SUMMARY AND OUTLOOK .....</b>	<b>88</b>
<b>6</b>	<b>MATERIALS AND METHODS .....</b>	<b>89</b>
6.1	MATERIALS.....	89
6.1.1	Instruments .....	89
6.1.2	Chemicals .....	90
6.1.3	Antibodies .....	95
6.1.4	Culture media .....	95
6.2	METHODS .....	98
6.2.1	Culture Conditions .....	98
6.2.2	Culturing and Preparation of Chemical Competent <i>Top10TM E. coli</i> .....	98
6.2.3	Sequencing of DNA.....	99
6.2.4	Amplification of Reverse Transcripts and Rapid Amplification of cDNA Ends (RACE) Products 99	
6.2.5	Acquisition of the <i>C. horridum psbO</i> Sequence with RACE .....	100
6.2.6	EST Database .....	100
6.2.7	Acquisition of <i>A. carterae</i> cDNA Sequences.....	100
6.2.8	BLAST Analysis using a Local Database.....	101
6.2.9	Horizontal Gene Transfer Phylogenetic Analyses .....	101
6.2.10	<i>In silico</i> Transit Peptide Analyses.....	102
6.2.11	Transient Transfection of <i>Pisum sativum</i> Leaves.....	103
6.2.12	Stable Transfection of <i>Phaeodactylum tricornutum</i> .....	104
6.3	PROTEIN STUDIES .....	105
6.3.1	Brefeldin A Radioactive Labeling of <i>Amphidinium carterae</i> Proteins .....	105
6.3.2	Cell lysis (repeated 3 times): .....	106
6.3.3	Semidiscontinuous Sucrose Gradient .....	106
6.3.4	Fraction Preparation for Immunoprecipitation (IP): .....	107
6.3.5	Sephacrose A Bead Preparation and Immunoprecipitation .....	108
6.3.6	Semi-Dry Western Blot.....	108
6.3.7	Immunodetection of Proteins .....	108
6.3.8	Stripping Western Blots .....	109
6.4	ELECTRON MICROSCOPY .....	110
6.4.1	Freeze Substitution .....	110
6.4.2	Immunogold Labeling .....	110
<b>7</b>	<b>APPENDIX.....</b>	<b>112</b>
7.1	MICROSOFT EXCEL MACRO .....	112
7.3	HETEROLOGOUS TRANSFECTION OF <i>PISUM SATIVUM</i> WITH eGFP FUSED N-TERMINALLY TO TRUNCATED TPS FROM <i>CERATIUM HORRIDUM</i> <i>PSBO</i> AND <i>PRK</i> N-TERMINAL EXTENSIONS.....	114
7.4	1:50 A- <i>PSBO</i> IMMUNOGOLD LABELING OF UNTREATED AMPHIDIUM CARTERAE CELLS FIXED VIA FREEZE SUBSTITUTION.....	115

---

7.5	1:50 A-PsBO IMMUNOGOLD LABELING OF AMPHIDINIUM CARTERAE CELLS TREATED WITH 2.5 $\mu$ G BFA/ML AND FIXED VIA FREEZE SUBSTITUTION. ....	116
7.6	1:2200 A-RbCL IMMUNOGOLD LABELING OF AMPHIDINIUM CARTERAE UNTREATED CELLS FIXED VIA FREEZE SUBSTITUTION. ....	117
7.7	1:2200 A-RbCL IMMUNOGOLD LABELING OF AMPHIDINIUM CARTERAE CELLS TREATED WITH 2.5 $\mu$ G BFA/ML AND FIXED VIA FREEZE SUBSTITUTION. ....	118
<b>8</b>	<b>REFERENCES.....</b>	<b>119</b>
<b>9</b>	<b>ACKNOWLEDGEMENTS.....</b>	<b>134</b>
<b>10</b>	<b>CURRICULUM VITAE.....</b>	<b>135</b>
<b>11</b>	<b>ERKLÄRUNG .....</b>	<b>136</b>

### Abbreviations:

<b><math>\alpha</math></b>	anti	<b>NCBI</b>	National Center for Biotechnology Information
<b>BFA</b>	Brefeldin A	<b>NJ</b>	Neighbor Joining
<b>BLAST</b>	Basic local alignment search tool	<b>Nm</b>	Nucleomorph
<b>Bp</b>	Base pairs	<b>Omp85</b>	85 kDa Outer (bacterial) Membrane Protein
<b>BTS</b>	Bipartite topogenic signal	<b>PAGE</b>	Polyacrylamide Gel Electrophoresis
<b>cDNA</b>	Complimentary DNA	<b>PBS</b>	Phosphat bufferd saline
<b>cER</b>	Chloroplast ER	<b>PIC</b>	Proteinase Inhibitor Cocktail
<b>CLSM</b>	Confocal Laser Scanning Microscope	<b>PPC</b>	Periplastidial Compartment
<b>ddH<sub>2</sub>O</b>	Wasser, demineralized & distilled	<b>PPM</b>	Periplastidial Membrane
<b>DIC</b>	Differential interference contrast	<b>Prk</b>	Phosphoribulokinase
<b>Der</b>	Degradation at the ER	<b>PsbD</b>	Photosystem II Subunit D2
<b>DMSO</b>	Dimethylsulfoxide	<b>PsbO</b>	Photosystem II Oxygen Evolving Enzyme
<b>DNA</b>	Desoxyribonucleic acid	<b>RACE</b>	Rapid Amplification of cDNA Ends
<b>eGFP</b>	Enhanced green fluorescence protein	<b>RbcL</b>	Rubisco, Large Subunit
<b>EDTA</b>	Ethylenediaminetetraacetic acid	<b>RNA</b>	Ribonucleic Acid
<b>EGT</b>	Endosymbiotic Gene Transfer	<b>RT</b>	Reverse Transcriptase
<b>EM</b>	Electron Microscope	<b>Rubisco</b>	Ribulose-1,5-bisphosphate carboxylase oxygenase
<b>ER</b>	Endoplasmatic Reticulum	<b>SD</b>	Standard Deviation
<b>ERAD</b>	ER-associated degradation	<b>SELMA</b>	Symbiont-specific ERAD-like machinery
<b>EST</b>	Expressed SequenceTag	<b>SL</b>	Spliced leader
<b>Gya</b>	Giga (billion) years ago	<b>SP</b>	Signal Peptide
<b>hr</b>	Hour(s)	<b>STD</b>	Stop-transfer Domain
<b>HRP</b>	Horse radish peroxidase	<b>TP</b>	Transit Peptide
<b>HGT</b>	Horizontal Gene Transfer	<b>TBS</b>	Tris buffered saline
<b>HSP</b>	Heat Shock Protein	<b>TCA</b>	Trichloroacetic Acid
<b>IMS</b>	IMS	<b>TIC</b>	Translocator of Inner Chloroplast membrane
<b>IP</b>	Immunoprecipitation	<b>TL</b>	Thylakoid Lumen
<b>IPTG</b>	Isopropyl- $\beta$ -D-Thiogalactoside	<b>TMHMM</b>	Transmembrane helix prediction program
<b>kB</b>	kilobase pairs	<b>TOC</b>	Translocator of Outer Chloroplast membrane
<b>kDa</b>	Kilo Dalton	<b>TTD</b>	Thylakoid Targeting Domain
<b>min</b>	Minutes	<b>TTS</b>	Tripartite Targeting Signal
<b>MB</b>	Megabase	<b>WGA</b>	Wheat Germ Agglutin
<b>ML</b>	Maximum Likelihood		
<b>Mya</b>	Million years ago		



**Index of Figures**

<b>Fig. 1.</b> A Schematic Depiction of Evolution and Protein Transport involved with Primary Endosymbiosis	4
<b>Fig. 2.</b> A Schematic Depiction of the Evolution of Alveolates and Chromists as per the Chromalveolate Hypothesis	6
<b>Fig. 3.</b> Summary of Plastid Exchanges leading to Complex Plastids as per Modern Molecular Data	7
<b>Fig. 4.</b> A Schematic Depiction of Protein Transport in Chromists	10
<b>Fig. 5.</b> A Schematic Depiction of Protein Transport in Apicomplexa	13
<b>Fig. 6.</b> General Morphological Features of Dinoflagellates	15
<b>Fig. 7.</b> Schematic Depiction of Class I, II, and III Proteins and Vesicle-Mediated Plastid Protein Transport in Dinoflagellates and Euglenophytes	22
<b>Fig. 8.</b> Differential Interference Light Microscope Image of <i>Ceratium horridum</i>	23
<b>Fig. 9.</b> Differential Interference Light Microscope of <i>Amphidinium carterae</i>	24
<b>Fig. 10.</b> Exemplary ClustalX Protein Alignment of ESTs GT59_E7.u and GT61_H9.u	27
<b>Fig. 11.</b> Comparison of <i>Ceratium horridum</i> EST Contig Homologies to Total Dinoflagellate EST Homologies using Local BLAST	28
<b>Fig. 12.</b> Phylogenetic Relationship of 4 <i>Ceratium horridum</i> Unigenes	30
<b>Fig. 13.</b> Functional Distribution of Sequenced <i>C. horridum</i> ESTs	32
<b>Fig. 14.</b> Weblogo of 12 Amino Acids Preceding SignalP Predicted Signal Peptidase Cleavage Site	33
<b>Fig. 15.</b> Exemplary ClusalX Alignments of High Relative Amino Acid Exchanges in the BTS Region of Varying Plastid Protein Isoforms	36
<b>Fig. 16.</b> Weblogo of Transit Peptides from <i>Ceratium horridum</i> , Total Dinoflagellate, Plants and Diatoms	37
<b>Fig. 17.</b> Difference between <i>Ceratium horridum</i> Transit Peptides and those of Peridinin Dinoflagellates, Diatoms, and Plants	39
<b>Fig. 18.</b> General Trend in Charge Separation in <i>Ceratium horridum</i> Transit Peptides.	40
<b>Fig. 19.</b> Web Logo of Occurrence of Charged Amino Acids at Discrete Positions in Transit Peptides	42
<b>Fig. 20.</b> Schematic Depiction of PsbO and Prk Sequence Demarcation and Transport	43
<b>Fig. 21.</b> Initial Transfections of Plants using the pAVA393 Vector	44
<b>Fig. 22.</b> Topogenic Signals Employed for <i>in vivo</i> Transfection Experiments in <i>Pisum sativum</i> and Construct Amino Acid Composition Compared to Plant TP Composition	45
<b>Fig. 23.</b> Heterologous Transfection of <i>Pisum sativum</i> with eGFP Fused N-terminally to Full-Length and Truncated TPs from <i>Amphidinium carterae</i> PsbO and Prk N-terminal Extensions	46

## Index of Tables and Figures

---

<b>Fig. 24.</b> Heterologous Transfection of <i>Pisum sativum</i> with eGFP Fused to Full-length Transit Peptides from Chromists	47
<b>Fig. 25.</b> Signal Peptides used for eGFP Constructs for Transfections of <i>Phaeodactylum tricornutum</i> from <i>Amphidinium carterae</i> and <i>Phaeodactylum tricornutum</i>	48
<b>Fig. 26.</b> Transfection of <i>Phaeodactylum tricornutum</i> with eGFP fused to Signal Peptides from <i>A. carterae</i> and <i>P. tricornutum</i>	49
<b>Fig. 27.</b> Schematic Depiction of <i>Amphidinium carterae</i> TTS and BTS from PsbO and Prk used as Topogenic Signals for eGFP Import Assays in the Diatom <i>Phaeodactylum tricornutum</i>	50
<b>Fig. 28.</b> Heterologous Transfection of <i>Phaeodactylum tricornutum</i> with eGFP Fused to C-terminally Truncated Topogenic Signals from <i>Amphidinium carterae</i> PsbO and Prk	51
<b>Fig. 29.</b> Empirical Evaluation of Maximal <sup>35</sup> S-Uptake and Incorporation into <i>Amphidinium carterae</i> Protein	52
<b>Fig. 30.</b> Sucrose Gradient and Fraction Compartment/Organelle Detection of Fractionated <i>Amphidinium carterae</i> cells	53
<b>Fig. 31.</b> ImageJ Quantification of Western Blot Relative Autoradiogram Signal Intensities of <sup>35</sup> S-Labelled Immunoprecipitated Proteins from Sucrose Gradient Fractionation of <i>Amphidinium carterae</i>	54
<b>Fig. 32.</b> Relative Autoradiogram Signal Intensities from Immunoprecipitated Proteins from <sup>35</sup> S-Labeled <i>Amphidinium carterae</i> Cells (BFA Untreated)	55
<b>Fig. 33.</b> Effect of Brefeldin A on the Location of ER in Sucrose Gradients	56
<b>Fig. 34.</b> Effect of Brefeldin A on the Location of Golgi Apparatus in Sucrose Gradients	57
<b>Fig. 35.</b> Relative Autoradiogram Signal Intensities from Immunoprecipitated Proteins from <sup>35</sup> S-Labeled <i>Amphidinium carterae</i> Cells treated with 7.5 µg BFA/mL	57
<b>Fig. 36.</b> Relative Autoradiogram Signal Intensities from Immunoprecipitated Proteins from <sup>35</sup> S-Labeled <i>Amphidinium carterae</i> Cells treated with 5 µg BFA/mL	58
<b>Fig. 37.</b> Relative Autoradiogram Signal Intensities from Immunoprecipitated Proteins from <sup>35</sup> S-Labeled <i>Amphidinium carterae</i> Cells treated with 2.5 µg BFA/mL	59
<b>Fig. 38.</b> Osmium Tetroxide Contrasted Electron Micrographs of <i>Amphidinium carterae</i> Cells (un)treated with 2.5 µg BFA/mL and Fixed via Freeze Substitution	60
<b>Fig. 39.</b> α-PsbO Immunogold Labeling of <i>Amphidinium carterae</i> Untreated Cells Fixed via Freeze Substitution	62
<b>Fig. 40.</b> α-PsbO Immunogold Labeling of <i>Amphidinium carterae</i> Cells Treated with 2.5 µg BFA/mL and Fixed via Freeze Substitution	63
<b>Fig. 41.</b> α-RbcL Immunogold Labeling of Untreated <i>Amphidinium carterae</i> Fixed via Freeze Substitution	64
<b>Fig. 42.</b> α-RbcL Immunogold Labeling of <i>Amphidinium carterae</i> Cells Treated with 2.5 µg BFA/mL and Fixed via Freeze Substitution	65

## Index of Tables and Figures

---

<b>Fig. 43.</b> Signal Peptide Peptidase Cleavage Site in Dinoflagellate BTS as per SignalP	70
<b>Fig. 44.</b> Model of Dinoflagellate Protein Transport to the Plastids via the Endomembrane System	82
<b>Fig. 45.</b> Possible Cytosolic and Non-Cytosolic Identities of Intermembrane Compartments in the Dinoflagellate Plastid	84
<b>Fig. 46.</b> Pipetting Scheme for Sucrose Fractionation	107

## Index of Supplementary Figures

Standard deviations (SD) Relative Amino Acid Abundances in Plant and Diatom TPs.	112
Heterologous Transfection of <i>Pisum sativum</i> with eGFP Fused N-terminally to Truncated TPs from <i>Ceratium horridum</i> PsbO and Prk N-terminal Extensions.	114
1:50 $\alpha$ -PsbO Immunogold Labeling of Untreated <i>Amphidinium carterae</i> Cells Fixed via Freeze Substitution.	115
1:50 $\alpha$ -PsbO Immunogold Labeling of <i>Amphidinium carterae</i> Cells treated with 2.5 $\mu$ g BFA/mL and Fixed via Freeze Substitution.	116
1:2200 $\alpha$ -RbcL Immunogold Labeling of <i>Amphidinium carterae</i> Untreated Cells Fixed via Freeze Substitution.	117
1:2200 $\alpha$ -RbcL Immunogold Labeling of <i>Amphidinium carterae</i> Cells treated with 2.5 $\mu$ g BFA/mL and Fixed via Freeze Substitution.	118
Microsoft Excel Macro.	112

## Index of Tables

Table 1. <i>Ceratium horridum</i> ESTs encoding Proteins involved in Protein Transport and Vesicle Formation.	31
Table 2. Homologies for 29 of 34 Plastid-Targeted Unigenes.	34
Table 3. Amino Acid Compositions of Plastid Protein Transit Peptides from 34 <i>Ceratium horridum</i> , 184 Peridinin Dinoflagellate, 123 Diatom, and 134 Plant Sequences.	38
Table 4. Charged Amino Acids in the First and Second Halves of Dinoflagellate, Diatom, and Plant Transit Peptides.	41
Table 5. Hydroxylated Amino Acids Content of Transit Peptides in Plastid-Containing Organisms.	71

## Abstract

Expressed Sequence Tag (EST) data from *Ceratium horridum* generated and analyzed in this thesis conform to the general parameters of dinoflagellate EST libraries. Comparison with diatom and plant transit peptides, revealed that transit peptides from peridinin-containing dinoflagellate conform to general trends for transit peptides but are relatively deficient in hydroxylated amino acids, have a slight net positive charge, and contain N-terminal basic amino acids among the most N-terminal amino acids. Like transit peptides in the alveolate *Plasmodium falciparum*, dinoflagellate transit peptides contain positively charged amino acids, have a depleted acidic residue content, and mostly contain one or more chaperone binding sites. The feature of dinoflagellate transit peptides that has gone unnoticed heretofore is the low overall positive charge, in addition to the significant division of charge between C- and N-termini.

Despite its overwhelming prominence in dinoflagellate transit peptides, C-terminal negative charge clearly had no impact on the import competence of *Amphidinium carterae* targeting signals in heterologous *in vivo* systems. Based on results from transfections of *Pisum sativum* and *Phaeodactylum tricornutum*, targeting mediated by transit peptides is not merely dependent on net positive charge, N-terminal positive charge, or amino acid content. Therefore, it was concluded that plastid transport into plant and diatom plastids also depended on sequence-specific patterns or motifs that are not present and/or not identical to those in dinoflagellate transit peptides. Based on the partial interchangeability of topogenic signals between an alveolate and a chromist but not between an alveolate and a plant – despite high homologies in mature protein sequences – it was deduced that plastid targeting signals evolve more expediently than the mature protein domains that they intracellularly target.

Analysis of the homologous intracompartamental transport of three *Amphidinium carterae* plastid proteins showed that differing transport routes exist for plastid proteins. While PsbO and Prk are transported by a Golgi-mediated route to the plastid, RbcL is transported directly from the ER to the plastids. In conclusion, a previously undescribed, possibly protein class-dependent, ER-mediated route seems to exist.

## Zusammenfassung

Die in dieser Arbeit generierten und analysierten Expressed Sequence Tag (EST) Daten von *Ceratium horridum* entsprechen in vielen Hinsichten den allgemeinen Kriterien verglichen mit bekannten ESTs aus anderen Dinoflagellaten. Ein Vergleich von Transitpeptiden aus Dinoflagellaten mit Transitpeptiden aus Diatomeen und Pflanzen zeigte ein vergleichsweise geringeres Vorkommen hydroxylierter Aminosäuren, eine geringere positive Gesamtladung und ein vermehrtes Vorkommen basischer Aminosäuren am N-Terminus. Ähnlich zu den Transitpeptiden des Alveolaten *Plasmodium falciparum*, sind Transitpeptide aus Dinoflagellaten insgesamt positiv geladen, verarmt an sauren Aminosäuren und beinhalten zu größten Teilen eine Chaperonbindestelle. Die niedrige positive Gesamtladung der Transitpeptide aus Dinoflagellaten sowie eine signifikante Trennung dieser Ladung in eine negative C-terminale Hälfte und positive N-terminale Hälfte konnten als neue Besonderheiten identifiziert werden.

Trotz des häufigen Vorkommens der negativen C-terminalen Ladung, hatte dieses Merkmal keine eindeutige Wirkung auf die Importkompetenz der topogenen Signale von *Amphidinium carterae* in heterologen *in vivo* Systemen. Basierend auf den Ergebnissen von Transfektionen in *Pisum sativum* und *Phaeodactylum tricornutum*, hängt die Information eines Transitpeptids weder von der positiven Gesamtladung, noch von der N-terminalen positiven Ladung oder der Aminosäurezusammensetzung ab. Proteinimport in Plastiden von Diatomeen und Pflanzen scheint folglich von bislang unidentifizierten sequenzspezifischen Mustern oder Motifen abhängig zu sein. Eine partielle Austauschbarkeit von topogenen Signalen zwischen einem Dinoflagellaten und einem Chromisten ist trotz hoher Homologien der maturen Proteinsequenzen nicht auf Alveolaten und Pflanzen übertragbar. Somit scheinen Zielsteuerungssequenzen schneller zu evolvieren als die maturen Proteindomänen.

Die Untersuchung des homologen intrakompartimentalen Transports dreier plastidärer Proteine in *Amphidinium carterae* zeigte Unterschiede in Bezug auf den Transportweg. Während die Proteine PsbO und Prk über einen Golgi-vermittelten Transport in die Plastide gelangen, scheint RbcL dieses Kompartiment zu umgehen und direkt über das ER in die Plastiden zu gelangen. Daher ist davon auszugehen, daß ein für Dinoflagellaten bislang unbekannter, möglicherweise proteinklassenabhängiger Transportweg existiert.

# 1 INTRODUCTION

## 1.1 The Evolution of Photosynthetic Eukaryotes

### 1.1.1 Primary Endosymbiosis

Approximately 5 billion years ago, adverse conditions prevailed upon the surface of the earth. Upon the advent of ambient temperatures and liquid oceans, life was cultivated from a sea of complex organic compounds over the course of billions of years and is thought to have originally been similar to modern archaean chemolithotrophs (Cavalier-Smith 2002; Yoon et al. 2004). From these humble beginnings, photosynthetic bacteria are thought to have developed oxygenic photosynthesis about 3.8 billion years ago (Gya) (Buick 2008). According to the fossil record, cyanobacteria-like organisms then came into existence about 3.5 Gya (Schopf 1993). By about 2.45 Gya, heterocyst forming cyanobacteria had unambiguously come into existence and had given rise to atmospheric oxygen around 2.3 Gya (Falcon et al. 2010). It was this set of photosynthetic bacteria that brought about the oxygen-containing atmosphere that supplied the environmental conditions for aerobic respiration to come into existence.

Eukaryotes came into existence at least 1.45 Gya and had the aptitude to feed on chemolithotrophs, heterotrophs, and autophototrophs (Embley and Martin 2006). It was this advent of phagotrophy, the feeding of organisms upon one another by engulfment, which became a hallmark of eukaryotes, and the progenitor of all eukaryotes may have been the result of a symbiotic event between a eubacterial and an archaean cell (Embley and Martin 2006; Margulis 1996). If this was the case, then host genes would have migrated into the symbiont, thus becoming the cell nucleus, and the membranes of the symbiont eventually became the nuclear envelope and ER, while the phagotrophic membrane was presumably lost (de Duve 2007; Yutin et al. 2009). Hence, the defining fundamental features of the existence of eukaryotes could very well have been premised by the capacity to phagocytize and engage endosymbiotic gene transfer (EGT).

Eukaryotic uptake of an aerobic heterotrophic prokaryote to respire with oxygen was probably prefaced by the increasingly aerobic environment on Earth (de Duve 2007), which had become increasingly prevalent in the atmosphere and oceans due to oxygenic photosynthesis from cyanobacteria (Archibald 2009). The internalized alpha-proteobacterium was reduced to the organellar mitochondrion and aerobic respiration generally became its primary function. As a result of this endosymbiosis, the three membranes (eukaryotic phagosomal membrane, inner/outer bacterial membranes) containing the cytosol of the bacteria were reduced to two during the course of evolution, presumably by the loss of the phagotrophic vacuole (Cavalier-Smith 2006; Gross and Bhattacharya 2009).

Reductive evolution of the proteobacterial genome then continued, consolidating it to the functions now associated with modern mitochondria, namely: aerobic ATP production coupled to electron transport, assembly of iron-sulfur clusters, and translation of mitochondrial proteins (Gray et al. 2001; Lill and Muhlenhoff 2008). This streamlining of the genome is attributed to mitochondrion-to-nucleus gene transfer, which can leave as few as 3 genes remaining in the mitochondrial genome, e.g. in dinoflagellates (Slamovits et al. 2007). On the other hand, some prokaryotic proteins were apparently substituted by phylogenetically unrelated proteins encoded on the eukaryotic nuclear genome and import post-translationally (Gray et al. 2001).

After the acquisition of mitochondrion, the stage was set for another primary endosymbiosis: a mitochondrion-containing heterotrophic eukaryote incorporated an intracellular cyanobacterium into its corpus, thus obtaining the ability to synthesize many of its own organic compounds (e.g., amino acids, heme, fatty acids) and energy photoautotrophically without having to resort to phagocytosis (Bodyl et al. 2009a; Yoon et al. 2004). This process of acquiring primary plastids is thought to have occurred for the first time about 1.332 Gya (Falcon et al. 2010) and is generally considered to be a monophyletic event (Embley and Martin 2006) except in the opisthokont lineage of *Paulinella*, which acquired its primary endosymbiont about 60 million years ago (Mya) (Yoon et al. 2009).

The initial phagocytized cyanobacterium-like cell was thus transformed from an autonomous cell, as first observed by Konstantin Mereschkowsky (Mereschkowsky 1905). Like in the case of the mitochondrion, a chimera formed from the initial endosymbiotic event. The cyanobacteria-like cell was originally encased in a eukaryotic phagosomal

membrane and was gradually transformed into a selectively permeable organelle surrounded by two membranes (Bodyl et al. 2009a).

Again like the mitochondrion, the transformation of the chimera involved massive genome reorganization by gene shuffling, elimination, and relocation to the nucleus, leading to genomic reduction of the endosymbiont. The majority of its coding capacity waned either via gene loss or transfer of genetic material into the nuclear genome (Bolte, Bullmann et al. 2009). In modern plants, over 90% of cyanobacterial genes were relocated to the nucleus and not only encode 98% of plastid proteins but also constitute 20% of the genes in the nuclear genome (Martin et al. 2002; Strittmatter et al. 2010). The enslaved phototroph became an obligate symbiont when genes were transferred from its genome to the host's chromosomes (Stoebe and Maier 2002), thus sustaining the trend that probably started upon the very inception of eukaryotes and continued with the genomic reduction of mitochondria.

After the monophyletic progenitor of modern photosynthetic eukaryotes established the chloroplast as an intracellular organelle, speciation occurred. A broad array of the progenitor's descendants constitutes the group of archaeplastida and came to colonize terrestrial and aquatic habitats from the equator to the poles. Members of archaeplastida are divided into three phyla: the rhodophytes, the glaucophytes, and the chlorophytes (Adl et al. 2005; Cavalier-Smith 1998; Reyes-Prieto et al. 2008; Stoebe and Maier 2002; Weber et al. 2006). Despite their diversity, oceanic phytoplankton primarily consisted of cyanobacteria and green algae that were only slightly larger than bacteria until 190 Mya, according to the fossil record (Falkowski et al. 2004).

### 1.1.2 Protein Targeting to Primary Plastids

Gene products with a plastid function and encoded by relocated genes must necessarily be redirected back to the primary plastid. Targeting to the plastid has however changed since the establishment of the photosynthetic chimera, and multiple models exist to explain how protein translocation into primary plastids evolved into being almost exclusively mediated by translocators of the chloroplast envelope (Bodyl et al. 2009a; Cavalier-Smith 2003; Steiner and Löffelhardt 2002). The perhaps most accepted theory of the evolution of plastid protein import dictates that the transport systems for proteins and compounds evolved



## Introduction

from pre-existing cyanobacterial transport systems (Weber et al. 2006). The chloroplast is contained by two envelope membranes, which are orthologous to the outer and inner cyanobacterial membranes, whereby the phagosomal membrane is thought to have been eliminated early on in evolution (Cavalier-Smith 1987b).

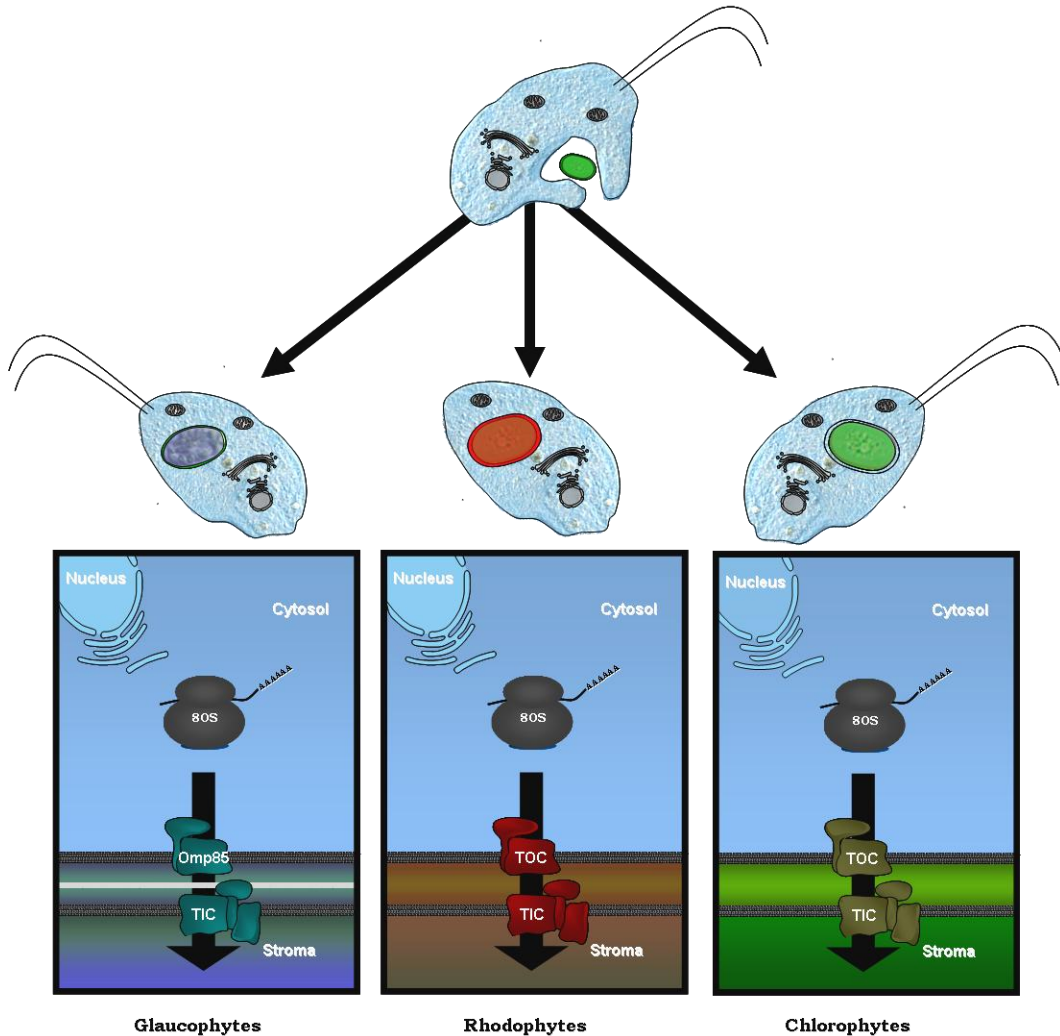


**Figure 1. A Schematic Depiction of Evolution and Protein Transport involved with Primary Endosymbiosis. Above:** A phagotrophic eukaryote ingested a cyanobacterium some 1.3 Gya, resulting in the three lineages shown: glaucophytes, rhodophytes, and chlorophytes (left to right). **Below:** Depiction of protein transport in each lineage. Cytosolic ribosomes synthesize proteins, which are transported across the two plastid envelope membranes by way of Omp85-related/TOC and TIC machinery.

Posttranslational protein targeting to and import into the plastid involves cytosolic heat shock proteins (Hsp70) that interact with unfolded preproteins. The Hsp70 then interacts with the Translocator of the outer chloroplast membrane (TOC) complex, in order to mediate transport across the first plastid membrane. The channel protein of Toc is thought to be an

ortholog of a cyanobacterial Omp85 protein (Weber et al. 2006). Cytosolic components of Toc recognize the plastid-targeting N-terminal extension of the preprotein, which is then delegated across the inner envelope membrane by the Translocator of the innner chloroplast membrane (TIC) complex.

Translocator-mediated transport is not the exclusive means of import into plant and green algal chloroplasts, as the endomembrane system has been shown to play a role in the import of proteins into the plastid stroma (Jarvis 2008). Furthermore, a number of proteins have been shown to have Golgi-to-plastid plastid targeting mediated in a signal-dependent manner (Hummel et al. 2010; Kitajima et al. 2009). A vesicle transport system to primary plastids is thus thought to exist for some proteins.

### 1.2 Secondary Endosymbiosis and the Chromalveolate Hypothesis

Phagotrophic eukaryotes fed not only on bacteria but also consumed fellow eukaryotes – including those with enslaved primary plastids. In a process analogous to primary endosymbiosis, phagocytic eukaryotes were able to enslave eukaryotes containing a primary symbiont. Multiple secondary endosymbioses are thought to have occurred about 1 to 1.5 Gya (Archibald 2009; Falkowski et al. 2004; Yoon et al. 2004). The currently predominant albeit controversial hypothesis suggests that three main lineages arose: the chromalveolates, the euglenoids and chlorarachniophytes, each which resulted from a monophyletic secondary endosymbiosis: of a red alga and of green algae, respectively (Cavalier-Smith 1999; Delwiche 1999; Keeling 2004; Rogers et al. 2007).

The chromalveolate hypothesis suggests that there was a single secondary endosymbiosis of an engulfed red alga by the putative common ancestor of chromists and alveolates (Cavalier-Smith 1999). This postulate stipulates that secondary plastid endosymbiosis involves a complex series of evolutionary events that is most easily reconciled with a single origin of the chromalveolate plastids (Cavalier-Smith 2002). Molecular data from plastid-encoded and plastid-targeted proteins, targeting systems, and targeting information have generally bolstered the idea that the successful establishment of a secondary endosymbiont is so complex that multiple recurrences of secondary endosymbiosis were restricted (Archibald 2009; Keeling 2009).

Although this monophyletic origin of chromists and alveolates conveniently and parsimoniously clarifies both morphological data and the diversity of eukaryotes with secondary endosymbionts, the origins of secondary plastids may actually be more complex. Recent data from molecular, biochemical, genomic and phylogenomic methods have come to light that seemingly contradict the chromalveolate hypothesis. Two of the most important observations are that red lineage complex plastids have been spread laterally between distantly related groups of eukaryotes on multiple occasions and that green lineage genes have been found in diatoms and alveolates currently harboring red algal symbionts (Archibald 2009; Elias and Archibald 2009; Funes et al. 2002; Harper et al. 2009; Moustafa et al. 2009; Petersen et al. 2006; Stelter et al. 2007; Waller et al. 2006a), as depicted in figure 3.

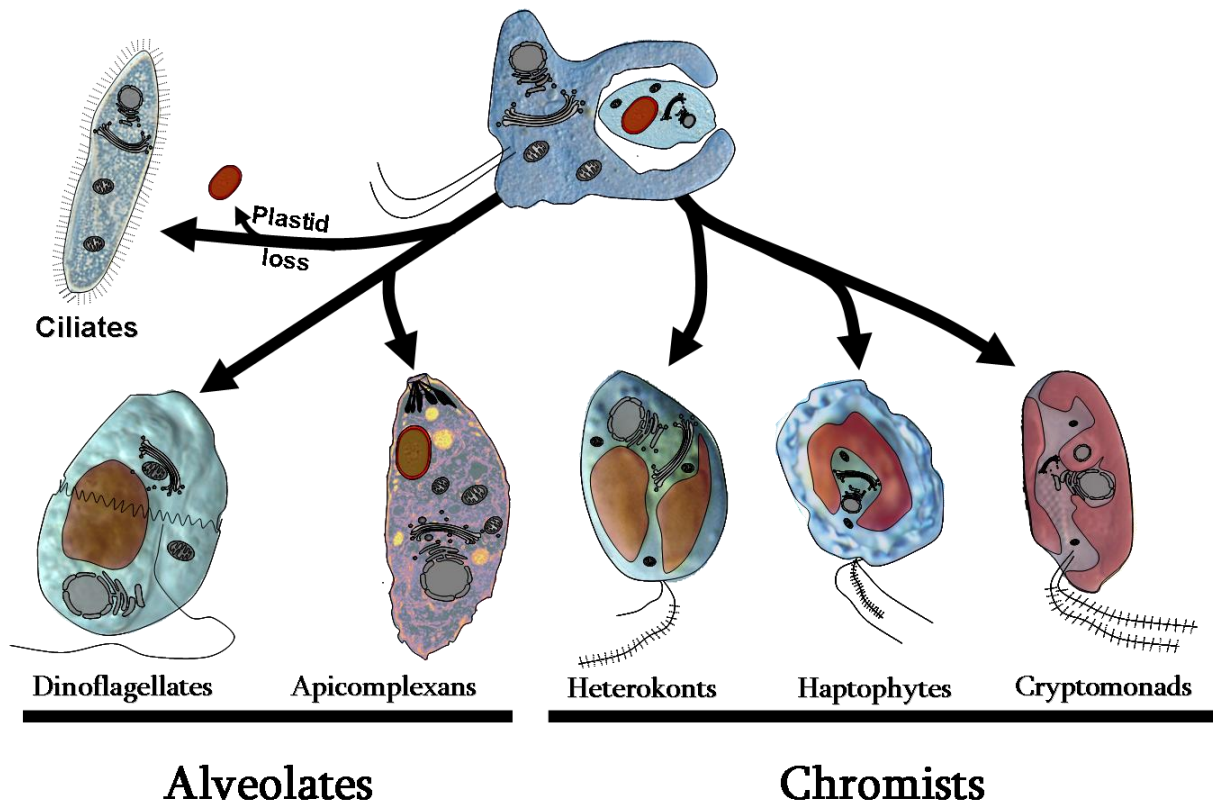


**Figure 2. A Schematic Depiction of the Evolution of Alveolates and Chromists as per the Chromalveolate Hypothesis.** A heterotrophic eukaryote phagocytized a red alga and split into two lineages of chromalveolates: Alveolates (left) and Chromists (right).

Current data thus implicate eukaryotic hosts as indeed being capable of obtaining new endosymbionts and disposing of the old ones, seemingly weakening the theory of a

monophyletic origin of secondary endosymbionts for the red lineage – the main tenet of the chromalveolate hypothesis (Bodl et al. 2009b). The clout of the chromalveolate hypothesis has also been diminished by highly unstable relationships among heterokont, haptophyte, and peridinin-containing dinoflagellate plastids in phylogenetic analyses using nuclear host genes and plastid genes (Baurain et al. 2010; Sanchez Puerta and Delwiche 2008). It has even been suggested that the endosymbionts in chromalveolates are in fact tertiary endosymbionts that arose perhaps on multiple occasions from the engulfment and reduction of hacrobian by alveolates and stramenopiles (Archibald 2009; Elias and Archibald 2009; Okamoto et al. 2009), as seen in figure 3.

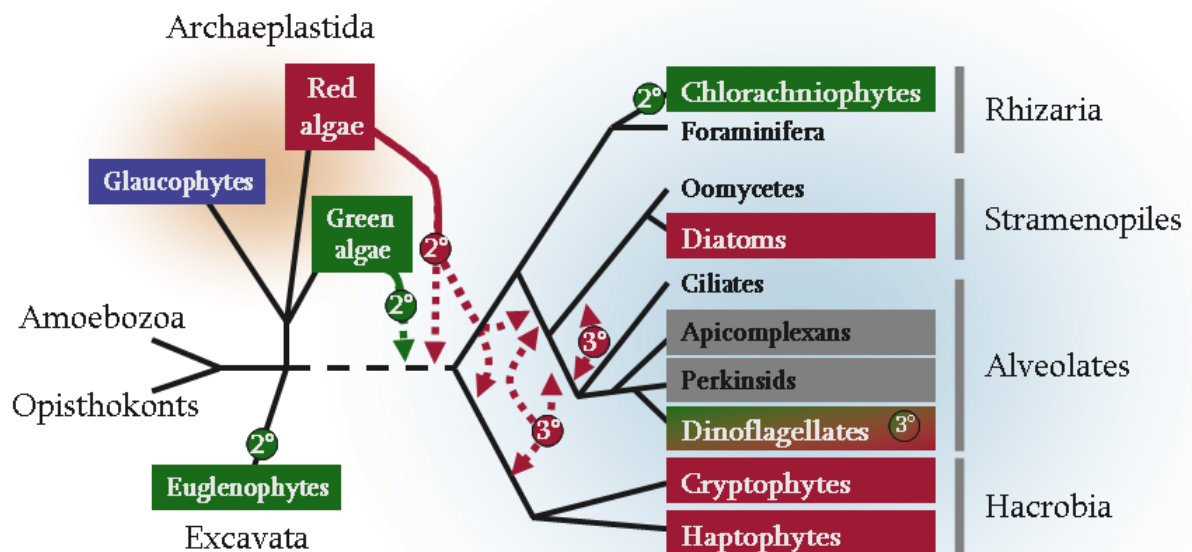


**Figure 3. Summary of Plastid Exchanges leading to Complex Plastids as per Modern Molecular Data** (modified from Elias and Archibald, 2009). The Chromalveolate theory has come under fire due to such incongruencies in molecular data as those shown here. **Dashed lines:** uncertainties in timing and/or directionality of secondary (2°) or tertiary (3°) endosymbiotic events. **Grey boxes:** presence of non-photosynthetic plastid. Dinoflagellates can contain both green and red tertiary plastids.

Nonetheless, alveolates and chromists are indubitably sister groups of photosynthetic eukaryotes that often branch together closely in phylogenetic analyses (Bachvaroff et al. 2005; Cavalier-Smith 1999). Moreover, heterokonts and alveolates have been repeatedly documented to be sister groups in multiple phylogenetic studies with differing data sets (Fast et al. 2002; Harper et al. 2005; Janouskovec et al. 2010; Van de Peer and De Wachter 1997). What's more, phylogenetic studies using genes from the host nuclear genomes shows that

alveolates, heterokonts, and members of the supergroup Rhizaria group together (to form the SAR supergroup) (Archibald 2009). The latter clade consists mainly of parasitic or free-living unicellular eukaryotes, thus implicating chromalveolate endosymbiosis involved multiple host organisms from the Rhizaria lineage (Burki et al. 2007, Hackett et al. 2007, Not et al. 2007).

### 1.3 Consequences of Harboring Eukaryotic Endosymbionts

#### 1.3.1 Genomic Reorganization

Upon the transition of the enslaved chromalveolate endosymbiont into an obligate symbiont, gene transfer occurred from endosymbiont's genomes to the host's chromosomes, as occurred after the incorporation of primary plastids (Elias and Archibald 2009; Stoebe and Maier 2002). In the cases of the cryptophytes and chlorachniophytes, some genes were not transferred from the eukaryotic endosymbiont's nucleus to the host nucleus, resulting in the smallest eukaryotic genomes in existence, i.e. the nucleomorph (Archibald and Lane 2009). Phylogenetic analyses of the sequence from the *Guillardia theta* nucleomorph's three chromosomes resulted in a clear association of the sequence with red algal homologs (Douglas et al. 2001). The nucleomorph is located in the remnant cytoplasm of the symbiont, termed the periplastidial compartment (PPC), which is located between the outer and inner pairs of membranes in the secondary plastid (Bolte et al. 2009).

As in primary plastids, most of the proteome of complex plastids is encoded by the host's genome (Armbrust et al. 2004; Douglas et al. 2001; Gilson et al. 2006; Rogers et al. 2007). Whereas extensive genomic reduction occurred during the confluence of host and endosymbiont, the number of membranes surrounding the complex plastid was not reduced to the extent found in primary plastids, as three or four membranes still surround complex plastids (with the exception of tertiary endosymbionts). Thus, hundreds of proteins encoded by the host's nuclear genome that are necessary for essential plastid functions must cross either three or four membranes to reach the plastid stroma.

### 1.3.2 Protein Transport into Chromist Plastids

The chromist plastid came to be fully encased in the endoplasmic reticulum lumen, i.e. the chloroplast ER (cER), which is continuous with the rest of the endoplasmic reticulum (Gibbs 1979). Reduction of the secondary endosymbiont, however, contrasts from the reduction of a primary endosymbiont inasmuch as symbiotic eukaryote membranes, cytosol, and nucleus persisted in some cases, thus necessitating a complex targeting strategy for proteins encoded by relocated, now nucleus-encoded genes.

Like for primary plastids, gene transfer to the host nucleus in secondary endosymbiosis implicates a mechanism for redirecting plastid proteins back into the organelle, and a coevolution of plastid-specific topogenic signals and transport/translocation machineries for directing proteins into the plastid (Cavalier-Smith 2003; Steiner and Löffelhardt 2002). In organisms with primary endosymbionts, nucleus-encoded proteins with plastid destinations require an N-terminal targeting signal, the transit peptide (TP). A number of theories exist as to how these N-terminal topogenic signals came into existence, ranging from frame-shifts in tandem duplicated genes (Ueda et al. 2006) to random mutational acquisition (Cavalier-Smith 2003) to spliceosomal introns (Kilian and Kroth 2004) to exon shuffling and recruitment of random coding and non-coding sequences (Tonkin et al. 2008a).

Plastid-targeted proteins encoded by nuclear genes in algae with complex plastids require an additional layer of intricacy for targeting that reflects their evolutionary history and complex cell biology. To accommodate for differences in the number of plastid membranes, nucleus-encoded TPs of plastid-targeted proteins acquired a signal peptide (SP) to direct them via the host cell's endomembrane system. In chromists and apicomplexa, plastid protein TPs acquired the capacity to direct proteins across an additional membrane than in primary plastids, namely the second outermost plastid membrane, i.e. the former plasma membrane of the eukaryotic endosymbiont. The resultant bipartite targeting signal (BTS) is composed of a signal and a transit peptide, which consist of specific amino acid sequences for ensuring reliable transport. These are cleaved from the N-terminus by an ER and a plastid protease, respectively (Bolte et al. 2009).

Recently, a translocator complex of chromist plastids has been identified. This former ER-associated degradation (ERAD) complex originally had a function in the protein quality control of the red algal symbiont and is thus called the Symbiont-specific ERAD-Like



Machinery (SELMA) (Hempel et al. 2009). The SELMA complex now translocates proteins from the ER lumen into the remnant symbiotic cytosol (Periplastidial Compartment or PPC), whence proteins can be translocated across the two inner plastid membranes via cyanobacterial translocators analogous to TOC and TIC (Bullmann et al. 2010; Hempel et al. 2007; Sommer et al. 2007).

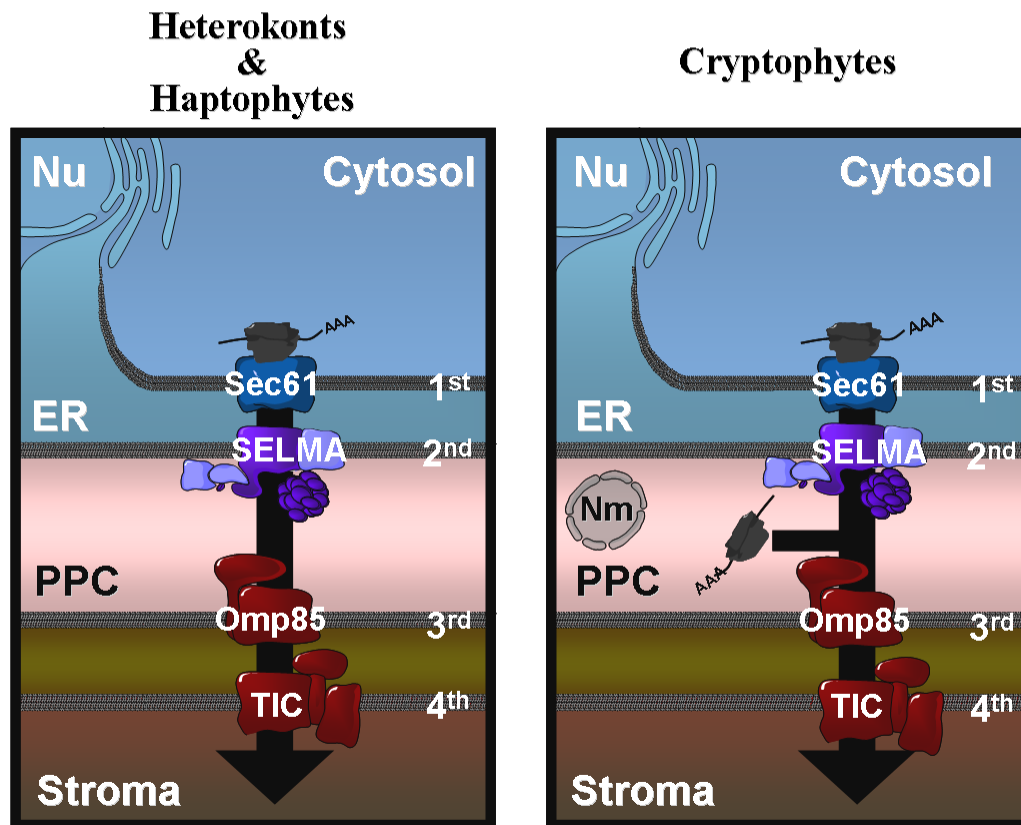


**Figure 4.** A Schematic Depiction of Protein Transport in Chromists (modified from Bolte et al. 2009). Heterokonts, haptophytes, and cryptomonads cotranslationally import proteins into the ER lumen by having localized their plastids in the ER lumen. 1<sup>st</sup>, 2<sup>nd</sup>, 3<sup>rd</sup>, 4<sup>th</sup> refer to the plastid four membranes. **Nm**: cryptomonads have a nucleomorph, the vestigial nucleus of the red algal symbiont, which still encodes plastid and periplastidial compartment (PPC) proteins. SELMA complex, Omp85-related, and TIC translocators have been identified in heterokonts, haptophytes, and cryptophytes (Bullmann et al. 2010).

Despite general traits that have been identified and can be used for *in silico* predictions (Bruce 2001; Emanuelsson et al. 1999), the defining qualities of TPs beyond primary structure, e.g. amino acid content, remain elusive (Steiner et al. 2005). For the most part, TPs are 20 to 100 amino acids long (Bruce 2001) and contain an elevated level of the hydroxylated amino acids (Soll and Schleiff 2004), a net positive charge (Patron and Waller

2007), and N-terminal basic amino acids (Tonkin et al. 2006a). A feature unique to chromists and dinoflagellates is a phenylalanine at position +1 of TPs (Gould et al. 2006b; Patron et al. 2005). TPs for transport into secondary plastids are thought to adhere to the same general trends as TPs for primary plastids (Wastl and Maier 2000), and have not differentiated so significantly during the course of evolution as to eliminate compatibility of TPs among chromists (Gould et al. 2006b; Gruber et al. 2007), which could be attributed to the use of the same ancestral symbiotic machinery, e.g. the SELMA complex and orthologs of TOC and TIC.

## 1.4 Infrakingdom Alveolata

### 1.4.1 Alveolates as Such

Dinoflagellates, ciliates, apicomplexans, and various other genera were first grouped together based on morphological features based upon such criteria as distinct flagella/cilia, tubular cristae of their mitochondria, similar chromosome division, and the system of single-membrane flattened sacs under the plasma membrane, i.e. alveoli (Cavalier-Smith 1987a; Cavalier-Smith 1991; Saldarriaga et al. 2004). Molecular phylogeny using DNA sequences further bolstered the grouping of these organisms into the infrakingdom of Alveolata (Baldauf et al. 2000; Burki et al. 2007; Keeling et al. 2005; Simpson and Roger 2002), which is tremendously important clade in regards to its impact on health, the environment, and agriculture.

All three alveolate subgroups contain predatory and parasitic species. Dinoflagellates and the genus *Chromera* however are the only groups of alveolates known to harbor fully-integrated, photosynthetic plastids. Alveolate plastids are thought to have arisen from a common alveolate progenitor plastid, which was probably most reminiscent of a heterokonts (Janouskovec et al. 2010). Of all alveolates, only dinoflagellates are both heterotrophic and photoautotrophic (Obornik et al. 2009). Ciliates are a diverse group of aquatic heterotrophs commonly covered by short cilia that can only harbor photosynthetic symbionts as intermittent kleptoplastids (Johnson et al. 2007). Apicomplexans are intracellular parasites that contain an extremely reduced plastid, the function of which seems to be limited to the



synthesis of fatty acids (Sato and Wilson 2005). Analogous to their highly variable lifestyles and morphologies, alveolates contain alveoli that vary quite significantly in shape, function, and arrangement. In apicomplexans, alveoli are vital for the parasite's gliding motility system during host cell invasion (Gaskins et al. 2004; Sibley 2004; Soldati et al. 2004). Apicomplexan and ciliate alveoli function in movement and interact with cytoskeletal elements at the basal bodies of the cilia but differ in their conjunction with complex cortical epiplasm comprising ejectile structures known as extrusomes (Rosati and Modeo 2003).

Apicomplexans and dinoflagellates were originally grouped together in the superphylum miozoa and are considered to be more closely related to each other than to ciliates (Cavalier-Smith 1987a). Morphological features confirming this are their common possession of a plastid and of an anterior cone of microtubules, which is used for host cell invasion in apicomplexa and for prey ingestion in heterotrophic dinoflagellates (Saldarriaga et al. 2004). Genera like *Oxyrrhis*, *Colponema*, *Perkinsus*, *Parvilucifera*, *Rastrimonas*, and the Ellobiopsids are phylogenetically related to dinoflagellates and apicomplexa and have thus also been classified as miozoa (Hoppenrath and Leander 2009; Saldarriaga et al. 2003; Slamovits et al. 2007), especially since their flagellates mostly bear an apical structure common to miozoa (Saldarriaga et al. 2004).

### 1.4.2 Protein Transport into Apicomplexan Plastids

In contrast to chromists, which are embedded in the cER, apicomplexan plastids, i.e. apicoplasts, lack bound ribosomes on their surfaces, and there is no connection between their outermost plastid membrane and the ER (Bolte et al. 2009). The origin of the four membranes surrounding the apicoplast is a point of contention, but generally the outermost membrane is considered to be a derivative of the endomembrane system, whereas the second outermost membrane known as the periplastidial membrane (PPM) is considered to be the remnant of the secondary endosymbiont's plasma membrane (Cavalier-Smith 2003). The inner two plastid membranes are considered to correspond to the plastid envelope of the primary plastid (Gould et al. 2008).

Like for all complex plastid proteins, nucleus-encoded apicoplast proteins require a BTS, which is necessary and sufficient to mediate transport to the plastid and across all four apicoplast membranes into its stroma (Waller et al. 1998). Because the apicoplast is not

located within the ER, vesicles must be transported to and fuse with the outermost apicoplast membrane. In apicomplexans, it has been ascertained that protein transport is neither affected by Brefeldin A – a fungal metabolite known to block Golgi-to-ER retrograde transport in model eukaryotic systems (Nebenfuhr et al. 2002) – nor Golgi retention signals, meaning that protein transport to the plastid is down-stream of the ER and independent of the Golgi (DeRocher et al. 2005; Tonkin et al. 2006b). Like in chromists, apicoplast preproteins are recognized in the ER lumen as being plastid-destined by means of their TPs, which mediate the rest of the transport to the plastid stroma (Tonkin et al. 2008b). By and large, apicoplast TPs are similar to general trends of plastid TPs inasmuch as they vary extensively in length and are relatively enriched in hydrophilic and basic amino acids (Ralph et al. 2004).

### Apicomplexans

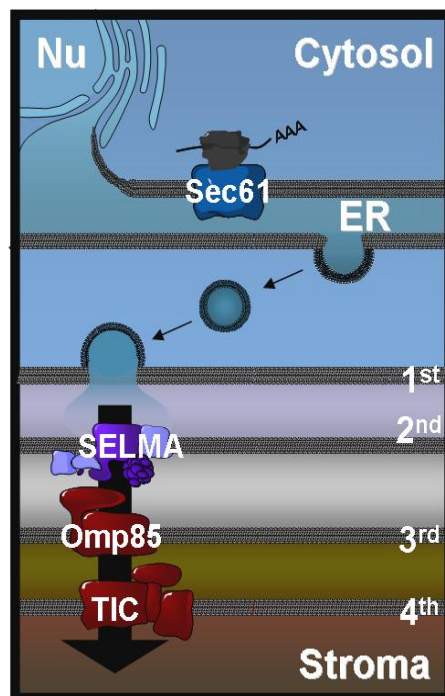


**Figure 5.** A Schematic Depiction of Protein Transport in Apicomplexa. (Agrawal et al. 2009; Bolte et al. 2009; Bullmann et al. 2010). Apicomplexans transport proteins to their alveolate plastids via vesicles, whereafter SELMA complex, Omp85-related, and TIC translocators are thought to mediate transport into the apicoplast. 1<sup>st</sup>, 2<sup>nd</sup>, 3<sup>rd</sup>, 4<sup>th</sup> refer to the four plastid membranes.

## 1.5 Dinoflagellates

### 1.5.1 Features of Dinoflagellate

Dinoflagellates are primarily unicellular eukaryotes possessing two angular ribbon-like flagella. One flagellum for lateral movement is located in the cingulum, i.e. the circumferential midline groove on the cell surface, and one for linear movement is located in a posterior flagellum originating in the sulcus, i.e. the anterior-posterior groove starting at the cingulum. A further typical feature of most dinoflagellates' ultrastructure is the presence of the dinokaryon nucleus, which contains fibrillar chromosomes without nucleosomal histones that remain condensed even after mitosis (Dodge and Gruet 1987).

Dinoflagellates' alveoli define the group, since they consist of cortical flattened amphiesmal vesicles immediately underneath the plasma membrane. Dinoflagellate alveoli can contain cellulose in the form of armored plates, or theca, which contribute to cellular structural integrity (Saldarriaga et al. 2004). In thecate orders (Gonyaulacales, Peridinales, Dinophysiales, Procentrales), thecal plate tabulation is well-characterized due to the low number of alveoli. In athecate dinoflagellate orders (Gymnodiniales, Syndiniales, Noctilucales), the alveoli have no elucidated function and may number in the hundreds, making classifications based on homologies and locational relationships exceedingly difficult (Dodge and Gruet 1987; Saldarriaga et al. 2004).

Dinoflagellates are probably some of the most enigmatic organisms. In contrast to the obligate phagotrophic lifestyle of ciliates or the obligate parasitic lifestyle of apicomplexans, dinoflagellates as a whole can be photosynthetic, mixotrophic, predatory, and parasitic (Hackett et al. 2004a). Roughly half of all dinoflagellates contain some sort of plastid and rely to some degree on photosynthesis, and although the rest are no longer photosynthetically active, they still seemingly retain intact genes for plastid proteins (Sanchez-Puerta et al. 2007).

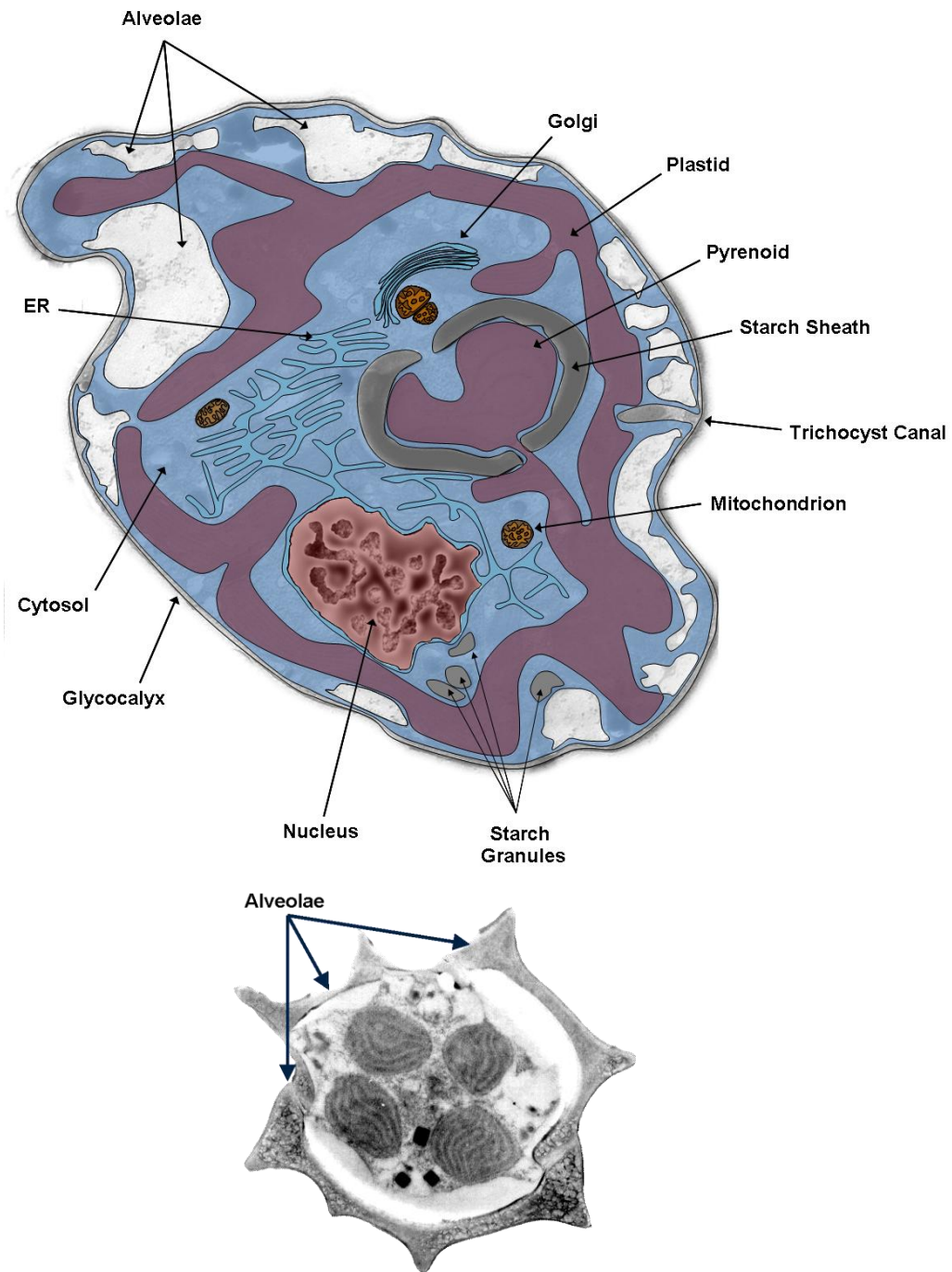


**Figure 6. General Morphological Features of Dinoflagellates: Above:** Schematic Composite of the Exemplary Dinoflagellate *Amphidinium carterae*. Common dinoflagellates features include constantly condensed nuclear chromosomes, the Golgi apparatus surrounding elongated tubular mitochondria, and peripheral alveolae, which are numerous and amorphous in athecate dinoflagellates like *A. carterae*. **Below:** A Cross-Section of a Horn from the Thecate Dinoflagellate *Ceratium horridum*. 3 alveolae are depicted containing cellulose plates.

A further defining feature of photosynthetic dinoflagellates is their light harvesting carotenoid: peridinin. Whereas most photosynthetic dinoflagellates use chlorophyll a,

chlorophyll c, and peridinin as the major photosynthetic pigments, an anomalously pigmented group of dinoflagellates contain a tertiary haptophytic plastid and utilize 19'-hexanoyloxy-fucoxanthin and/or 19'-butanoyloxy-fucoxanthin instead of peridinin (Yoon et al. 2002). Tertiary symbiosis is best characterized in dinoflagellates: the genera of *Dinophysis*, *Karlodinium/Karenia*, and (*Krypto*)*Peridinium* resulted from the endosymbioses of a cryptophyte, haptophyte, and diatom, respectively (Stoebe and Maier 2002).

### 1.5.2 Ecological Impetus

Organisms resembling dinoflagellates enter the fossil record during the Silurian period about 400 Mya, whereas modern dinoflagellate fossils are found in sediments from the late Triassic period from about 200 Mya. Haptophytes and diatoms had already been in existence for 20 to 100 million years by the time dinoflagellates became prominent according to the fossil record (Armbrust 2009; Morden and Sherwood 2002). These three groups have played a very prominent role in the carbon cycle since they came into existence, when they replaced cyanobacteria and green algae as the most predominant clades of oceanic phytoplankton 190 Mya (Falkowski et al. 2004). The most extreme example of their ecological contributions occurred about 100 Mya during the Cretaceous period when they sequestered four fifths of atmospheric CO<sub>2</sub> into biomass (Armbrust 2009). These three chromalveolate groups constitute a great portion of modern oceanic phytoplankton. Diatoms and dinoflagellates alone are responsible for roughly half the primary production on earth and contribute significantly to carbon cycling (Nassoury et al. 2003).

Dinoflagellates are considered to be of significant ecological and economic impetus. Dinoflagellate blooms, or so-called "red tides", occur when elevated nutrients, e.g. phosphates and nitrates, in coastal waters ameliorate dramatic algal growth that either directly or indirectly chokes out other aquatic life. Intense blooms even of non-toxic dinoflagellate species can physically clog gills of shellfish and finfish and even suffocate them by actually *reducing* aquatic oxygen levels (Chen and Chou 2001). Bloom-forming dinoflagellate species, e.g. *Gymnodinium catenatum*, *Alexandrium minutum*, *Alexandrium tamarense* and *Alexandrium catenella*, lay dormant as cysts in sediments for several years, whereupon a favorable environment is sensed. Massive cyst germination and subsequent

asexual reproduction then result in an overabundance of free-swimming cells (Bravo et al. 2010). Cell growth and division can result in rapid albeit short-lived blooms over large areas. Cells then reproduce sexually to produce another generation of resting cysts.

Members of the dinoflagellates genus *Symbiodinium* lodge themselves within the tissues of the host cnidarian and serve as symbionts. This symbiosis results in high levels of primary productivity as well as the rapid deposition of  $\text{CaCO}_3$  that serves as the rock substrate of coral reefs. Primary productivity from coral reefs is among the highest in the tropical seas, ranging from 300 to 5,000 g Carbon/m<sup>2</sup>/year (compared to 8-50 g Carbon/m<sup>2</sup>/year for non-reef tropical marine environments) (Longhurst et al. 1995). Dinoflagellate symbionts (zooxanthellae) of corals and other invertebrates are thus vital for coral reef survival in that they provide the animal hosts with carbon and energy in otherwise depleted tropical waters (Little et al. 2004). Coral bleaching is the disruption of symbiosis between the coral host and their dinoflagellate symbionts and has been increasing in frequency in the last few decades, resulting in diminished overall coral health (Lukes et al. 2009). The predominant consensus on the cause of coral bleaching is that high water temperatures results in a loss of pigment in the dinoflagellates and/or loss of algae in the holobiont (Lajeunesse et al. 2010; Rosenberg et al. 2009).

### 1.5.3 Genomic Arrangement of Dinoflagellates

Several unique features of genomic organization set dinoflagellates apart from other alveolates. For instance, dinoflagellates post-transcriptionally splice a leader sequence to the 5'-end of many if not all of their mRNA sequences. Spliced leader (SL) trans-splicing has a common mechanism in dinoflagellates; a 22-nt sequence is transferred from the 5'-end of a non-coding RNA of tandem repeats of SL to the 5'-end of mRNA (Zhang et al. 2007). Phylogenetically and ecologically diverse groups of dinoflagellates have been shown to all possess SL RNA transcripts of 50–60 nt, implicating the SL tandem repeat RNA as being an ancient and widespread feature among dinoflagellates as a whole (Lidie and van Dolah 2007). Although rampant genomic duplication and recombination continues to cause complex and diverse genomic arrangements in dinoflagellate lineages, important features like the length and structure of the functional SL RNA varies only slightly (Zhang et al. 2009).

Based on the extreme degree of endosymbiont gene transfer (EGT) from the plastid and mitochondrial genomes to the nucleus, the sheer size of dinoflagellate nuclear genomes, and the puzzling organizations of both nuclear and organelle genomes, it has been suggested that dinoflagellates' genetic material evolves under different constraints than is typical for other organisms with smaller, more conventional genomes (McEwan et al. 2008). Many if not all genomic coding regions are present as multiple copies that can vary at up to 2.2% of the nucleotide sites, which can even lead to changes in the physical properties of encoded proteins. Mutations among isoform copies are both as silent and non-silent and may represent low level concerted evolution (Reichman et al. 2003).

Besides ongoing evolution of transcribed sequences, dinoflagellates contain a number of characteristics that are unique to their nuclear genomes, including permanently condensed chromosomes that vary in number from 4 to 200 and lack both histones and nucleosomes (Bhaud et al. 2000). A sequencing survey of over 230 kb of the *Heterocapsa triquetra* nuclear genome demonstrated that about half of the dinoflagellate genome is made up of high copy repeated sequences and transposons. Perhaps the most striking result from the survey is that ca. 90% of the genomic sequence is apparently random, non-repetitive sequence (McEwan et al. 2008). This implicates large portions of the genome as being structural in nature, which could explain why dinoflagellates harbor the largest known nuclear genomes. Dinoflagellate genomes can be over 75 times the size of the human genome (250 and 3.2 pg/cell, respectively) (Hackett et al. 2005). The incredible amount of non-coding DNA has hampered efforts at genome projects and has thus limited sequence information to Expressed Sequence Tag (EST) projects. As of February 2010, 96,036 dinoflagellate ESTs were present in the NCBI database, most of which had yet to be annotated.

A canonical plastid genome is not present in many, if not all, peridinin-containing dinoflagellates (henceforth termed peridinin dinoflagellates). Although the typical plastid genomes of non-dinoflagellates vary in size and content, they are generally circular molecules of about 150 kb, encoding 60–200 genes (Martin and Herrmann 1998). In contrast, DNA encoding plastid proteins in dinoflagellates is arranged as several circular plasmid-like molecules that typically encode 0, 1, or 2 plastid genes. In at least one dinoflagellate, minicircles are located in the nucleus (Laatsch et al. 2004). Fewer than 20 coding genes and ESTs for plastid proteins have identified thus far in dinoflagellates, including *atpA*, *atpB*, *petB*, *petD*, *psaA*, *psaB*, *psbA*, *psbB*, *psbC*, *psbD*, *psbE*, *petD*, *ycf16*, *ycf24*, *rpl28*, and *rpl23*



(Bachvaroff et al. 2006; Barbrook and Howe 2000; Barbrook et al. 2006; Hiller 2001; Laatsch et al. 2004; Nelson et al. 2007; Zhang et al. 1999).

The guiding principle behind the gene complement encoded by the typical eukaryotic autotroph's plastid genome is still a matter of contention. One hypothesis stipulates that properties of the proteins encoded by the plastid genome would hinder their own import if they were to be nuclear-encoded (Daley and Whelan 2005; Kugita et al. 2003). Another hypothesis dictates that proteins encoded in the plastid must be quickly synthesized and regulated in the plastid in order to control the organelle's redox potential and to avoid the formation of oxygen radicals (Allen 2003; Allen 2005). Peridinin dinoflagellates seem to have circumvented the evolutionary constraints that led to the retention of genes in the plastid, as the "universal" photosynthetic plastid gene set present in all other photosynthetic organisms is not present in the dinoflagellate plastid genome and has been at least partially if not totally relocated to the nucleus (Bachvaroff et al. 2004).

In short, dinoflagellates may very well have carried out the most extensive amount of endosymbiont gene transfer (EGT) of any photosynthetic organism, and the actual coding capacity of the dinoflagellate plastid genome still has yet to be determined. Non-minicircle encoded genes for other photosynthetic components are thought to have migrated as single gene insertions into the nuclear genome, e.g. in *Alexandrium tamarense*, *Amphidinium carterae*, and *Lingulodinium polyedrum*, and to have acquired bipartite targeting sequences after their arrival there (Bachvaroff et al. 2004; Hackett et al. 2004b). The mitochondrial genome has been found to only contain multiple, redundant copies of *cox1*, *cox3*, and *cob* (Nash et al. 2007; Wang et al. 2005).

### 1.5.4 Protein Targeting in Dinoflagellates

Very little is known about the transport of plastid proteins in dinoflagellates, despite the vital role that they play in the survival of dinoflagellates. Because dinoflagellate plastids lack bound ribosomes on their surfaces and are external to the ER lumen, a secretory pathway vesicle transport system has been suggested in mitigating protein transport to the plastid, according the commonly accepted hypothetical model (Nassoury et al. 2003; van Dooren et al. 2001).



Like other organisms with complex plastids, plastid targeting of dinoflagellate proteins is mitigated with the BTS. In contrast to other organisms, dinoflagellate BTSs often contain a hydrophobic stop transfer sequence (STD) at the C-terminus of their TPs. Proteins containing STDs are classified into two groups: stromal class I proteins and thylakoid luminal class III proteins (Durnford and Gray 2006; Patron et al. 2005). According to Patron et al. 2005, Class III proteins can also be devoid of STDs, as is the case with stromal class II proteins. According to the hypothetical model from van Dooren et al. 2001, the mature domains of proteins containing STDs are located outside of the vesicle lumen during transport to plastids.

Regardless of class, proteins transported to the dinoflagellate plastid are thought to be trafficked via the Golgi apparatus in a BFA-sensitive manner, unlike vesicle-mediated transport in apicomplexans (Nassoury et al. 2005). Dinoflagellate plastid protein transport is thus thought to be more similar to vesicle-mediated protein transport to the likewise three-membraned plastids of the euglenophyte *Euglena gracilis*, in which fusion of Golgi vesicles with the plastid have been shown to occur *in vitro* (Slavikova et al. 2005; Sulli and Schwartzbach 1995).

Import of nucleus-encoded plastid proteins into dinoflagellate plastids is thought to differ from that of apicomplexans and chromists, because dinoflagellate plastids are surrounded by three membranes instead of four. Import of dinoflagellate preproteins into plastids after vesicle fusion must differ by en large from apicomplexa, because after fusion with the outermost plastid membrane of vesicles, the majority of protein precursors, i.e. those containing stop transfer domains, remain membrane-anchored with their functional domain in the cytosol (Nassoury et al. 2003; van Dooren et al. 2001). It has been postulated that a hypothetical translocator exists in the outermost plastid membrane that would facilitate the passage of class I and class III preproteins (containing STDs) across the outermost plastid membrane (Sulli et al. 1999; van Dooren et al. 2001). This suggested translocation machinery could then possibly recruit translocators of the second and third outermost plastid membranes. Translocation of soluble class II and class III preproteins (without STDs) across the inner two plastid membranes employs as yet unidentified translocators that are not necessarily the same ones used for class I and class III membrane-bound proteins. Cleavage of remaining targeting signals from the mature protein takes place upon the arrival of the

## Introduction

---

preprotein at its final destination by a compartment-specific protease (Chaal et al. 2003; Gomez et al. 2003).

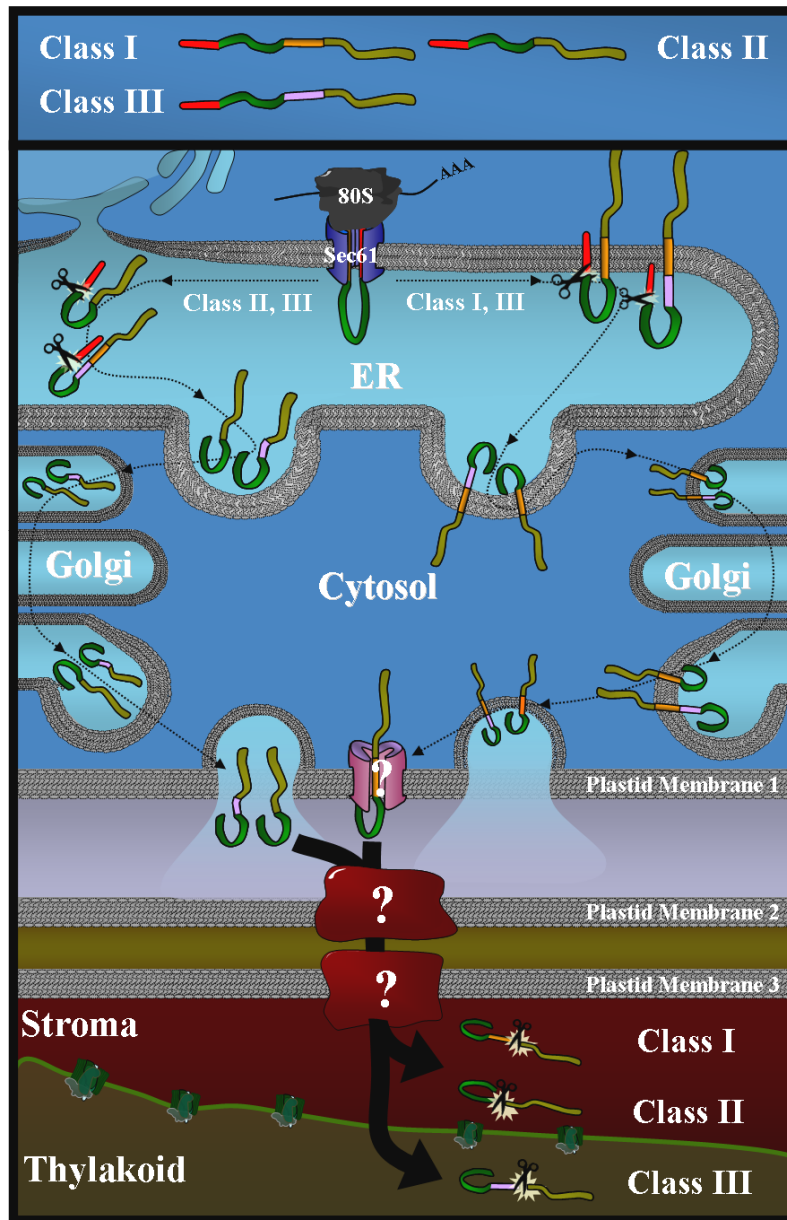


**Figure 7. Schematic Depiction of Class I, II, and III Proteins and Vesicle-Mediated Plastid Protein Transport in Peridinin Dinoflagellates and Euglenophytes** (as per van Dooren, Schwartzbach et al. 2001). Targeting signals include N-terminally located a signal peptide (**red**) preceded by a transit peptide (**green**). In all class I proteins, a hydrophobic domain (**orange**) is located between the transit peptide and the protein functional domain (**tan**). Class III proteins differ from class I and II contain topogenic signals for thylakoid lumen (**lilac**) and can contain a hydrophobic domain. After vesicles fuse to the first plastidial membrane, an hypothetical translocator may mediate the transport of class I and III membrane-bound preproteins across plastid membrane 1 and may then recruit translocators of membranes 2 and 3 (van Dooren et al. 2001). Transport of non-membrane-bound class II and III proteins across plastid membranes 2 and 3 probably utilizes unidentified translocators, albeit not necessarily the same translocators as class I and III membrane-bound proteins (Bolte et al. 2009). Cleavage of the signal peptide is thought to occur in the ER lumen, thus exposing the transit peptide to transport machinery. Remaining targeting signals are cleaved from the mature protein when the protein arrives at its final destination.

### 1.5.5 *Ceratium horridum*

*Ceratium horridum* is about 230 $\mu$ m–260 $\mu$ m in size. One defining characteristic is its three horns, which vary in their length and probably have an impact on its ability to tread water (Kofoid 1908). Motility is instilled by one longitudinal flagellum and one transverse flagellum, which allow the cell to move at a rate of about 0.03 – 0.12 m/hr (Peters 1929). Asexual reproduction is asymmetrical, and both daughter cells have two horns directly after mitosis, the third of which grows back over time. One feature that differentiates *C. horridum* from other dinoflagellates is its containing multiple small plastids and not one or two. *Ceratium horridum* minicircles are located in its nucleus, are independent of the chromosomes, and either are targeted by alternative means or have yet to acquire a topogenic presequence in the coding sequence (Laatsch et al. 2004).



**Figure 8.** Differential Interference Light Microscope Image of *Ceratium horridum*. Three horns protrude from the corpus of the cell. Plastids are on the cell periphery of the cell corpus and extend into the horns. The circular structure under the sulcus is the nucleus.

### 1.5.6 *Amphidinium carterae*

*Amphidinium carterae* is one of the best known and researched dinoflagellates. It is between 7 and 20 $\mu$ m large and has the capacity to flourish in sea water as well as brackwater in axenic culture (Nayak and Karunasagar 1997). Its generation time is about 1½ days and

## Introduction

---

does not possess cellulose theca, but is nonetheless very robust and can survive centrifugation (up to 2000 x g). *A. carterae* only contains one plastid that has many lobes that are mainly located at the cell's periphery. The lobes of the plastid connect to one another at the pyrenoid.



**Figure 9.** Differential Interference Light Microscope of *Amphidinium carterae*. The space seen between plastids on the right side of the cell is the nucleus. The circular structure proximal to the protrusion on the left is the pyrenoid. Plastids appear as dark organelles with a white periphery.

## 2 Aims

The aims of this doctorate thesis were threefold:

- Acquire novel insights into dinoflagellate plastid targeting sequences by establishing an EST library for *Ceratium horridum*, from which plastid proteins will be identified and analyzed.
- Using the trends identified from EST analysis, obtain information about the heretofore uncharacterized transport of dinoflagellate class II and III proteins (Prk and PsbO) heterologously in the transfectable systems of *Phaeodactylum tricorutum* and *Pisum sativum*.
- Establish a functional protocol for radioactive labeling of and sucrose fractionation in the dinoflagellate *Amphidinium carterae*, and determine the identity of fractions relevant to plastid protein transport by finding suitable markers for ER, Golgi, and Plastid fractions. Using this protocol, obtain information about the homologous transport of dinoflagellate class I, II, and III proteins (RbcL, Prk, and PsbO).

### 3 RESULTS

#### 3.1 Analysis of Synthesized *Ceratium horridum* ESTs

##### 3.1.1 Analysis of *Ceratium horridum* cDNA Library

cDNA synthesis was executed according to section 6.2.6, and 1651 sequences were acquired for the *Ceratium horridum* EST library. Clones with the prefix “On” and “Ch” were sequenced using the Sanger method for Licor4200 (bidirectional) and ABI sequencing (5’ unidirectional). All sequences with the prefix “Gt” signifies that sequencing occurred commercially at the Agowa company (now LGC genomics, Berlin). The global G+C content of thus acquired ESTs was 54.2%. *C. horridum* ESTs had an average length of 676 bp. The 1651 acquired ESTs could be aligned into 222 contigs and 720 singlets, totalling in 922 unigenes (56% of total EST number), of which 748 (81% of unigenes) contained a spliced leader sequence.

Preliminarily, stringent alignment parameters required a minimum overlap of 100 bp and 90% minimum match percentage resulted in the extrapolation of 213 contigs (clusters of assembled ESTs), consisting of 913 ESTs (55% of total). Alignment of the 753 remaining non-redundant singlet ESTs was performed with less stringent parameters (20 bp overlap, 70% minimum match). The contig containing the most sequences was by far the peridinin-chlorophyll binding protein contig, which constituted 148 (9%) of the 1651 clones. A single EST and a contig of 21 sequences coding peridinin-chlorophyll binding protein did not align with this contig. The sum of ESTs coding peridinin-chlorophyll binding protein was 160 out of the 1651 sequences (~10% of total ESTs). The second most abundant EST (2% of total ESTs) encoded a 743 bp ORF with no homology to known nucleotide translations.

Both BLASTX and tBLASTx were employed for EST analysis with an expect value cut-off of  $e^{-10}$ . The 213 contigs consisting of 913 ESTs resulting from the EST stringent alignment were found to have homologies with annotated proteins from a wide range of organisms as per BLASTX. 46 contigs consisting of 79 ESTs were found to be most homologous to dinoflagellate EST translations as per tBLASTx.

## Results

Of the 700 non-redundant singleton sequences remaining after the stringent EST alignment, 20 pairs of ESTs were observed to be most homologous to the same BLASTX hit. Of these, 9 pairs were aligned with the less stringent parameters. The 11 pairs of singletons remaining after low-stringency alignment were determined by BLAST homologies to encode the same region of two genes of analogous function. All such sequence pairs were observed to have substantial nucleotide sequence variation, and the proteins they encode were found to be divergent yet clearly homologous, as seen in figure 10. Therefore, these singletons encode different genes for one protein and are not non-overlapping ESTs of a single gene.

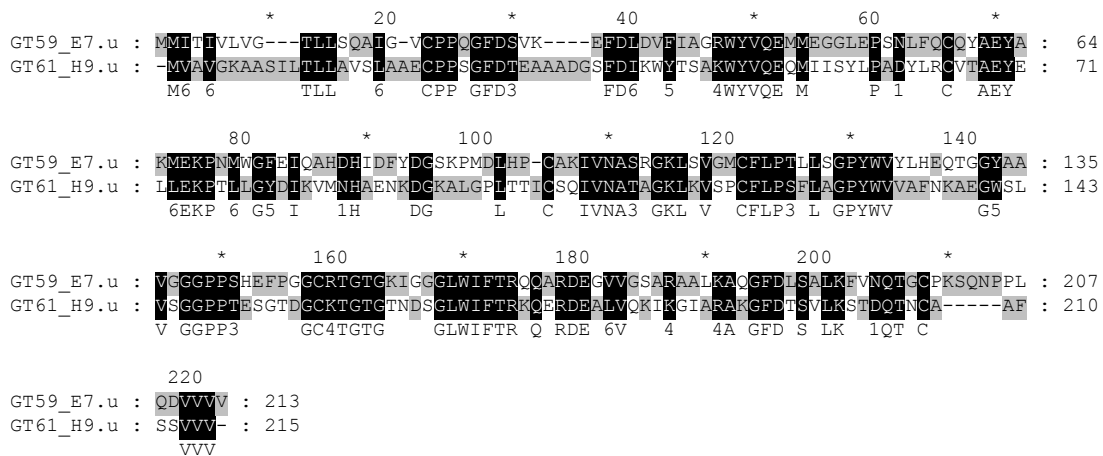


**Figure 10.** Exemplary ClustalX Protein Alignment of ESTs GT59\_E7.u and GT61\_H9.u. This depiction is a typical representation of the 11 pairs of ESTs encoding protein isoforms, of which the nucleotide sequences were not able to be aligned.

### 3.1.2 *C. horridum* EST Sequence Homologies

*Ceratiium horridum* sequences were each collated according to the organism with the best BLASTX or tBLASTX homology. The most significant EST homologies were observed in dinoflagellates (59%), chromists (12%), viridiplantae (9%), and alveolates (8%), as seen in figure 11. To determine whether this data set was representative for all dinoflagellates, a local BLAST search was extended to include all organisms that were determined to be most homologous to *C. horridum* unigenes for BLAST analysis of all 96,036 known dinoflagellate ESTs as of February 2010. The totality of protein sequences for each organism (or most related model organism, if adequate sequence information for the BLAST hit was lacking) were blasted against concatenated dinoflagellate ESTs. Special emphasis was given to including chromalveolate protein sequences in further the BLAST analyses. Thus, all



obtainable protein sequences from apicomplexa, oomycete, cryptophyte, haptophyte, and ciliates were included in further EST analyses, regardless of whether or not these organisms were present in the list of *C. horridum* EST BLAST hits.

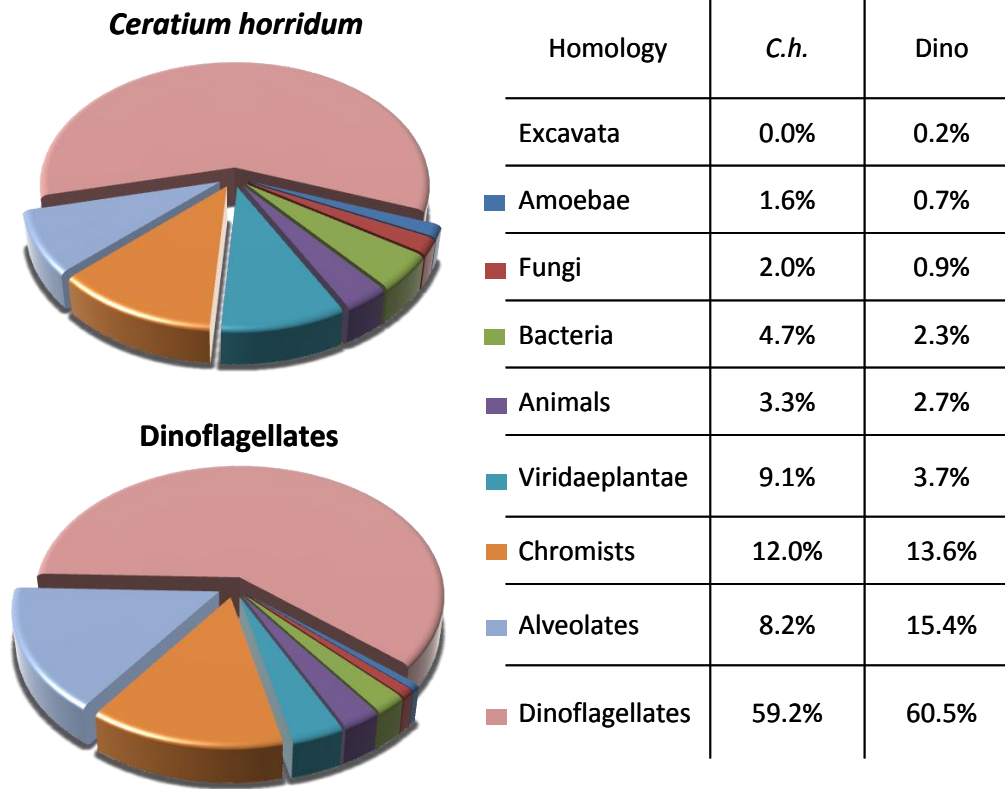


**Figure 11. Comparison of *Ceratium horridum* EST Contig Homologies to Total Dinoflagellate EST Homologies using Local BLAST.** All available protein sequences for chromists, alveolates, dinoflagellates, and all organisms found to be the best BLASTX hits from *C. horridum*. tBLASTn was used for blasting these sequences against the *C. horridum* and dinoflagellate EST library. **Left:** Pie diagram of *C. horridum* and Dinoflagellate EST sequence homologies. **Right:** Percentage of ESTs most homologous to each clade.

Utilizing the downloadable local BLAST program 2.2.22 from NCBI, a local database was created from all available dinoflagellate EST sequences available at NCBI together with the acquired *C. horridum* EST unigene library. Protein sequences from chromalveolates and all organisms with a *C. horridum* EST BLASTX hit were blasted against the *C. horridum* and dinoflagellate databases using tBLASTn, after which the database was compared to itself with tBLASTX. A macro was written in Microsoft Excel to retain only the most homologous BLAST hit for each EST that was not identical to itself. In this manner, differences in dinoflagellate and *C. horridum* EST homologies were extrapolated. It was thus determined that the most striking difference between the two data

sets is that the *C. horridum* EST library had markedly fewer homologies (10%) with other chromalveolates than other dinoflagellates do. *C. horridum* however had a comparative abundance of ESTs with homologies to viridiplantae, bacteria, animals, and amoebae.

For a number of BLASTX results, the most homologous hits did not originate from members of the chromalveolate superkingdom, which could implicate these unigenes as possibly not having chromist or alveolate origins. A list was compiled of *C. horridum* ESTs that had non-chromalveolate BLASTX hits. A list of homologous proteins from throughout the tree of life was compiled for phylogenetic analysis. To this end, phylogenetic methodology was employed in the exact manner as has been previously demonstrated to detect HGTs in dinoflagellates (Nosenko and Bhattacharya 2007; Nosenko et al. 2006), which was similar to the methodology for identifying red algal EGTs in *Oxyrrhis marina* (Slamovits and Keeling 2008). Of the initial 88 candidates for HGT, 88 were closely homologous to chromist and alveolate sequences and branched with them, whereas 2 clearly were and did not. The unigenes gt57c03 and gt62\_f11 were identified as being more closely related to the green lineage than to chromists.

The *C. horridum* EST gt57c03 is most homologous to 57 uncharacterized dinoflagellate ESTs (represented in the phylogenetic tree by a single *Karlodinium veneficum* EST). The closest non-dinoflagellate homolog with an identified function was the AMP-activated protein kinase from *Chlamydomonas reinhardtii*, as seen in figure 12. Bootstrap values of 86% and 100% were obtained from both Neighbor-Joining and Maximum Likelihood methods, respectively, in addition to a Bayesian posterior output value of over 0.95 separate the dinoflagellate sequences from chromist sequences, thus strongly confirming that the Gt57c03 and its 57 dinoflagellate homologs are most similar to proteins from primary plastid-harboring green algae and plants.

Gt62\_f11 is most homologous to the functionally identified *Amphidinium carterae* UDP-glucose dehydrogenase, which is involved in the reaction  $\text{UDP-glucose} + 2\text{NAD}^+ + \text{H}_2\text{O}$  to UDP-glucuronate, 2 NADH, and  $2\text{H}^+$ . This enzyme is a central to biosynthesis and energy metabolism, and thus plays a role in a number of biochemical pathways like the pentose phosphate pathway, glycolysis, and the metabolic pathways for ascorbate, aldarate, starch, sucrose, amino sugars, nucleotide sugars, inositol phosphate, and galactose. Phylogenetically, dinoflagellate homologs and Gt62\_f11 strongly group with plants, cyanobacteria, and green

algae, whereas the chromists are clearly the most phylogenetically distant group of examined organisms.

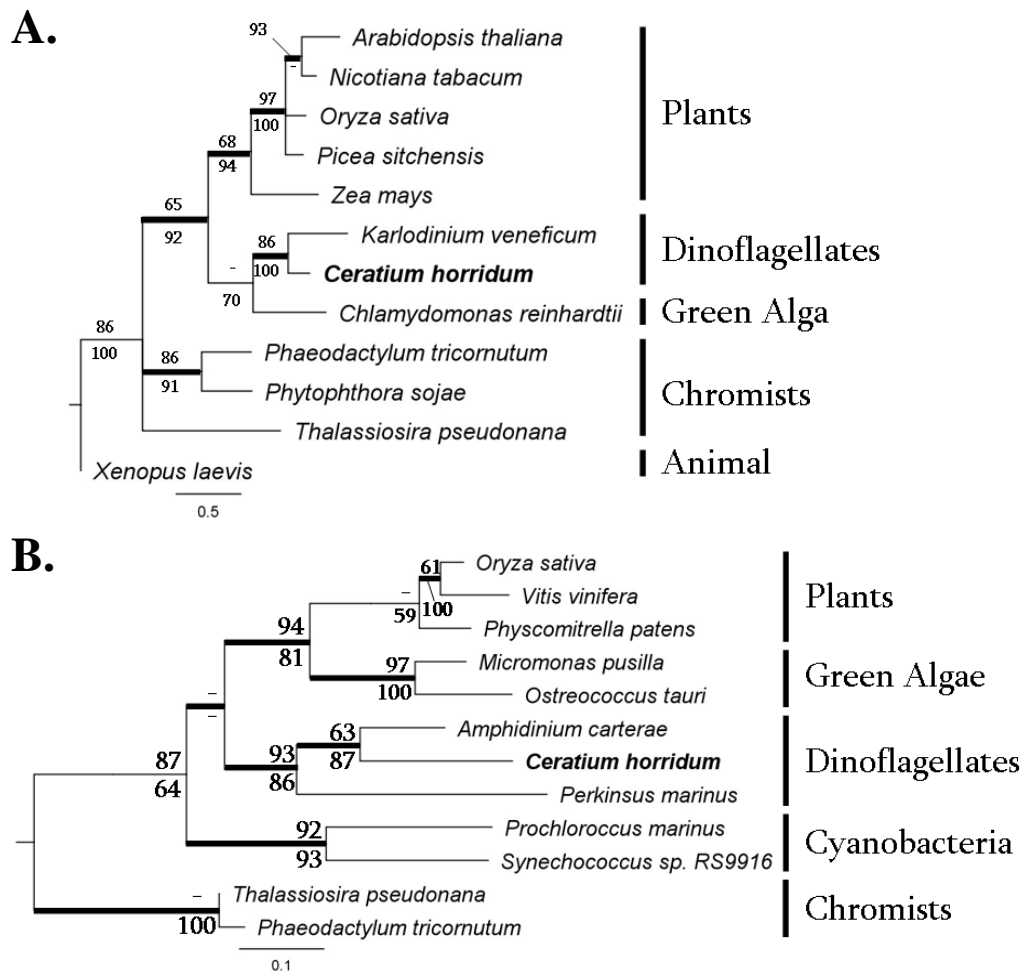


**Figure 12. Phylogenetic Relationship of 4 *Ceratium horridum* Unigenes.** Bold faced branches denote  $\geq 0.9$  Bayesian Posterior Output. Numbers above and below each branch denote bootstrap values calculated with ML and NJ bootstrap analyses, respectively. The thick branches indicate 0.95 posterior probability from Bayesian inference. Bar indicates exchanges per position. **A.**: Calcium-dependent protein kinase (Gt57c03), **B.**: UDP-glucose dehydrogenase (Gt62\_f11).

### 3.1.3 *C. horridum* EST Sequence Functions

All *Ceratium horridum* ESTs with identified homologies were classified into functional groups of four or more unigenes that belong to a single pathway. Enzymes catalyzing reactions were categorized according to the most prevalent cellular process or metabolic pathway that utilizes the enzymatic reaction product. This resulted in 13 categories. Gene products with low abundances (<4 unigenes) were grouped into the

## Results

category “other”. The four most represented groups of proteins corresponded to protein metabolism (21%), intracellular signaling (15%), photosynthesis (13%), and protein transport (9%).

<i>C. horridum</i> EST	BLASTX Hit	Organism	E value
on334	ADP-ribosylation factor	<i>Pfiesteria piscicida</i>	e-108
GT56c04.M13-21	rab GDP dissociation inhibitor alpha_ putative	<i>Toxoplasma gondii</i> ME49	3e-106
Gt62_C1.u	small GTP-binding protein Sar1, putative	<i>Toxoplasma gondii</i> ME49	1e-81
ON563	ADP-ribosylation factor	<i>Pfiesteria piscicida</i>	5e-67
on236	ADP-ribosylation factor family	<i>Phytophthora infestans</i> T30-4	e-58
ON317	adaptin or adaptin-related protein 8	<i>Brugia malayi</i>	e-42
ON373	small GTP-binding protein Sar1	<i>Cryptosporidium hominis</i>	1e-42
Gt63_H10.u	GTP-binding protein, putative	<i>Toxoplasma gondii</i> ME49	3e-41
Gt63_D2	Os06g0342100 signal recognition protein	<i>Oryza sativa</i> Japonica Group	3e-26
on45f	Sec61-gamma subunit of protein translocation complex	<i>Cryptosporidium parvum</i> Iowa II	7e-25
Gt58_D3.u	vacuolar sorting receptor protein, putative	<i>Toxoplasma gondii</i> VEG	6e-22
GT53c11.F	guanine nucleotide exchange family protein	<i>Ostreococcus lucimarinus</i> CCE9901	3e-20
on208	FAD-linked sulfhydryl oxidase Erv1p	<i>Saccharomyces cerevisiae</i> JAY291	1e-15
on539	mitochondrial inner membrane protein	<i>Theileria annulata</i> strain Ankara	2e-12
ON575	protein transport protein Sec13, putative	<i>Pediculus humanus corporis</i>	3e-11
GT61_H8.u	vesicle-associated membrane protein 4	<i>Danio rerio</i>	4e-08

**Table 1. *Ceratium horridum* ESTs encoding Proteins involved in Protein Transport and Vesicle Formation.** All results were determined with BLASTX or tBLASTn with a cut-off of  $e^{-4}$ .

The categories in which dinoflagellate homologies constituted less than 50% of hits were ABC Transporters, Alveolae and Cell Membrane Proteins, RNA Metabolism, “Other”, Protein Modifications, and Intracellular Signaling. Whereas 2 of the 4 ABC transporter proteins were most similar to fungal sequences, alveolae and cell membrane proteins were most homologous to an oomycete, a bacterium, and a fungus. RNA metabolism hits were most similar to other alveolates. Hits from the “Other” category were expectedly diverse and included BLAST hits from green algae/plants, animals, chromists, bacteria, and fungi. BLAST hits for enzymes catalyzing protein modifications originated from an animal, a

diatom, and an alveolate. Intracellular signaling homologies included a fungus, a plant, an animal, chromists, and bacteria.

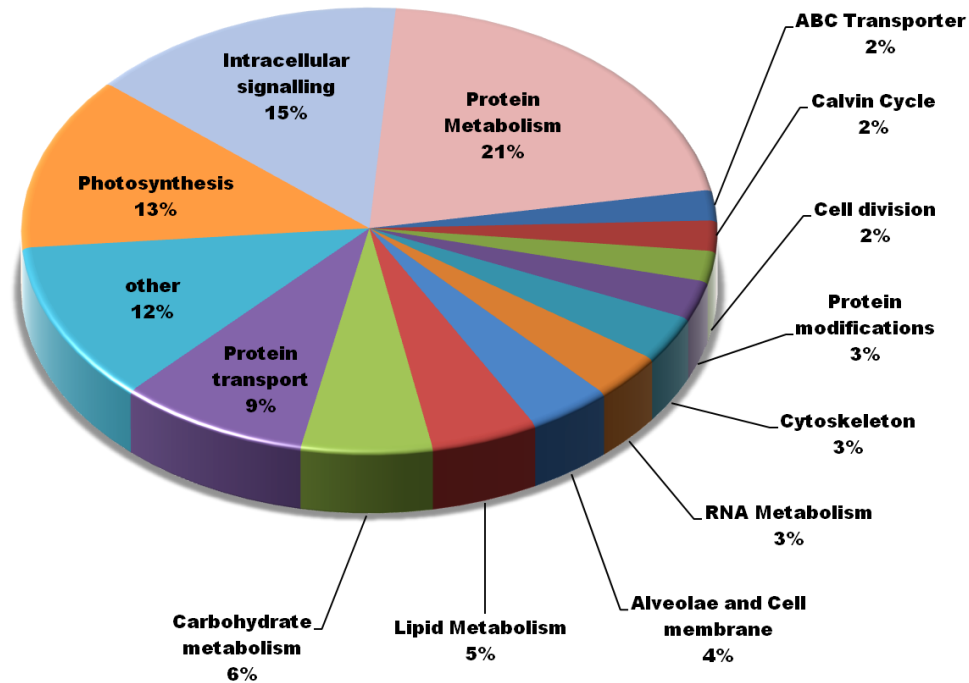


**Figure 13. Functional Distribution of Sequenced *C. horridum* ESTs.** ESTs are grouped according to biochemical and cellular functions. All components of biochemical pathways have been summarized according to the end products they produce, e.g. the category protein metabolism ranges from enzymes catalyzing reactions of amino acid anabolism to post-translational modifications.

### 3.1.4 Determination of *Ceratium horridum* Plastid-Targeted Proteins

Identification of plastid-associated ESTs was carried out by compiling a list of BLASTX hits that play a role in photosynthesis and dark reactions. All sequences encoding photosynthetic proteins were considered to contain a BTS, if the 5' terminus of the unigene was fully sequenced, as signified by the presence of a 5' SL sequence. 17 unigenes with functions in the plastid were determined in this manner.

For unigenes not encoding proteins with a clear plastid function, the longest frame was determined, and the first methionine in frame with the coding region after the spliced leader sequence was considered to be the start of the coding region. If no spliced leader sequence was present, then the first methionine in the sequence was used under the

assumption that an *ApaI* restriction site was present between the coding sequence and the spliced leader, which would have truncated the splice leader during cloning (see section 6.2.6). From this collated list of putative unigenes preprotein coding regions, SignalP was employed to determine SP length. SPs determined in this manner were truncated *in silico* for ChloroP analysis.

Of the 210 signal peptides identified by SignalP, SP lengths were from on average 24 amino acids long with a maximum length of 55 residues and minimum length of 12 residues. Of the 157 sequences determined to have a SP, 15 were determined as containing a plastid TP by ChloroP, 7 of which had no homology to any NCBI database entry. Combined with sequences identified by plastid-associated function, a total of 34 unigenes consisting of 15 singlets and 19 contigs (4% of total unigenes) were considered to have a plastid targeting presequence. These plastid-targeted proteins had functions related photosynthesis (50%), unknown (42%), or related to other plastid-localized reactions (8%).

The three most abundant amino acids in SPs of the 34 BTSs were alanine (23%), leucine (14%), and valine (12%). BTS SPs mostly contained non-polar neutral amino acids (72%), had an net positive charge (+1.75), and contained a noteworthy level of hydroxylated amino acids (13%). Most of the positive charge is located in the N-terminus of the SP. In figure 14, a weblogo of the positions of the SP directly preceding the TP are depicted. From this, an AXA-like motif seems to be present to some degree in *C. horridum* sequences.

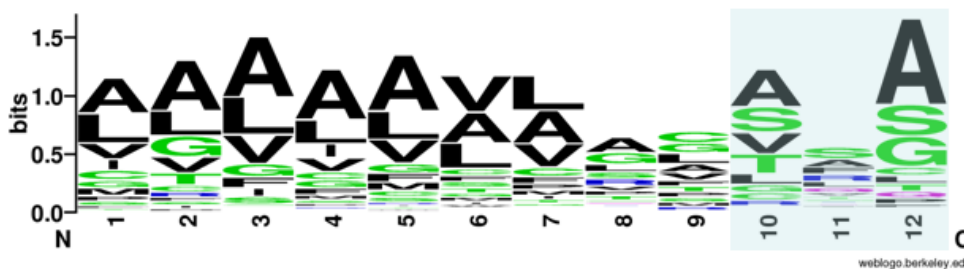


**Figure 14.** Weblogo of 12 Amino Acids Preceding the Signal Peptidase Cleavage Site Predicted by SignalP. Blue box highlights the AXA motif directly preceding the end of the signal peptide.

Accession	Description	Total score	Query coverage	E value	Organism	<i>C. horridum</i> Clone Reference
AAAX13962.1	chloroplast phosphoribulokinase	401	100%	1.00E-110	<i>Pyrocystis lunula</i>	on510
AAM77465.1	oxygen evolving enhancer I precursor	301	90%	1.00E-80	<i>Heterocapsa triquetra</i>	psbO_cDNA_contig
AAW79405.1	unknown protein	226	92%	8.00E-58	<i>Heterocapsa triquetra</i>	on590
ABV22122.1	chloroplast ATP synthase subunit C (AtpH)	206	99%	9.00E-52	<i>Alexandrium tamarense</i>	on303
AAW79346.1	chloroplast photosystem I subunit XI (PsaL)	197	98%	3.00E-49	<i>Heterocapsa triquetra</i>	Gt58_H5
EX461188.1	sqb34c1bd9	192	55%	4.00E-15	<i>Alexandrium catenella</i>	GT57h05.M13-21
CF947692.1	UI-D-GC1-aah-e-13-0-UI.s1	187	50%	9.00E-15	<i>Alexandrium tamarense</i>	on533
AAW79342.1	chloroplast cytochrome f	171	48%	2.00E-41	<i>Heterocapsa triquetra</i>	GT54a05.F
Q5ENN5.1	Ribulose biphosphate carboxylase, chloroplastic	157	68%	2.00E-17	<i>Heterocapsa triquetra</i>	on197
ABV72565.1	hypothetical protein	146	57%	7.00E-34	<i>Heterocapsa rotundata</i>	on73
AAW79333.1	chloroplast cytochrome c6	145	98%	2.00E-33	<i>Heterocapsa triquetra</i>	Gt58_B2.u
BP743201.1	BP743201	137	54%	8.00E-09	<i>Lingulodinium polyedrum</i>	ON327
AAW79314.1	chloroplast ferredoxin-NADP(+) reductase	135	86%	2.00E-30	<i>Heterocapsa triquetra</i>	Gt58_E7
AAW79388.1	unknown protein	135	81%	1.00E-30	<i>Heterocapsa triquetra</i>	Ch757
AAN39441.1	peridinin chlorophyll-a binding protein apoprotein precursor	132	47%	1.00E-15	<i>Symbiodinium kawagutii</i>	SZ2
AAW79343.1	chloroplast photosystem I protein E	129	99%	8.00E-29	<i>Heterocapsa triquetra</i>	on398
DT381197.1	HTE00008158	124	36%	5.00E-07	<i>Heterocapsa triquetra</i>	GT59_A2
BP743085.1	BP743085	110	34%	8.00E-06	<i>Lingulodinium polyedrum</i>	on276
YP_635799.1	Photosystem I subunit VII	107	48%	4.00E-22	<i>Chara vulgaris</i>	ON328
AAW79348.1	chloroplast cytochrome b559 subunit beta	106	99%	7.00E-22	<i>Heterocapsa triquetra</i>	on318
AAW79333.1	chloroplast cytochrome c6	103	61%	7.00E-21	<i>Heterocapsa triquetra</i>	on195
AAW79349.1	chloroplast photosystem II protein L	89	99%	1.00E-16	<i>Heterocapsa triquetra</i>	on182
CO061354.1	est_k_brevis923	82	40%	6.00E-16	<i>Karenia brevis</i>	GT52f12.F
ABV72575.1	unknown	55.5	22%	5.00E-06	<i>Heterocapsa rotundata</i>	on266
NP_043691.1	photosystem II protein K	64.7	0.37	0.000000003	<i>Odontella sinensis</i>	on269
AAG37859.1	Ribulose biphosphate carboxylase, chloroplastic	50.4	0.2	0.00005	<i>Symbiodinium sp.</i>	GT52a12.F
ZP_01470365.1	cytochrome b6-f complex subunit V	47.8	0.37	0.0004	<i>Synechococcus sp. RS9916</i>	on461
CF948083.1	UI-D-GC1-aah-o-16-0-UI.s1	45.8	0.46	0.00002	<i>Alexandrium tamarense</i>	on231.1
FE865729.1	ZooX20012E21.g_091	43.1	0.29	0.0001	<i>Symbiodinium sp.</i>	Gt62_C8.u

**Table 2. BLAST Homologies for 29 of 34 Plastid-Targeted Unigenes.** Hits are arranged in order of highest to lowest bit score. The homologies up to ABV22122.1 were ascertained by utilizing BLASTX and the remaining homologies by tBLASTX. An e value cutoff of  $e^{-4}$  was used. All sequences were most homologous to dinoflagellates except for on328, on461, and on269. 5 plastid-targeted unigenes had no homologies to known sequences.

### 3.1.5 *Ceratium horridum* Transit Peptide Classification

Classification of TPs took into account whether each sequence contained a hydrophobic domain. 23% of the plastid-targeting TPs identified contained a putative

## Results

membrane-spanning domain that could act as an STD. Of these, one was determined to be a class I protein, whereas the rest were class III (containing a putative STD).

Function	<i>C. horridum</i> Clone Reference	Protein Class
Ribulose biphosphate carboxylase, chloroplastic	GT54a05.F	class I
peridinin chlorophyll-a binding protein apoprotein precursor	SZ2	class II
Ribulose biphosphate carboxylase, chloroplastic	on197	class II
chloroplast phosphoribulokinase	on523	class II
chloroplast ferredoxin-NADP(+) reductase	Gt58_E7	class III
oxygen evolving enhancer I precursor	psbO_cDNA_contig	class III
chloroplast ATP synthase subunit C (AtpH)	on318	class III
chloroplast cytochrome b559 subunit beta	ON328	class III
chloroplast photosystem I protein E	on461	class III
chloroplast cytochrome f	GT57h05.M13-21	class III (w/o)
chloroplast cytochrome c6	Gt58_D12.u	class III (w/o)
chloroplast photosystem I subunit XI (PsaL)	Gt58_F10.u	class III (w/o)
chloroplast photosystem II protein L	Gt63_B2.u	class III (w/o)
chloroplast cytochrome c6	on182	class III (w/o)
photosystem II protein K	on269	class III (w/o)
photosystem I subunit VII	on398	class III (w/o)
cytochrome b6-f complex subunit V	on510	class III (w/o)
unknown	on266	class I or III (w/o)
unknown	on276	class II or III(w/o)
unknown	ON383	class II or III(w/o)
unknown	on533	class II or III(w/o)
unknown	on590	class II or III(w/o)
unknown	on73	class II or III(w/o)
unknown	Ch757	class II or III(w/o)
unknown	on231.1	class II or III(w/o)
unknown	GT55f09.F	class II or III(w/o)
unknown	Gt58_B2.u	class II or III(w/o)
unknown	Gt58_H5	class II or III(w/o)
unknown	GT60_F4.u	class II or III(w/o)
unknown	Gt62_C8.u	class II or III(w/o)

**Table 3. Classification of *Ceratium horridum* Plastid-Targeted Proteins.** Classification of proteins was accomplished by identifying whether TPs potentially contained membrane-spanning domains. Class I and III proteins contain putative stop-transfer domains, and class II and III(w/o) do not. Without knowing their localization, proper classification was not possible for unknown proteins.

Except for one protein with an unknown function, proteins containing hydrophobic domains were classified based on the location of their function: class I corresponds to a stromal localization and class III indicates a thylakoid lumen localization. 10% of TPs were



class II proteins and 27% class III proteins (without putative STDs). Class III proteins (with and without STDs) constituted 50% of sequenced unigenes encoding plastid proteins. 40% of proteins had unidentified functions and could not be classified.

### 3.1.6 *Ceratium horridum* Transit Peptide Variations between Isoforms

Some contigs encoding plastid proteins were noted to have a number of point mutations between different contig sequences. Of the 3220 nucleotide positions for contigs encoding 7 plastid proteins, 208 nucleotide positions (6%) contained point mutations at discreet positions in at least one EST. The majority of mutations (58 %) that led to amino acid exchanges or deletions were located in BTSs. Of the remaining 42% of mutations, the majority (81%) were silent in the mature sequence.

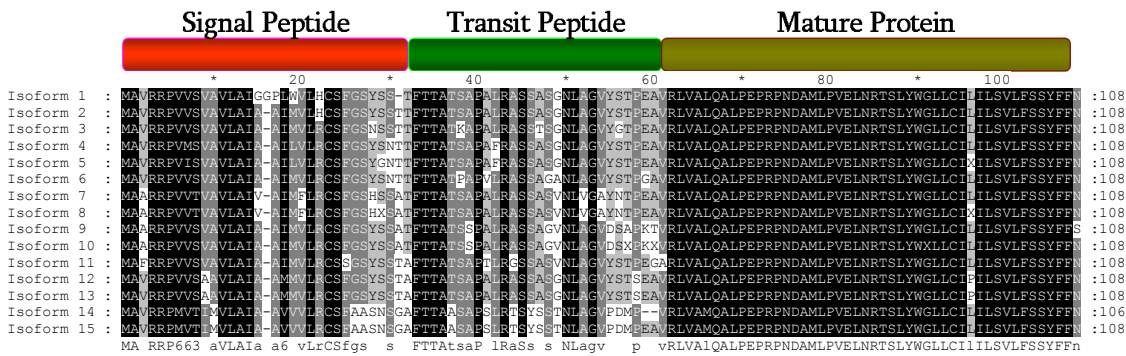


**Figure 15. Exemplary ClusalX Alignments of High Relative Amino Acid Exchanges in the BTS Region of Varying Plastid Protein Isoforms.** The entire coding preprotein coding region of *Ceratium horridum* PsbL isoforms.

ESTs encoding PsbL were sequenced numerous times to acquire the 15 non-redundant isoforms, displayed in figure 15. In the mature domain of the isoforms, two amino acid exchanges were present, which led to exchanges within a biochemical class of amino acid (non-polar neutral: leucine-to-proline and polar neutral: serine-to-asparagine). Of the 62 BTS amino acid positions, 42% differ between isoforms. These exchanges account for 52% of SP and 66% of TP amino acid positions. 85% of exchanges in the signal peptide are within the same biochemical class, whereas 83% of TP exchanges are from one biochemical group to another.

Thus, point mutations between *C. horridum* PsbL isoforms in the SP and mature domain of the protein are either silent or result in amino acid exchanges within the same biochemical category. Mutations in the TP sequence conversely showed exactly the opposite trend: most amino acid exchanges altered the biochemical properties of the TP.

### 3.1.7 Comparison of *Ceratium horridum* Transit Peptides with Those of Other Phototrophs

A broader spectrum of TPs from plastid-carrying organisms was included to approximate whether TP composition was representative for dinoflagellates and whether TPs from dinoflagellates and *Ceratium horridum* differed from one another. To this end no more than three non-repetitive sequences from TPs of dinoflagellate isoforms were used in further analyses, as not to bias results. Visualization of differences between *C. horridum*, dinoflagellate, diatom, and plant TPs was conducted by producing a weblogo for each data set, which included 32 *C. horridum* TPs, 163 peridinin dinoflagellate TPs, 123 diatom TPs, and 134 plant TPs from proteins with a documented plastid function.

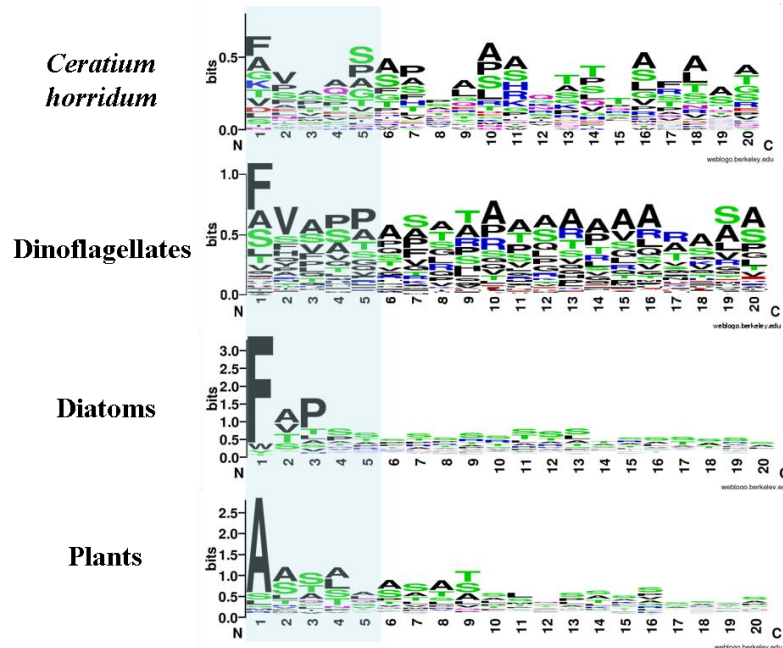


**Figure 16. Weblogo of Transit Peptides from *Ceratium horridum*, Total Dinoflagellate, Plants and Diatoms.** Weblogo of 32 *C. horridum* TPs, of 163 TPs from isoforms of 124 dinoflagellate plastid-targeted proteins, of 123 diatom TPs, and of 134 plant TPs. For plant TPs, the starting methionine was removed as not to make the other amino acids unreadable. Blue highlighted box depicts the first 5 amino acids of the TP, where conserved motifs can be located in TPs.

It was observed that an FVAP-related motif was present within 20 amino acids of the SignalP signal peptidase cleavage site in the majority (87%) of *C. horridum* plastid preprotein sequences. The FVAP motif is visible in the weblogo of 163 dinoflagellate TPs and appears to be more prominent than in *C. horridum* TP sequences. In contrast to the FVAP motif in dinoflagellate sequences, FAP motif is much more prominent in diatom sequences. Indeed, bit scores in figure 16 for both *C. horridum* and other dinoflagellate TPs are lower in general than the plant and diatom TPs, indicating more diversity at discreet TP positions.

Amino Acid	<i>C.h.</i>	Dino	Diatoms	Plant
Alanine (A)	20%	21%	11%	13%
Serine (S)	10%	11%	18%	16%
Threonine (T)	9%	8%	11%	8%
Proline (P)	9%	8%	7%	8%
Isoleucine (I)	3%	2%	7%	8%
Glycine (G)	6%	7%	3%	3%
Valine (V)	8%	9%	1%	1%
Methionine (M)	2%	2%	9%	6%
Leucine (L)	7%	7%	1%	3%
Glutamine (Q)	4%	4%	4%	5%
Trypsine (W)	1%	1%	6%	6%
Phenylalanine (F)	4%	3%	3%	4%
Histine (H)	2%	2%	3%	5%
Arginine (R)	4%	5%	1%	2%
Cysteine (C)	0%	1%	7%	4%
Lysine (K)	3%	2%	3%	3%
Glutamate (E)	3%	4%	2%	1%
Aspartate (D)	2%	2%	2%	2%
Asparagine (N)	2%	2%	2%	2%
Tyrosine (Y)	2%	1%	1%	0%
<b>Non-Polar Neutral</b>	<b>61%</b>	<b>60%</b>	<b>48%</b>	<b>52%</b>
<b>Hydroxylated</b>	<b>19%</b>	<b>19%</b>	<b>29%</b>	<b>24%</b>
<b>Polar neutral</b>	<b>6%</b>	<b>6%</b>	<b>13%</b>	<b>11%</b>
<b>Basic</b>	<b>9%</b>	<b>9%</b>	<b>7%</b>	<b>10%</b>
<b>Acidic</b>	<b>5%</b>	<b>6%</b>	<b>4%</b>	<b>3%</b>

**Table 4. Amino Acid Compositions of Plastid Protein Transit Peptides from 21 *Ceratium horridum*, 163 Peridinin Dinoflagellate, 123 Diatom, and 134 Plant Sequences.** Amino acids and amino acid classes are listed from highest to lowest average abundance. Dinoflagellate TPs have a relative abundance of non-polar residues and deficiency in hydroxylated residues.

*Ceratium horridum* TP amino acid compositions were compared to other dinoflagellates, to diatoms, and to plants, which revealed multiple differences, as depicted in table 4. The features already visible in figure 16 were specified in the numerical analyses: hydrophobic amino acids are about 10% more common in the *C. horridum* and dinoflagellate sequences than in diatoms and plants. Furthermore, hydroxylated and polar neutral residues are relatively less abundant in dinoflagellate sequences than in TPs from plants and diatoms. Also, only plants and diatoms were shown to have a preference for serine over threonine (~2:1). Perhaps the most interesting difference is that dinoflagellates have the same relative amount of positive charge in their TPs as diatoms and plants, but contain about 1.5 times more negative charge.

The average composition of *C. horridum* TPs correlates very closely to that of other dinoflagellates and falls within the standard deviations (SD) for plant TP amino acids classes (see appendix). It does not however fall within the range of SD for most diatom TPs. Hydroxylated and polar neutral residues are below the diatom TPs SD, and non-polar amino acids are too abundant to fall within the SD of diatom TPs. Altogether, compositions were species-specific, as noted by a general lack of variations among TPs within species ( $\leq 6\%$  SD).

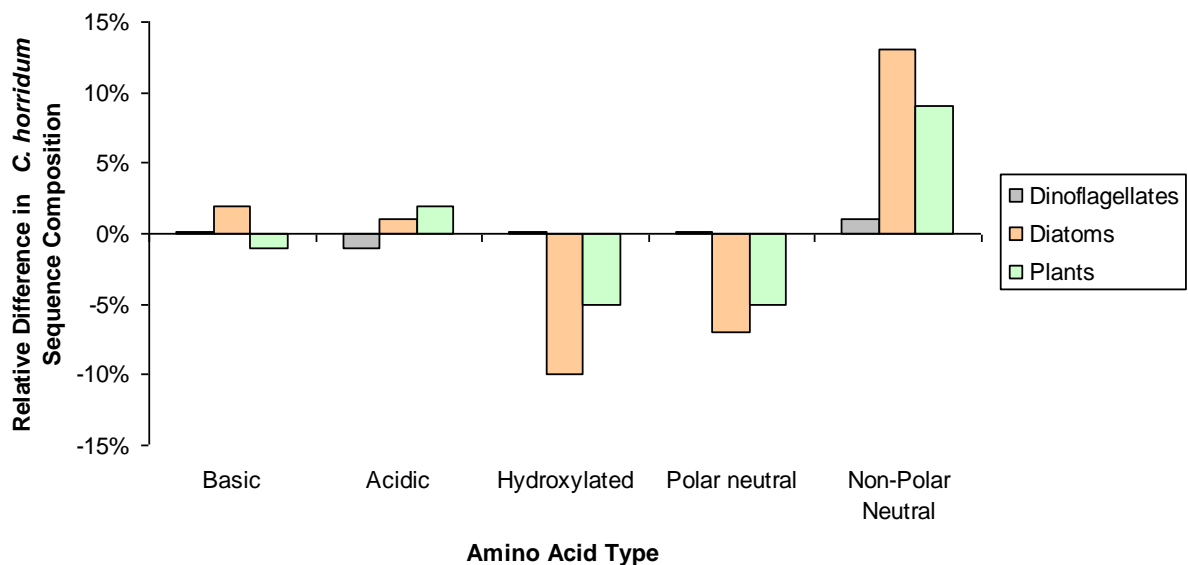


**Figure 17. Difference between *Ceratium horridum* Transit Peptides and those of Peridinin Dinoflagellates, Diatoms, and Plants.** Above: x-axis indicates the average composition for given amino acid in dinoflagellates, diatoms, or plants. A negative percentage indicates depletion in *C.*

## Results

*horridum* TPs, whereas positive percentage indicates dinoflagellates TPs being replete in the given amino acid class.

The majority of *C. horridum* TPs (75%) contained HSP70 binding sites as determined by the PlasmAP algorithm, but only one half (50.0%) of them were located in TP N-termini (Foth et al. 2003). In contrast to the homogenous distribution of HSP70 binding sites, *C. horridum* TPs contained the majority of their negatively charged amino acids (60%) in the TP C-termini, although positively charged amino acids were homogeneously distributed among the N- and C-termini (49% and 51%, respectively), as depicted in figure 18.

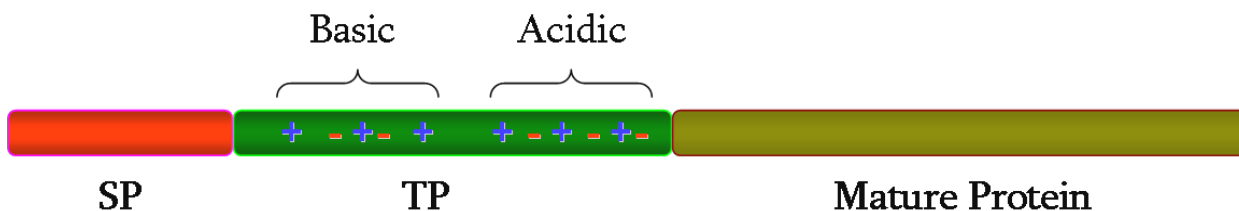


**Figure 18.** General Trend in Charge Separation in *Ceratium horridum* Transit Peptides. SP: signal peptide. TP: transit peptide.

### 3.1.8 Statistical Comparative Analysis of Dinoflagellate Transit Peptides

Analysis of the other 163 peridinin dinoflagellate TPs was performed to identify C-terminal negative charge using the average length of TPs as a cutoff and including no more than three isoforms of each protein, 67% of negatively charged residues were found to reside in the C-terminal halves of TPs, while 70% of positively charged residues were concentrated in the first N-terminal half of the average dinoflagellate TP. *C. horridum* thus has 7% less negative charge concentrated in the C-terminal TP half and 20% less in the N-terminal half of TPs than the average dinoflagellate TP.

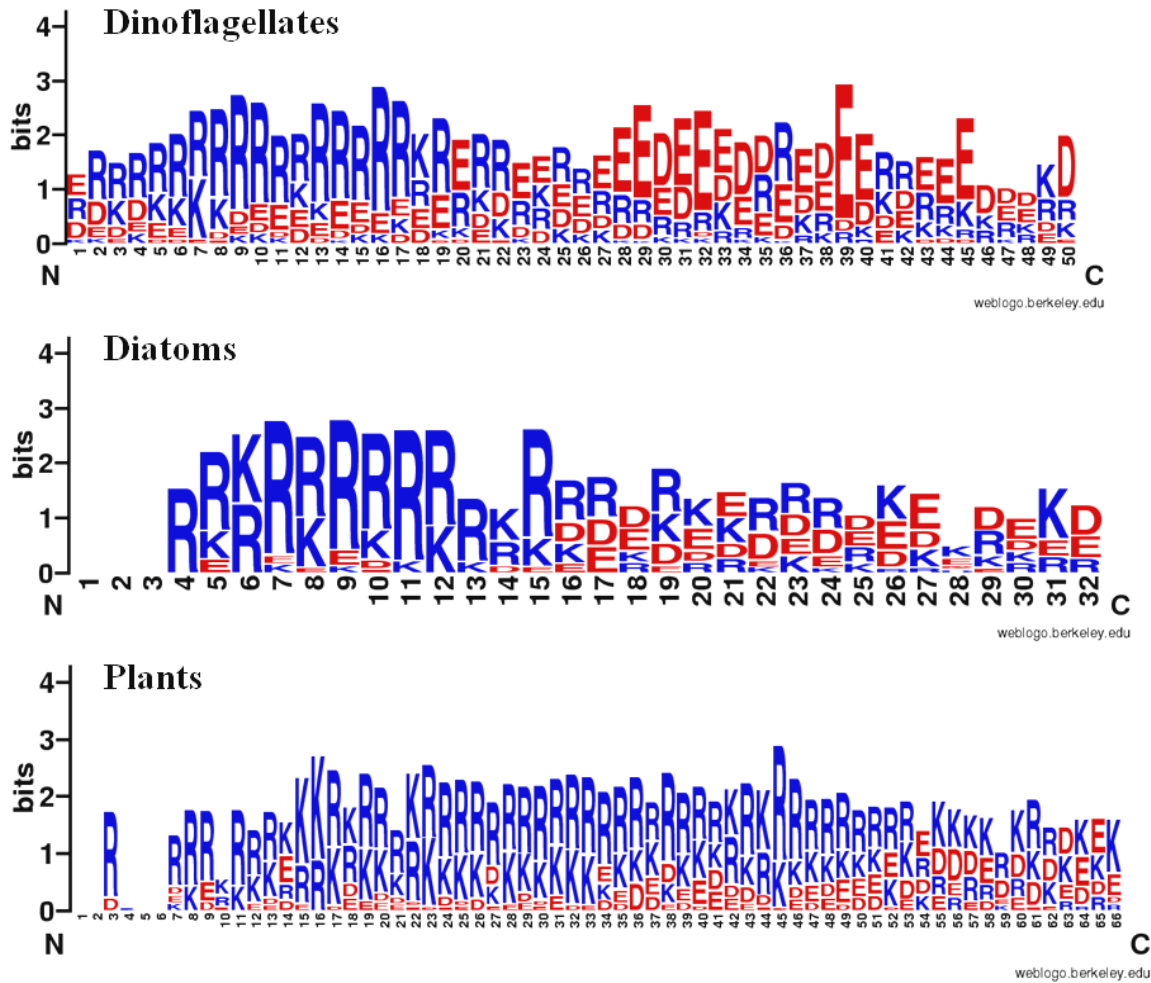
As seen in table 5, the first half of the average dinoflagellate TP was found to have a net positive charge of +2.08 more than the second half. The following trend could be ascribed to 79% of 184 non-redundant dinoflagellate TPs (now including all *C. horridum* TP sequences): a positive charge from basic amino acids is present in the first half of the TP and followed by an acidic patch consisting of the majority of the TP's negatively charged amino acids. Analysis of 123 diatom TPs, and 134 plant TPs in the same manner, led to the

observation that this trend is not absolutely absent in diatoms and plants but is much less distinct.

<b>Dinoflagellates</b>	N-terminal Charge in Relation to C-terminal Charge	Charged Residues per TP
From Acidic AA	+0.85	3.01
From Basic AA	+1.23	2.45
Sum	+2.08	5.46
<b>Diatoms</b>	N-terminal Charge in Relation to C-terminal Charge	Charged Residues per TP
From Acidic AA	+0.7	2.43
From Basic AA	+0.73	0.98
Sum	+1.43	3.41
<b>Plants</b>	N-terminal Charge in Relation to C-terminal Charge	Charged Residues per TP
From Acidic AA	+1.26	2.16
From Basic AA	-0.82	7.46
Sum	+0.44	9.62

**Table 5. Charged Amino Acids in the First and Second Halves of Dinoflagellate, Diatom, and Plant Transit Peptides. Above:** Charged amino acids in the first 50 amino acids of 184 dinoflagellate TPs. **Middle:** Charged amino acids in the first 32 amino acids of 123 diatom TPs. **Below:** Charged amino acids in the first 65 amino acids of 134 plant TPs.

The average diatom TP contains the least amount of charge (charged residues per TP), followed by dinoflagellates. The average plant TP has by far the most charged residues in their TPs, exceeding diatoms by a factor of >2.5 and dinoflagellates by >1.5. Roughly half of this charge (45%) is present in the form of arginine, which is consistent with the average diatom TP (48%) and in the average N-terminus of dinoflagellate TPs (55%). Of these charged amino acids, 78% were positively charged in plants, 71% in diatoms, and 57% in dinoflagellates. Dinoflagellate TPs therefore contain ~20% and ~15% more negative charge than plants and diatoms, respectively. To illustrate this data, a weblogo was produced as before except that all amino acids were omitted, which are not charged at physiological conditions. As can be seen in figure 19, the first 25 amino acid positions (half) of the average dinoflagellate TP most predominantly contains positive charge in the form of arginine, whereas in the second half negative residues predominate, especially glutamate.



**General Trend**

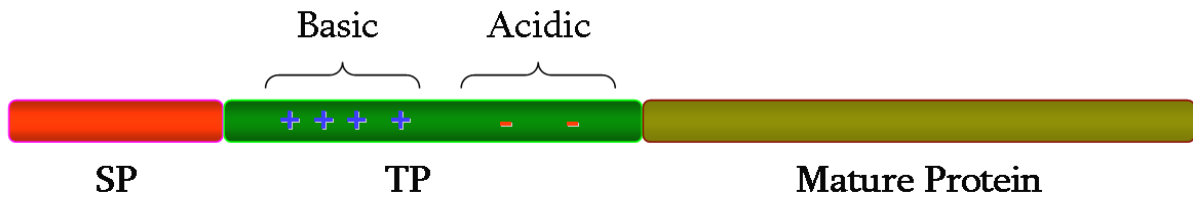


**Figure 19. Web Logo of Occurrence of Charged Amino Acids at Discrete Positions in Transit Peptides. Dinoflagellates:** First 50 amino acids (average TP length) of 184 peridinin dinoflagellate TPs. **Diatoms:** First 32 amino acids (average TP length) of 123 diatom TPs. **Plants:** First 65 amino acids (average TP length) of 134 plant TPs. **General Trend:** Format of Charge Separation in Dinoflagellate Transit Peptides. SP: signal peptide. TP: transit peptide.

### 3.2 Heterologous *in vivo* Import Studies

Because a protocol for transfection of dinoflagellates unfortunately does not exist, *in vivo* GFP targeting experiments with dinoflagellate targeting signals could only be performed in heterologous systems. *In vivo* import assays were performed to determine to what degree dinoflagellate targeting signals are viable for mediating transport into the ER of diatoms and into plant plastids. Because transport of stroma-localized class I proteins had already been partially characterized, viable candidates were limited to class II and class III proteins. As a stromal protein with no hydrophobic domains, Phosphoribulokinase (Prk) from the dinoflagellate *Amphidium carterae* was chosen to represent class II proteins. As a thylakoid luminal protein containing a thylakoid targeting domain (TTD), the *A. carterae* oxygen-evolving enzyme of Photosystem II (PsbO) was chosen to represent class III proteins. As seen in figure 20, both Prk and PsbO were exemplary proteins for dinoflagellate charge separation.

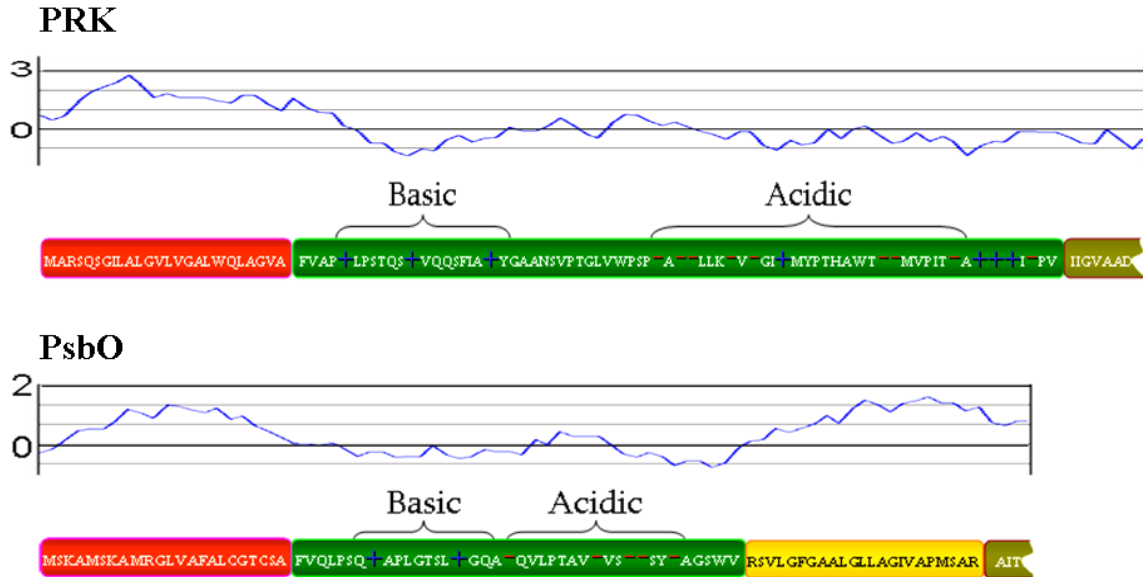


**Figure 20. Schematic Depiction of PsbO and Prk Sequence Demarcation and Transport.** Depictions of *A. carterae* PsbO and Prk Kyte-Doolittle plots (above, window size = 11) and amino acid sequences with charge of N-terminal extensions. Numbers next to Kyte-Doolittle plots indicate relative hydrophobicity units (max.: 4.5, min.: -4.5), whereby >1.7 usually indicates a membrane-spanning domain (Kyte and Doolittle 1982). **Red:** SP, **green:** TP, **yellow:** putative stop-transfer domain, and **tan:** mature protein.



### 3.2.1 Heterologous *in vivo* Import into the *Pisum sativum* Chloroplasts using *Amphidinium carterae* PsbO and Prk Transit Peptides

A protocol for the transfection of the plant *Pisum sativum* was established to investigate the *in vivo* targeting capacity of *A. carterae* PsbO and Prk TP sequences (section 6.2.11). Positive and negative controls were first tested using pAVA393 with the PsbO targeting signal from *Pisum sativum* and without a targeting sequence N-terminally fused to GFP, as seen in figure 21.

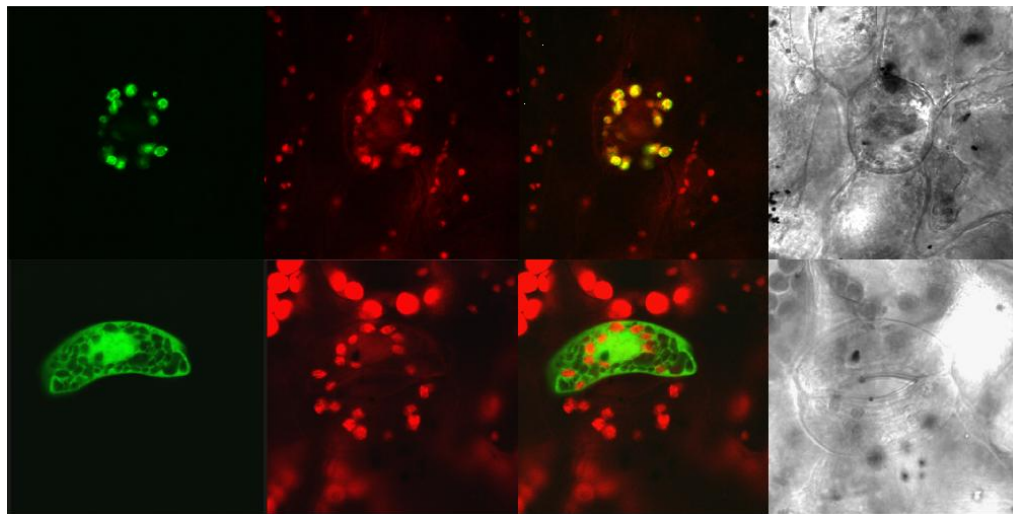


**Figure 21.** Initial Transfections of the Plant *Pisum sativum* using the pAVA393 Vector. **Above:** Transfection of *Pisum sativum* PsbO TP N-terminally fused to eGFP served as a positive control for further experiments. **Below:** Transfection of *Pisum sativum* with empty pAVA vector, which served as the negative control in subsequent experiments. **From left to right:** eGFP fluorescence, chloroplast autofluorescence, merge, DIC. **Green:** eGFP fluorescence, **Red:** Autofluorescence.

For *in vivo* *Pisum sativum* transfections, genetic constructs were produced with *A. carterae* TPs N-terminally fused to eGFP. Constructs of *A. carterae* PsbO and Prk TP sequences were devised to be as comparable to one another as possible. The first 19 and 20 amino acids of respective Prk and PsbO TPs contained the majority of positive charge ( $\geq 60\%$ ) and no negatively charged residues. In order to determine the effect of the C-terminal charge of dinoflagellate TPs, the negative C-terminal charge from Prk and PsbO TPs was truncated. Truncated construct TPs resembled plant TPs more closely in relative composition and charge than full-length *A. carterae* TPs. Since the hydrophobic domain in the plant PsbO

## Results

sequence is not present in plant sequence, a construct was produced without this hydrophobic domain. As seen in figure 22, features of truncated *A. carterae* TPs varied .

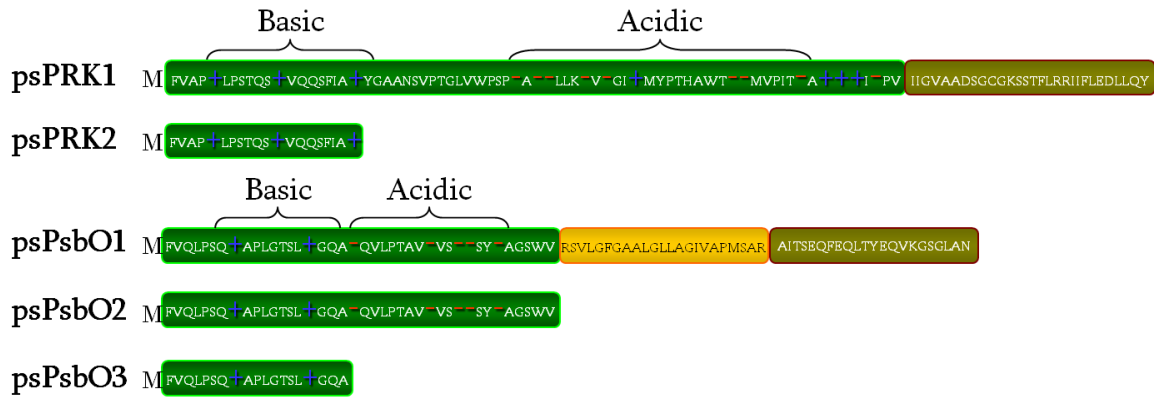


**Figure 22. Topogenic Signals Employed for *in vivo* Transfection Experiments in *Pisum sativum* and Construct Amino Acid Composition Compared to Plant TP Composition. psPrk1:** Prk full length TP sequence, **psPrk2:** truncated TP sequence fused to eGFP. **psPsbO1:** Full-length PsbO TP sequence containing the hydrophobic TTD, **psPsbO2:** PsbO TP sequence without the hydrophobic domain, **psPsbO3:** truncated TP sequence fused N-terminally to eGFP. **Red:** SP, **green:** TP, and **yellow:** putative stop-transfer domain, **tan:** mature protein.

Transfection of *P. sativum* with constructs psPrk1, psPsbO1, and psPsbO2 resulted in an eGFP localization outside of the plant's chloroplasts, as did the corresponding constructs containing Prk and PsbO SPs (not shown). Dinoflagellate targeting signals were unable to mediate protein import into pea chloroplasts *in vivo* as noted by the cytosolic eGFP localization.

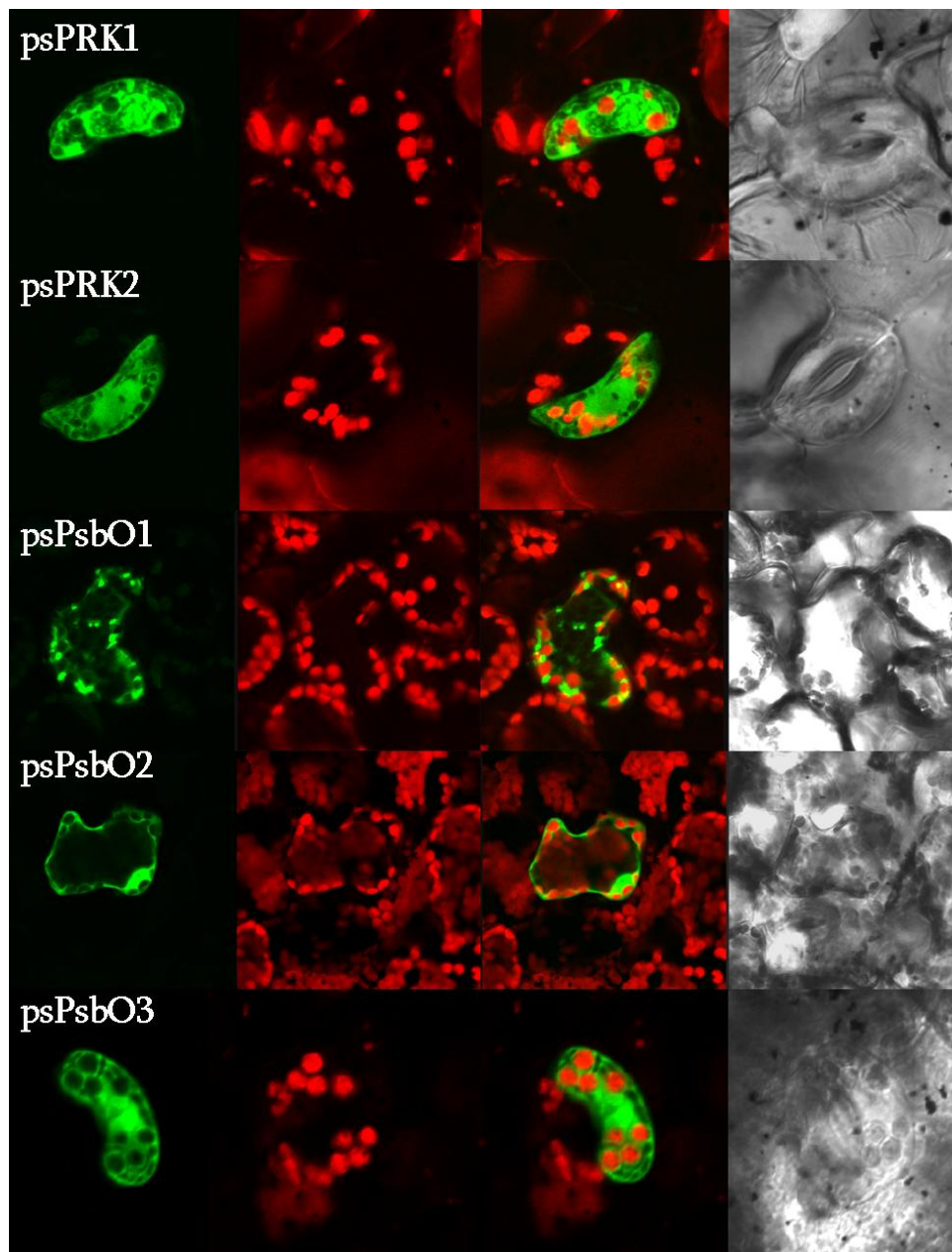


**Figure 23.** Heterologous Transfection of *Pisum sativum* with eGFP Fused N-terminally to Full-Length and Truncated TPs from *Amphidinium carterae* PsbO and Prk N-terminal Extensions. **psPsbO1:** Transfection of a mesophilic cell with construct. **psPsbO2:** psPsbO2 transfection of a mesophilic cell containing a central vacuole. **psPrk1:** Cytosolic eGFP localization seen in an epithelial guard cell with construct psPrk1. **psPsbO3:** Transfection of a mesophilic cell with construct psPsbO3. **psPrk2:** Cytosolic eGFP localization seen in an epithelial guard cell with construct psPrk2. **From left to right:** eGFP fluorescence, chloroplast autofluorescence, merge, DIC. **Green:** eGFP fluorescence, **Red:** Autofluorescence.

### 3.2.2 Heterologous *in vivo* Import into the *Pisum sativum* Chloroplasts using Chromalveolate PsbO and Prk Transit Peptides

To differentiate whether unique features of dinoflagellate TPs influence *in vivo* import competence in *P. sativum* or whether other chromalveolate sequences also cannot mediate transport, chromist TPs were also used for *in vivo* transfections of *P. sativum*. To this end, the well-characterized AtpC TP from the diatom *Phaeodactylum tricornutum* as well as AtpC and GapC1 TPs from the cryptophyte *Guillardia theta* were fused to eGFP as above. Import of eGFP into the chloroplasts of *P. sativum* did not occur using any one of these constructs, as seen in figure 24.

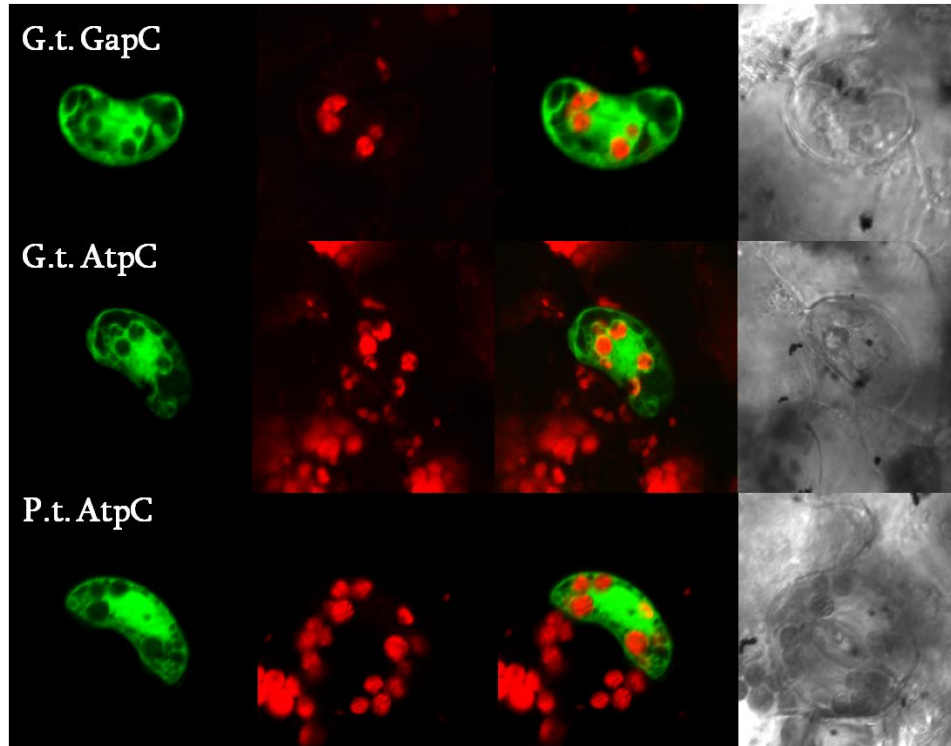


**Figure 24. Heterologous Transfection of *Pisum sativum* with eGFP Fused to Full-length Transit Peptides from Chromists. Above: *Guillardia theta* GapC TP. Middle: *Guillardia theta* AtpC TP. Below: *Phaeodactylum tricornutum* AtpC TP. From left to right: eGFP fluorescence, chloroplast autofluorescence, merge, DIC. Green: eGFP fluorescence, Red: Autofluorescence.**

### 3.3 Heterologous *in vivo* Protein Import into the Plastids of *Phaeodactylum tricornutum* using *Amphidinium Carterae* PsbO and Prk Targeting Signals

Although dinoflagellates and diatoms are thought to have a common ancestor according to the chromalveolate hypothesis, they have a differing number of membranes surrounding their plastids. In both organisms, however, the first membrane that is crossed during transport to the plastid is the ER membrane. This translocation is thought to be mediated by the signal peptide in both chromists and dinoflagellates. The capacity of heterologous signal peptides in mediating *in vivo* translocation across the first membrane of the diatom plastid was tested. Constructs were also tested that contained not only the signal peptide but also variations of the transit peptide used for *P. sativum* transfections.

#### 3.3.1 Heterologous *in vivo* Protein Import in *Phaeodactylum tricornutum* using *Amphidinium Carterae* PsbO and Prk Signal Peptides

Because no *in vivo* data exists as to whether dinoflagellate signal peptides can mediate import into a heterologous ER lumen, signal peptides from PsbO and Prk were tested in the transfectable diatom *Phaeodactylum tricornutum*. Figure 25 portrays both of the *Amphidinium carterae* SPs used for constructs used in transfections.



**Figure 25.** Signal Peptides used for eGFP Constructs for Transfections of *Phaeodactylum tricornutum* from *Amphidinium carterae*. **spPrk:** signal peptide from *A. carterae* Phosphoribulokinase fused N-terminally to eGFP. **spPsbO:** signal peptide from *A. carterae* Oxygen Evolving Enzyme fused N-terminally to eGFP.

Signal peptide constructs used to transfect *P. tricornutum* resulted predominantly in a eGFP localization in the periplastidial compartment (PPC) for all constructs. As seen from fluorescence in the eGFP channel of figure 26, signal also arose from the ER albeit to a significantly lesser degree than the PPC fluorescence. There was however no signal present that colocalized with the plastid.

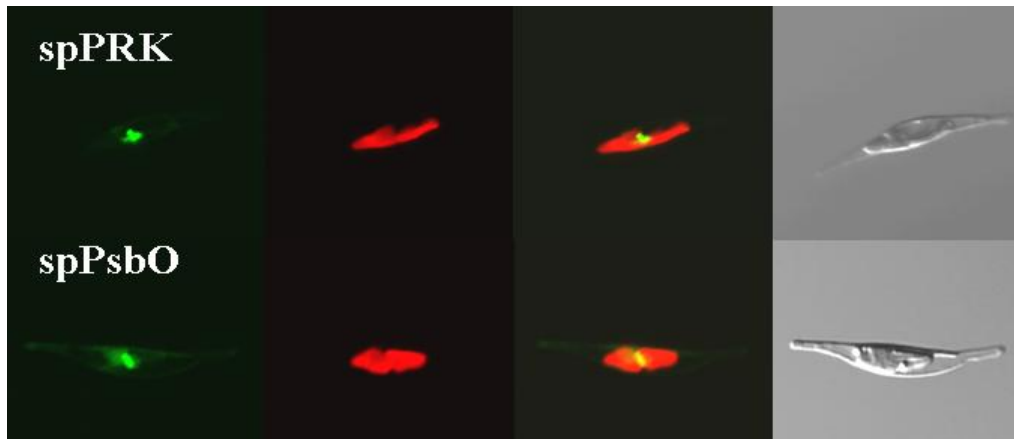


**Figure 26.** Transfection of *Phaeodactylum tricornutum* with eGFP fused to Signal Peptides from *A. carterae* and *P. tricornutum*. **Above:** *A. carterae* SP from Prk: predominant PPC and lesser ER eGFP localization. **Below:** *A. carterae* SP from PsbO: predominant PPC and lesser ER eGFP localization. **From left to right:** eGFP fluorescence with increased contrast and brightness to portray totality of eGFP signal, plastid autofluorescence, merge, DIC. **Green:** eGFP fluorescence, **Red:** Autofluorescence.

### 3.3.2 Heterologous *in vivo* Protein Import in *Phaeodactylum tricornutum* using *Amphidinium Carterae* PsbO and Prk Signal, Transit, and Thylakoid Targeting Peptides

Of the *A. carterae* BTS constructs, ptPsbO3 was the only PsbO construct that had a sufficient level of basic amino acids to be comparable to diatoms, whereas ptPrk1 was within the diatom TP SD, and ptPrk2 was not. Both ptPsbO1, ptPsbO2, and ptPrk1 contained a heightened level of acidic amino acids in comparison to diatoms, whereas ptPsbO3 and Prk2 fell within the range of the diatom TP SD. The most extreme difference noted between *A. carterae* PsbO and Prk constructs and diatom TPs was the lack of hydroxylated residues in constructs.



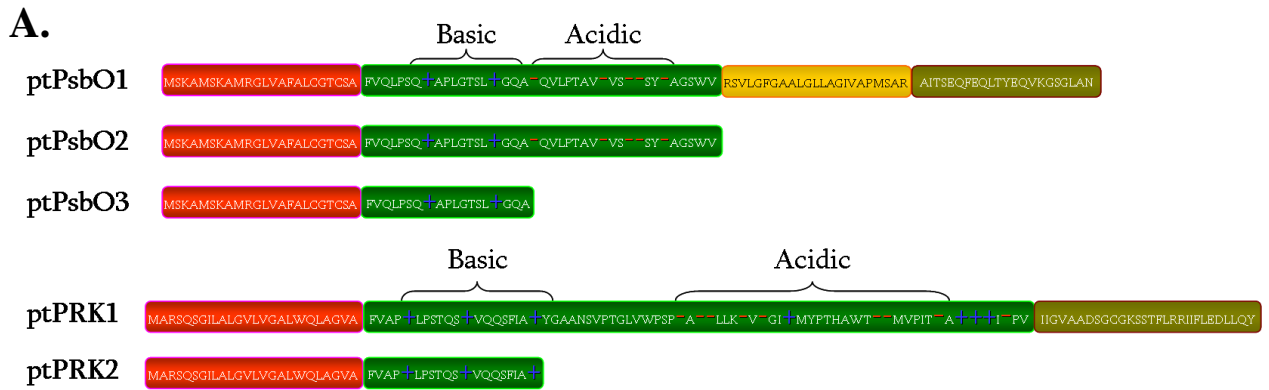


**Figure 27. Schematic Depiction of *Amphidinium carterae* TTS and BTS from PsbO and Prk used as Topogenic Signals for eGFP Import Assays in the Diatom *Phaeodactylum tricorutum*. Above:** Constructs used for transfection. **ptPrk1:** Prk full length BTS, **ptPrk2:** BTS sequence with TP truncated down to the 20 amino acids containing basic charge. **ptPsbO1:** PsbO full length TTS, **ptPsbO2:** PsbO BTS (without the hydrophobic domain), **ptPsbO3:** PsbO BTS with TP truncated to the 19 amino acids containing basic charge. **Red:** SP, **green:** TP, and **yellow:** putative stop-transfer domain, **tan:** mature protein.

Like in *Pisum sativum*, full-length PsbO and Prk targeting signals were unable to delegate the fusion proteins into the stroma of the plastid in *Phaeodactylum tricorutum* transformants. A blob-like PPC localization of eGFP fluorescence was observed for the full-length Prk BTS construct, whereas the construct for the full-length PsbO sequence (ptPsbO1, figure 28) resulted in an ER localization of eGFP. Transfection with ptPsbO2 resulted in a stromal localization of the eGFP signal. ptPrk1 localization was however not limited to the PPC, but also seemed to have a slight partial import into the diatom plastid. As denoted with blue arrows in figure 28, eGFP signal emanated to the left and right of the PPC and colocalized with plastid autofluorescence.

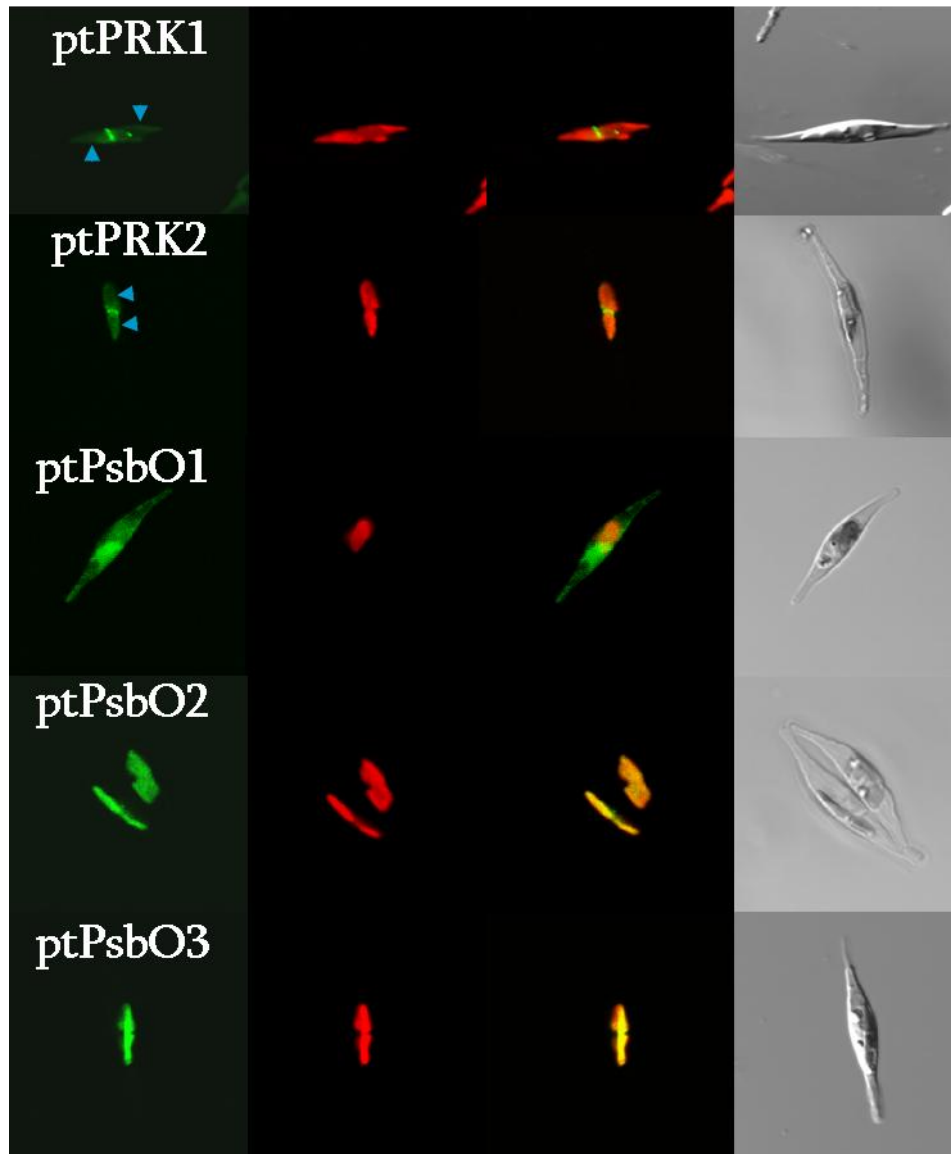


**Figure 28.** Heterologous Transfection of *Phaeodactylum tricornerutum* with eGFP fused to Full-length and Truncated *A. carterae* Targeting Signals. **ptPsbO1:** ER localization. **ptPsbO2:** plastid localization; **ptPrk1:** PPC/plastid localization; **ptPsbO3:** plastid eGFP localization. **ptPrk2:** PPC/plastid eGFP localization; **Blue arrows** indicate GFP signal colocalizing with the plastid autofluorescence. **From left to right:** eGFP fluorescence, plastid autofluorescence, merge, DIC. **Green:** eGFP fluorescence, **Red:** Autofluorescence.

Truncation experiments were performed to determine whether charge segregation plays a role in heterologous targeting in diatoms. Like ptPsbO2, ptPsbO3 was capable of fully mediating transport to the stroma of the diatom plastid. Correspondingly truncated Prk construct resulted in strong PPC localization of eGFP and a partial stromal localization of eGFP in *P. tricornerutum* similar to that from ptPrk1.



### 3.4 Tracking Homologous Protein Targeting in *Amphidinium Carterae*

One of the main focuses of this thesis was to establish and execute a method for tracking protein transport in dinoflagellates. This involved radioactively labeled proteins and determining location of individual proteins within the cell. To this end, radioactive labeling of *Amphidinium carterae* protein was of paramount importance.

To this end, an empiric evaluation of conditions for ideal uptake of  $^{35}\text{S}$ -labeling of *Amphidinium carterae* was undertaken. A paucity of sulfur in a minimal medium was ascertained not to ameliorate the uptake of  $^{35}\text{S}$ -sulfate,  $^{35}\text{S}$ -methionine, and  $^{35}\text{S}$ -Metmix and only served to decelerate growth and hamper uptake, which was measured according to section 6.3.5. In every case, cells were consistently able to uptake  $^{35}\text{S}$ -methionine and incorporate the amino acid into proteins. Uptake was highly dependent on the age of the culture, and it was determined that maximal incorporation of radioactivity occurred after six and a half days of growth after 1:5 inoculation with a full-grown culture.

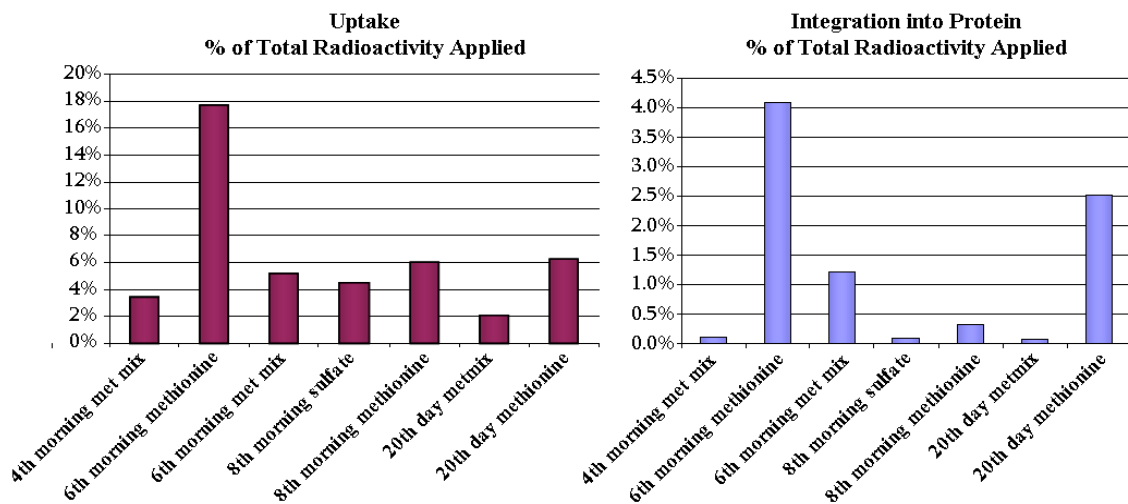


**Figure 29. Empirical Evaluation of Maximal  $^{35}\text{S}$ -Uptake and Incorporation into *Amphidinium carterae* Protein.** Varying compounds and culturing times were used to achieve maximum incorporation of  $^{35}\text{S}$  into the *A. carterae* protein, which was highly dependent on the length of culture growth and  $^{35}\text{S}$ -compound used. **Red:** *A. carterae* cells were only able to uptake 2% to 18% of  $^{35}\text{S}$ -compounds available in the culture medium. **Lilac:** 0.1 to 4.1% of  $^{35}\text{S}$  compounds applied to each culture were incorporated into proteins.

#### 3.4.1 Sucrose Fractionation of *Amphidinium Carterae*

The detection of plastid protein transport to the plastid necessitated the ability to fractionate *A. carterae* cells. A number of different cell fractionations were attempted with differing sucrose gradients, which differed in sucrose percentages and buffering systems (see section 6.3.3). Based on previous publications for organisms ranging from algae to plants to mammalian cells (Cramm-Behrens et al. 2008; Murata et al. 1979; Slavikova et al. 2005; Wagner and Hrazdina 1984; Zerges and Rochaix 1998), a sucrose gradient suitable for *A. carterae* was empirically determined. Culture conditions, harvesting of cells, <sup>35</sup>S-labeling, cell lysis, and sucrose fractionation were performed as noted in sections 6.3.1 to 6.3.3.

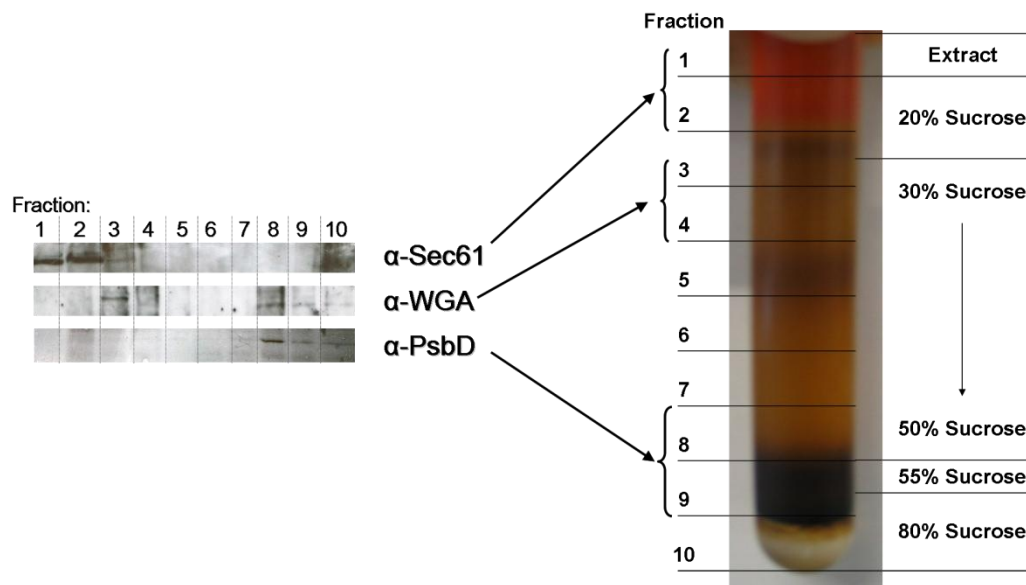


**Figure 30. Sucrose Gradient and Fraction Compartment/Organelle Detection of Fractionated *Amphidinium carterae* cells.** Left: Western blots of TCA precipitated fractions from a sucrose gradient. Right: Photograph of a sucrose gradient from *A. carterae* with sucrose concentrations.

In order to determine which sucrose gradient fraction corresponds to which compartment or organelle in the cell, proteins from each gradient fraction were precipitated, separated by SDS-polyacrylamide gel electrophoresis, and Western blotted according to sections 6.3.6. Antibodies for the alpha subunit of the mammalian Sec61 were effective in identifying the ER in sucrose gradients at the threshold between the 20% and 25% steps of semi-discontinuous sucrose gradients. The lectin Wheat Germ Agglutin (WGA) was used to detect the Golgi apparatus in gradient fractions. The photosystem II component PsbD was chosen to serve as a plastid marker in Western blot analyses.

These antibodies were tested via Western blot analysis of sucrose gradient fractions according to section 6.3.7. As seen in figure 30, protein from sucrose gradient fractions resulted in  $\alpha$ -Sec61 signals arising mainly in sucrose fractions 1 to 3 corresponding to 20% - 25% sucrose. WGA signals arising in fractions 3 to 6, and plastid-specific signals arising in fractions 8 to 10. WGA signal also arose in fraction 8, thus colocalizing with plastid-specific  $\alpha$ -PsbD signal.

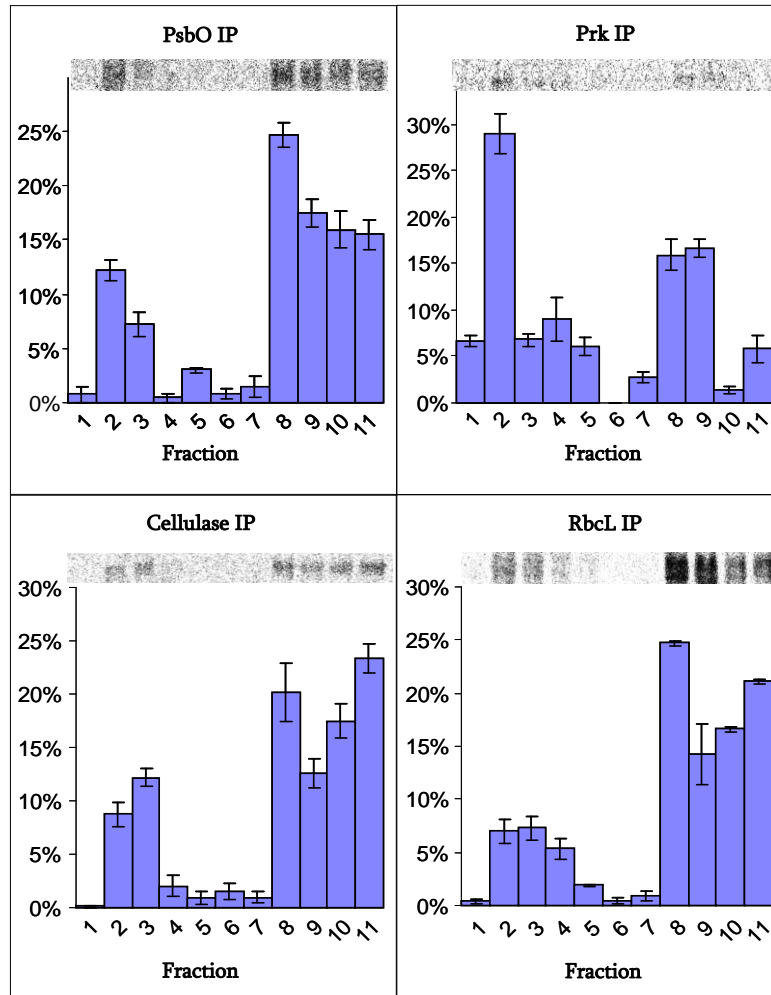


**Figure 31. ImageJ Quantification of Western Blot Relative Autoradiogram Signal Intensities of  $^{35}\text{S}$ -Labelled Immunoprecipitated Proteins from Sucrose Gradient Fractionation of *Amphidinium carterae*.** IPs from TCA precipitated fractionations from sucrose gradient were blotted 3 times for 3 quantifications with 50, 100, and 200  $\mu\text{m}$  StormJet scanner resolution settings. Percentages are a proportion of the total signal detected in the autoradiogram. Error bars indicate standard deviation. Fraction 11 originates from pelleting cell debris and intact cells before loading the sucrose gradient.

Using specific antibodies, it was possible to perform immunoprecipitation (IP) to obtain and quantify radioactively labeled proteins from sucrose gradients. IP was employed

to track the transport of plastid proteins RbcL, Prk, and PsbO which were representative of class I, II, and III proteins, respectively. Results from the initial test of protein localization in cells not treated with a vesicle inhibitor are summarized in figures 31 and 32.

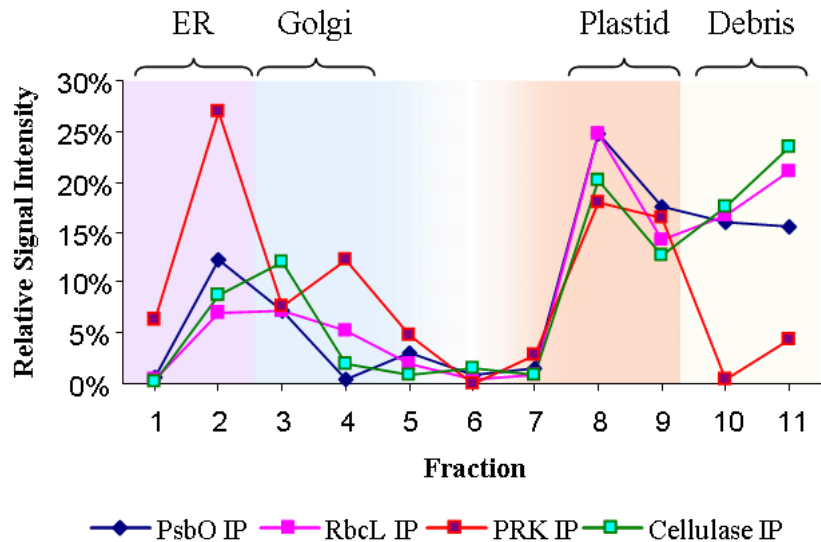


**Figure 32. Relative Autoradiogram Signal Intensities from Immunoprecipitated Proteins from <sup>35</sup>S-Labeled *Amphidinium carterae* Cells (BFA Untreated).** Graphic depiction of autoradiograph signals quantified with ImageJ, as for figure 31. Little to no signal was located in the Golgi fractions (5-6), the plastid fractions (8-9), or the cell debris (10-11). A significant level of Prk signal originated from the ER fractions (2-3).

Signals from <sup>35</sup>S-labeled Cellulase were strongest in fractions 10 and 11, which corresponded to the visible cell debris pellet at the bottom of the ultracentrifuge tube and left over from cell lysis, respectively. The majority of autoradiogram signals from plastid-localized proteins were present in the plastid fractions (8-9). The second most prevalent cellular location for autoradiogram signals from plastid-localized proteins come from intact cell fractions 10 and 11, which can most probably be attributed to incomplete cell lysis. Together, the plastid fractions constituted 44% of signals arising from PsbO IPs, 37% of Prk IP signals, and 40% of RbcL signals. 15-20% of total signal originated from the ER and Golgi fractions, except for Prk IP signal, which was present to a significant extent (~27%) in the ER and Golgi.

### 3.4.2 Effects of Brefeldin A on Protein Mobility in Sucrose Gradient Fractionations of *Amphidinium Carterae*

After verifying the viability of tracking protein transport in *A. carterae* cells, Brefeldin A was employed to interrupt vesicle flow to *A. carterae* plastids. An empiric determination of a BFA concentration was necessary to ascertain the lethal dosage. The initial concentration of 7.5  $\mu\text{g}$  BFA/mL was determined to be viable based on the retention of the secondary metabolic characteristic of motility in approximately 50% of treated cells. At this concentration, more than half of the cells were still visibly motile, whereas higher concentrations led to cell death.

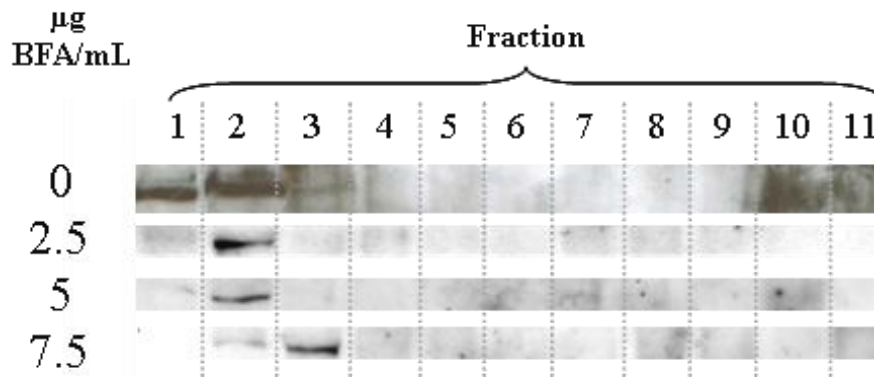


**Figure 33. Effect of Brefeldin A on the Location of ER in Sucrose Gradients.**  $\alpha$ -Sec61 signals shifted from fraction 1 and 2 in untreated cells to fraction 2 in cells treated with 2.5  $\mu\text{g}$  and 5  $\mu\text{g}$  BFA per mL.  $\alpha$ -Sec61 signals shifted to fraction 3 in cells treated with 7.5  $\mu\text{g}$  BFA/mL.

Because BFA in essence leads to a fusion of ER and Golgi apparatus, it was necessary to ascertain if a shift between Golgi and ER density had occurred as a result of BFA treatment. To this end, Western blots from fractionated cells treated with BFA were compared with the signal from untreated cells. As seen in figure 33,  $\alpha$ -Sec61 signals shifted from fraction 1 and 2 in untreated cells shifted to fraction 2 with 2.5  $\mu\text{g}$  and 5  $\mu\text{g}$  BFA per mL and to fraction 3 in cells treated with 7.5  $\mu\text{g}$  BFA/mL. As seen in figure 34, the localization of the Golgi apparatus in the third fraction of the sucrose gradient was not dependent on BFA concentration. At the highest BFA concentration,  $\alpha$ -Sec61 and  $\alpha$ -WGA signals overlapped in fraction 3.

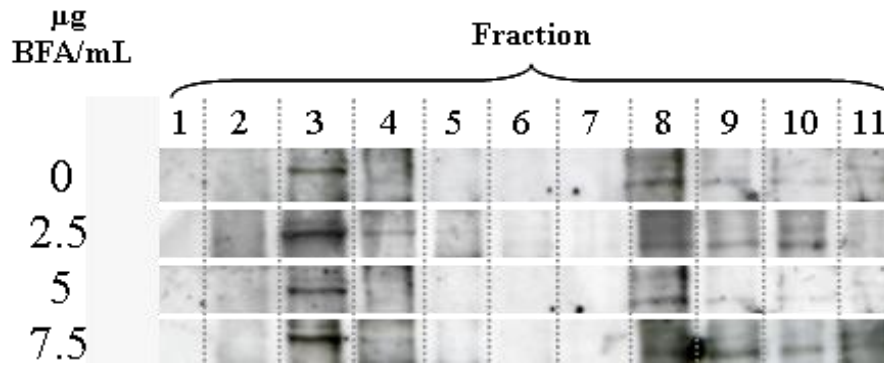


**Figure 34. Effect of Brefeldin A on the Location of Golgi Apparatus in Sucrose Gradients.** BFA had the effect that WGA signals from fraction 3 and 4 remained unchanged with and without BFA.

Radioactive labeling and BFA inhibition experiments were first executed using 7.5 µg BFA/mL. 50 – 90 % of autoradiograph signals from plastid proteins were observed in the ER and Golgi fractions at this concentration. Baseline IP signals were observed to have originated from the plastid-containing fractions and cell debris fractions. In addition to plastid proteins, Cellulase was also inhibited by the BFA treatment, as seen by the ER localization displayed in figure 35.

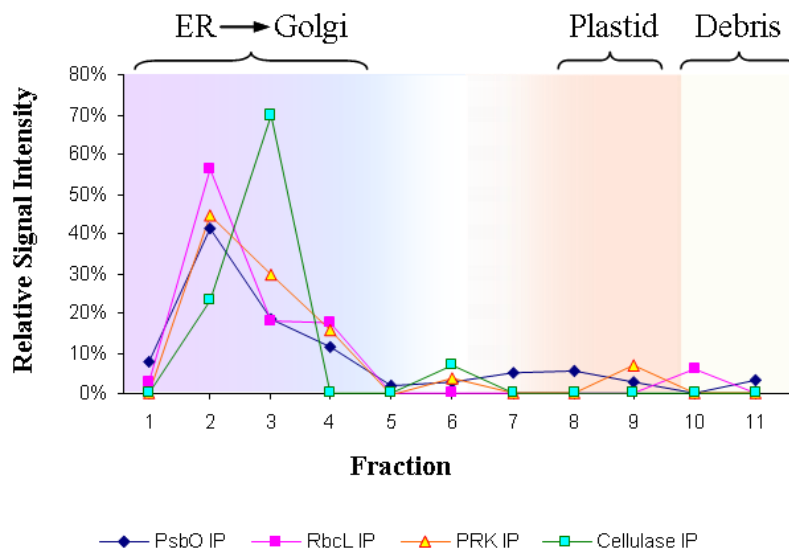


**Figure 35. Relative Autoradiogram Signal Intensities from Immunoprecipitated Proteins from <sup>35</sup>S-Labeled *Amphidinium carterae* Cells treated with 7.5 µg BFA/mL.** Signals were quantified with ImageJ as above. Little to no signal is located in the Golgi fractions (5-6), the plastid fractions (8-9), or the cell debris (10-11), because proteins are virtually exclusive to the ER fractions (2-3).

## Results

In comparison to the 7.5  $\mu\text{g}/\text{mL}$  treatment of *A. carterae*, a concentration of 5  $\mu\text{g}$  BFA/mL subsequently resulted in a marked difference. Except for RbcL, virtually all autoradiograph signals from examined proteins were located in the endomembrane fractions. In contrast to signals from 7.5  $\mu\text{g}$  BFA/mL inhibition, approximately 50% of RbcL autoradiograph signals were localized in the plastid and unlysed cell fractions (8-11). The rest of RbcL signal arose from the endomembrane fractions. The secretory system was also observed to have been inhibited at this BFA concentration, as seen by the ER fraction localization of Cellulase autoradiograph signal.

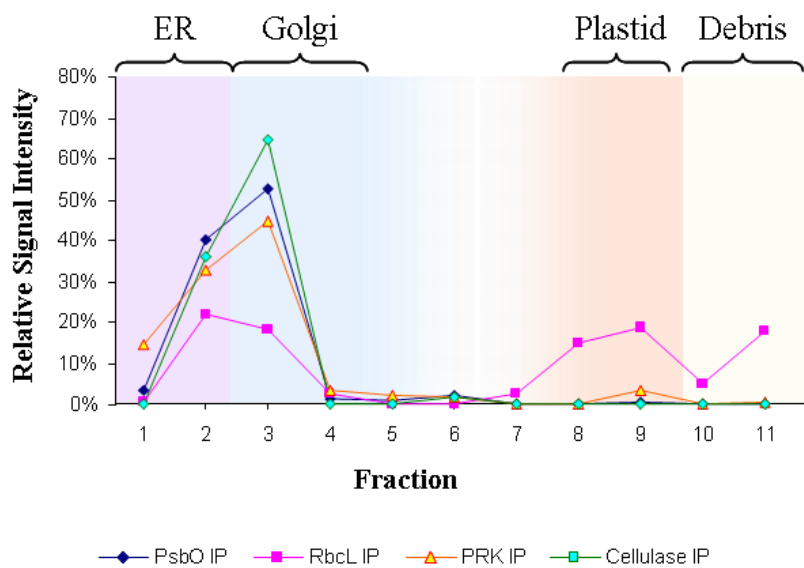


**Figure 36. Relative Autoradiogram Signal Intensities from Immunoprecipitated Proteins from  $^{35}\text{S}$ -Labeled *Amphidinium carterae* Cells treated with 5  $\mu\text{g}$  BFA/mL.** Signals were quantified with ImageJ as above. Little to no signal is located in the Golgi fractions (5-6), the plastid fractions (8-9), or the cell debris (10-11), because proteins are virtually exclusive to the ER fractions (2-3). The exception to this is displayed by RbcL, which apparently was partially transported to the plastid at this BFA concentration.

A comparative increase in RbcL transport, i.e. increase in autoradiogram signal from the plastid fractions, was observed in cells treated with 2.5  $\mu\text{g}$  BFA/mL. In comparison to the 7.5  $\mu\text{g}$  BFA/mL and 5  $\mu\text{g}$  BFA/mL treatments of *A. carterae*, a substantial shift in RbcL localization took place. 92% of RbcL signal arose in from the plastid fractions in this experiment. In contrast, 50-70% of autoradiograph signals from other examined proteins were located in the endomembrane fractions. Like at 5 $\mu\text{g}$  BFA/mL, RbcL was once again the sole protein to have been transported to any substantial degree to the plastids.

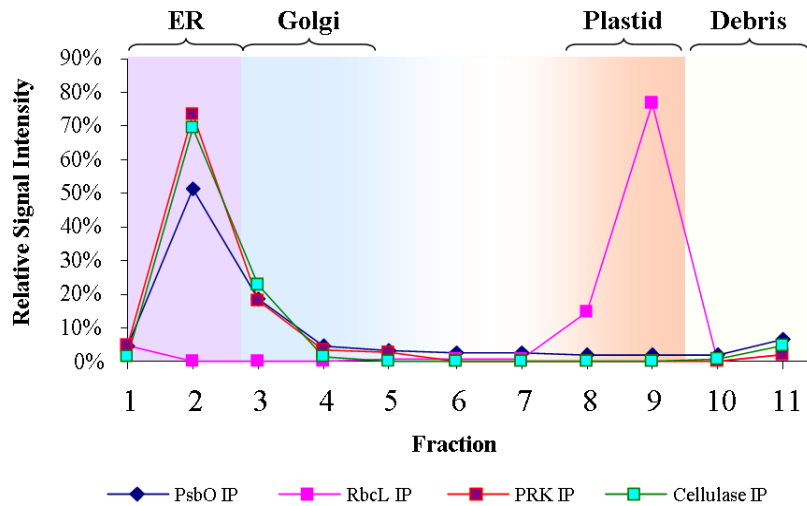


**Figure 37. Relative Autoradiogram Signal Intensities from Immunoprecipitated Proteins from <sup>35</sup>S-Labeled *Amphidinium carterae* Cells treated with 2.5  $\mu$ g BFA/mL.** Signals were quantified with ImageJ as above. Little to no signal is located in the Golgi fractions (5-6), the plastid fractions (8-9), or the cell debris (10-11), because proteins are virtually exclusive to the ER fractions (2-3). The exception to this is displayed by RbcL, which apparently can be normally transported at these BFA concentrations.

To summarize, the homologous transport of <sup>35</sup>S-labeled plastid-destined proteins in *Amphidinium carterae* is completely inhibited by the effects of Brefeldin A at a concentration above 5  $\mu$ g BFA/mL. Effects of BFA did not diminish by lowering the concentration to below half of the lethal dosage, except in the case of Rubisco, for which transport is restored to about 50%. Although all other proteins continue to be inhibited by the 2.5  $\mu$ g BFA/mL, Rubisco transport is not inhibited at all and even shows an increase in plastid localization in comparison with untreated cells, as seen in figure 37.

### 3.4.3 Electron Microscopic Examination of the Effects of Brefeldin A on Protein Localization in *Amphidinium carterae*

Results from tracking subcellular protein localization with sucrose gradients were supplemented with electron microscopy. Freeze substitution was used to fix cells treated with 2.5  $\mu$ g BFA/mL and untreated cells for electron micrograph analysis, according to section 6.4.1. Comparative analysis of electron micrographs led to the conclusion that cells treated with BFA did not contain a discernable intact Golgi apparatus or ER. Instead, an increase in



centrally located vacuoles (labeled “6” in figure 38) was observed around the pyrenoid in BFA-treated cells.

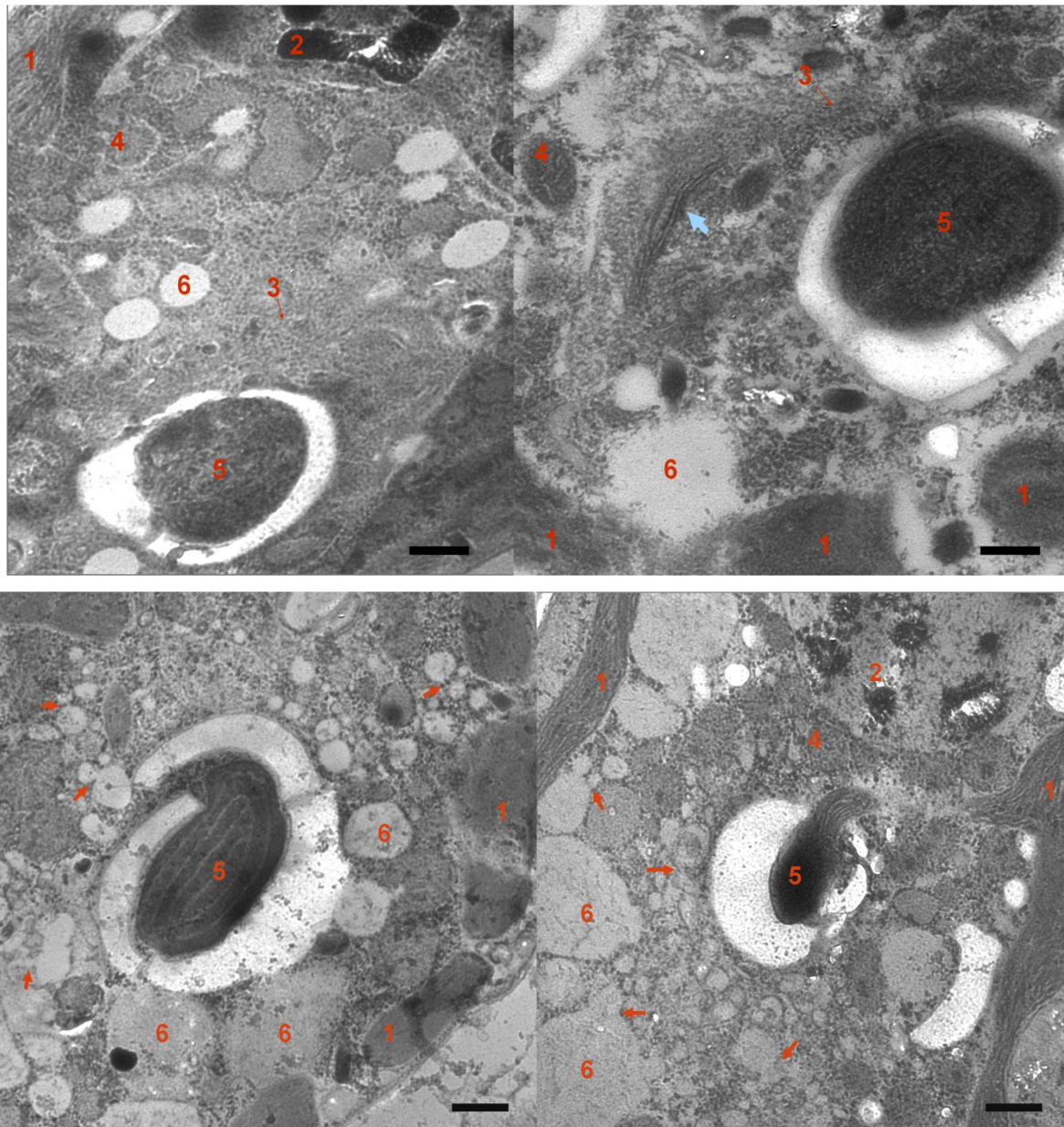


**Figure 38.** Osmium Tetraoxide Contrasted Electron Micrographs of *Amphidinium carterae* Cells (un)treated with 2.5 µg BFA/mL and Fixed via Freeze Substitution. Upper micrographs: Untreated cells. Lower micrographs: Cells treated with 2.5 µg BFA/mL. Blue arrow denotes the Golgi apparatus, 1: Plastid, 2: Cell nucleus containing condensed liquid crystalline chromosomes, 3: ER, 4: mitochondria, 5: pyrenoid, and 6: membrane-contained vacuole. Bold red arrows: Denote connections between vesicular protrusions of vacuolar system. Bar: 500 nm.

In BFA-untreated cells, internal membranous vacuoles were observed to be not nearly as prominent or as fragmented as in BFA-treated cells. In treated cells, the nuclear envelope

space was bloated in comparison to untreated cells (nucleus is “2” in figure 38). The perimeter of the pyrenoid in BFA-treated cells is veritably littered with interconnected vesicular protrusions of the endomembrane system. Markedly more material was located in the endomembrane system of BFA-treated cells than of untreated cells. Furthermore, no Golgi apparatuses were observed in BFA-treated cells. Although no visible effect resulting from BFA treatment was observed in the cells’ pyrenoids, thylakoid stacks within plastids are more interspersed and not as uniformly distributed in the plastid in comparison to untreated cells. Mitochondria were present in comparable number in treated and untreated cells. The pyrenoid and the starch sheath were entirely intact in treated as well as untreated cells.

### **3.4.3.1 Immunogold Labeling with $\alpha$ -PsbO in *Amphidinium carterae* Cells Treated with Brefeldin A**

As seen in figure 37, 2.5  $\mu\text{g}/\text{mL}$  BFA treatment led to an inhibition of PsbO transport to the plastid and a localization in the endomembrane system. Immunogold labeling of  $\alpha$ -PsbO in correspondingly 2.5  $\mu\text{g}$  BFA/mL-treated and untreated cells was performed according to section 6.4.2. Ca. 50 immunogold signals were used for statistical analysis of protein localization caused by BFA treatment. Immunogold labeling with the  $\alpha$ -PsbO antibody in untreated cells resulted in 80% of signals being located in the plastids. Immunogold labels that were not located in the plastids were located either directly next to the plastid or proximal to an endomembrane in untreated cells. Immunogold labeling with the  $\alpha$ -PsbO antibody in BFA-treated cells resulted in 74% of signals being located at the periphery of the bloated endomembrane vacuoles. No signals were located in the interior of the endomembrane vesicles/vacuoles, and 26% of signals were located in thylakoids in BFA-treated cells.

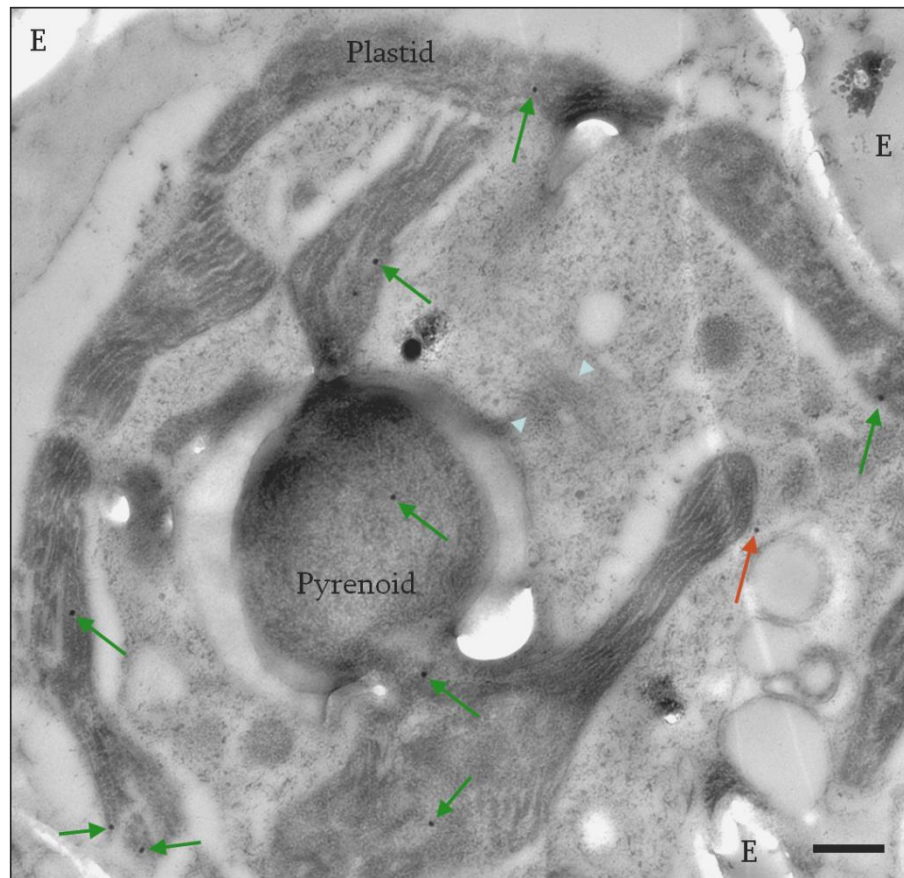


**Figure 39.**  $\alpha$ -PsbO Immunogold Labeling of *Amphidinium carterae* Untreated Cells and Fixed via Freeze Substitution. Green Arrows indicate signal arising from plastids. Red Arrow indicates signal arising from the endomembrane system. Blue arrows denote the Golgi apparatus. E: Exterior of cell. Bar: 500 nm.



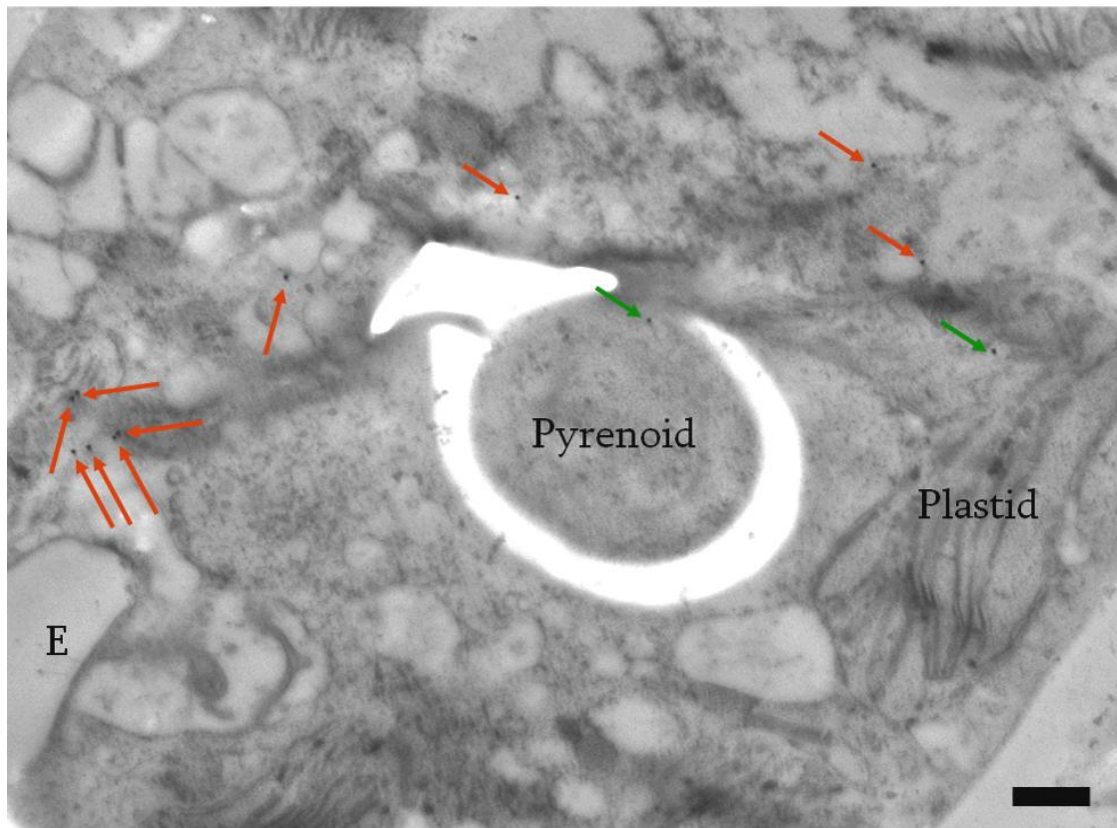


**Figure 40.**  $\alpha$ -PsbO Immunogold Labeling of *Amphidinium carterae* Cells Treated with 2.5  $\mu$ g BFA/mL and Fixed via Freeze Substitution. Green Arrows indicate signal arising from the periphery of fused endomembrane system. Red Arrows:  $\alpha$ -PsbO signals proximal to the membranes of the endomembrane system. A large amount of protein was present in vacuoles in comparison to figure 39. E: Exterior of cell. Bar: 500 nm.

### 3.4.3.2 Immunogold Labeling with $\alpha$ -RbcL in *Amphidinium carterae* Cells Treated with Brefeldin A

As seen in figure 37, 2.5  $\mu$ g/mL BFA treatment did not lead to an inhibition of RbcL transport to the plastid, as RbcL autoradiograph signals mainly originated from plastid fractions. Immunogold labeling of  $\alpha$ -RbcL in correspondingly 2.5  $\mu$ g BFA/mL-treated and untreated cells was performed according to section 6.4.2. Immunogold labeling with the  $\alpha$ -RbcL antibody in untreated cells resulted in 79% of signals being located in the plastids. Signals that were not located in the plastids were located in the endomembrane system. Immunogold labeling with the  $\alpha$ -RbcL antibody in BFA-treated cells resulted in 84% of signals being located in the plastids.

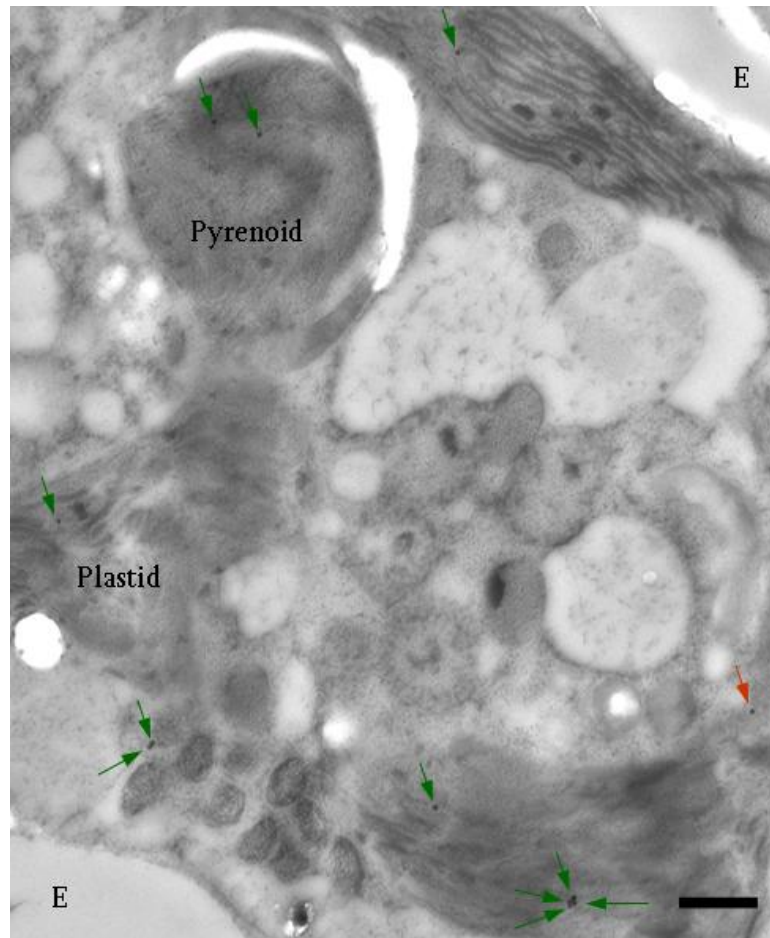


**Figure 41.**  $\alpha$ -RbcL Immunogold Labeling of Untreated *Amphidinium carterae* Fixed via Freeze Substitution. Green Arrows indicate signal arising from the endomembrane system membranes. Red Arrow:  $\alpha$ -RbcL signals proximal to the membranes of the endomembrane system. E: Exterior of cell. Bar: 500 nm.

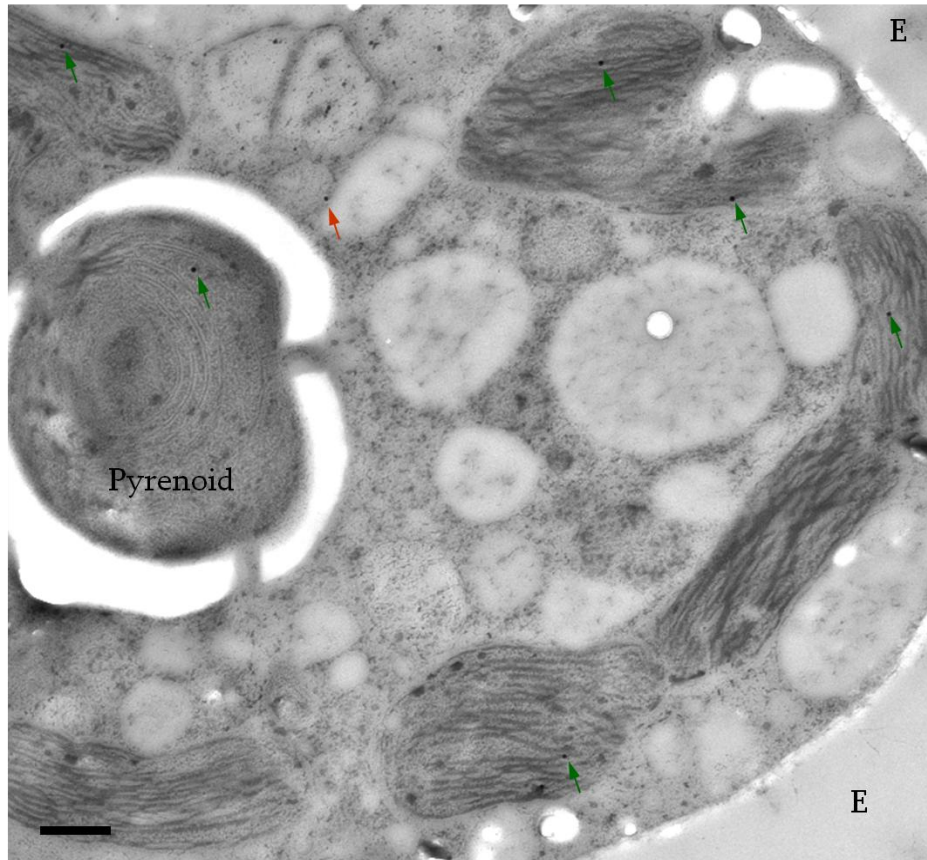


**Figure 42.**  $\alpha$ -RbcL Immunogold Labeling of *Amphidinium carterae* Cells Treated with 2.5  $\mu$ g BFA/mL and Fixed via Freeze Substitution. **Green Arrows:** indicate signal arising from the periphery of fused endomembrane system. **Red Arrow:**  $\alpha$ -RbcL signal proximal to the membranes of the endomembrane system. **E:** Exterior of cell. **Bar:** 500 nm.

## 4 DISCUSSION

### 4.1 *Ceratium horridum* EST Library

Comparative analyses resulted in the identification of *C. horridum* plastid proteins and topogenic signals. From these analyses, new insights were gained about general features of dinoflagellate targeting signals, which were tested in heterologous and homologous systems *in vivo*.

#### 4.1.1 General Features

EST data from *Ceratium horridum* corresponded to general parameters established for other published dinoflagellate EST libraries, such as G+C content, prominent constituents, genes transfers from non-dinoflagellates were present, and roughly half of homologies were dinoflagellate hits (Bachvaroff et al. 2004; Joseph et al. 2010; Kwok and Wong 2010; Tanikawa et al. 2004; Uribe et al. 2008). The ratio of ESTs to unigenes (55%) is higher than that reported for other dinoflagellate EST libraries. Similar to other EST libraries, genes encoding plastid-targeted products were the third largest constituent represented in the data set (13%), which showed little variety (4% of unigenes). Considering the fact that these proteins contribute to the cell's main source of energy, fatty acids, and carbon, this percentile is low.

*C. horridum* homologies differ slightly from a recently published *Perkinsus marinus* EST library, in which BLAST hits originated mainly from dinoflagellates, followed by stramenopiles, viridiplantae and other alveolates (Joseph et al. 2010; Toulza et al. 2010). *C. horridum* EST homologies however differed greatly from those of a recent dinoflagellate EST library from *Alexandrium catenella*, in which EST homologies were disproportionately bacterial hits in comparison to *C. horridum* and other dinoflagellates. Without the use of tBLASTX, 62% of *C. horridum* EST homologies would not have been identified, which was similar to the value for the *P. marinus* EST library (Joseph et al. 2010).

The lack of BLAST homologies for about half of *C. horridum* ESTs is quite commonplace among dinoflagellate EST libraries (Joseph et al. 2010; Kwok and Wong 2010; Toulza et al. 2010). Nonetheless, it is noteworthy that – unlike those from any other dinoflagellate – the second-most prominent gene cluster in this EST library was a protein of unknown function.

The lack of homologies obtained from dinoflagellate EST libraries can be attributed to the fact that many dinoflagellate proteins are simply not present in other clades with annotated genomes, as dinoflagellates are known to have unique morphological and biochemical traits that set them apart from all other organisms, including other alveolates (Kellmann et al. 2010; Kita et al. 2010; Kobayashi and Kubota 2007; Lukes et al. 2009). Of the *C. horridum* unigenes encoding proteins of unknown function, gene products were identified with a plastid localization. Analysis of proteins encoded by *C. horridum* ESTs resulted in the identification of gene transfers and of topogenic signals in proteins of unknown function as well as proteins with known plastid functions.

### 4.1.2 Gene Transfers

Whereas endosymbiotic gene transfers (EGTs) like those from the dinoflagellate plastid genome to the host genome are fairly common occurrences in eukaryotes, gene transfers from sources other than endosymbionts have yet to be actively investigated (Richardson and Palmer 2007). Such horizontal gene transfers (HGTs), i.e. transfers of genetic material between unrelated species, are much less prevalent than EGTs and typically account for only <1% of nuclear genes from eukaryotes in which such genes are identified (Andersson, 2005).

It is thus not unprecedented that 2 of 922 *C. horridum* unigenes identified by phylogenetic analyses arose from organisms outside the red lineage. Like Prk sequences from chromists and alveolates that originated from the green lineage (Petersen et al. 2006), robust bootstrap and posterior Bayesian position values support *gt57c03* and *gt62\_f11* as having been transferred from the green lineage. Based on the present understanding of the evolution of chromalveolates, the sources for these green lineage genes in *C. horridum* could be either 1) an HGT from an unrelated green plant/algae or 2) an EGT from a green algal



endosymbiont that preceded the present red one, as previously suggested (Elias and Archibald 2009). The latter posit implicates green lineage genes as having been present in alveolates since before the acquisition of their red lineage plastid. This would entail the elimination of the majority of green lineage genes from the host's nuclear genome and their replacement with red algal homologs. This posit is bolstered by the presence of numerous green lineage genes in the genomes of chromists and alveolates (Archibald 2009; Elias and Archibald 2009; Huang et al. 2004; Keeling and Palmer 2008; Moustafa et al. 2009; Nosenko and Bhattacharya 2007; Stelter et al. 2007).

From the data at hand, it cannot be definitively determined whether *gt57c03* (encoding AMP-activated protein kinase) and *gt62\_f11* (encoding UDP-glucose dehydrogenase) are HGTs from the green lineage or whether they arose from a more ancient EGT from a former green endosymbiont. It has however been suggested based on whole-genome phylogenetics of *Phaeodactylum tricornutum* and *Thalassiosira pseudonana* that at least diatoms may have originally contained a green endosymbiont prior to their present red algal endosymbiont (Moustafa et al. 2009). Furthermore, phylogenetic and biochemical analyses indicate that apicomplexans contain genes of green lineage origins, despite the presence of their current red algal endosymbiont (Funes et al. 2002; Harper et al. 2009; Janouskovec et al. 2010; Stelter et al. 2007). In light of these indications that a green endosymbiont preceded the present red one in other chromalveolates, it is probably more likely that the acquisition of these green lineage genes in *C. horridum* was the result of an EGT than an HGT.

Acquisitions of proteins like *Gt57c03* and *Gt62\_f11* often entail combining phylogenetically unrelated proteins in a single pathway (Elias and Archibald 2009). It is unknown what factors play a role in the acquisition, modification, and elimination of genes in dinoflagellate genomes (Lukes et al. 2009), so the factors involved in the selection for or against either a host gene or a transferred gene after HGT or EGT are likewise unknown. Hence, hypotheses as to which genes are retained in the dinoflagellate genome are effectively speculative. That being said, it can be inferred that the widespread occurrence of gene product hodgepodes from different lineages that interact with each other in identical cellular compartments (Elias and Archibald 2009) are an indication either that constructive neutral and/or concerted evolution is taking place (Lukes et al. 2009; Reichman et al. 2003) or that there is indeed a selective advantage to utilizing proteins from gene transfers. Any number of

factors may influence evolutionary selection of genes, including protein architecture for protein-protein interaction, biochemical rate-limiting steps influencing positive/negative feedback loops, substrate binding coefficients, and the possible presence of moieties for biochemical modifications serving in post-translational protein regulation. Only the cross-species comparison of specific pathways involving HGT and EGT proteins and the biochemical characterization thereof will shed light on this issue, such as those already performed for Prk (Maberly et al. 2009).

### 4.1.3 Plastid Targeting Signals

Topogenic signals encoded by *Ceratium horridum* ESTs conform to general trends of topogenic signals for organisms containing complex plastids and contain dinoflagellate-specific motifs (Patron et al. 2005). BTSs from *C. horridum* plastid proteins share some characteristics with related organisms. The AXA motif indicative of the signal peptide peptidase cleavage site in stramenopiles (Kilian and Kroth 2005) is indicated by the weblogo in figure 16. Despite this, it is present only in very few dinoflagellate presequences, as shown exemplarily in figure 43. Alanines are some of the most prevalent amino acids in dinoflagellate signal and transit peptides (see figure 14 and 16 as well as table 4), thus the AXA motif may simply be the result of alanine's prevalence in the three amino acid positions preceding the predicted signal peptide cleave site.

Close to the cleavage site predicted by SignalP, the majority of *C. horridum* signal and transit peptides are demarcated by an A<sup>F</sup> motif, like in most other red algae with secondary endosymbionts. Like other dinoflagellates, this phenylalanine is commonly located in the context of a motif that bears similarity to the FAP motif found in chromists (Patron et al. 2005). Unlike chromists, the dinoflagellate FVAP motif is usually not at the position +1 of the TP predicted by SignalP, and was found in only a third of TPs to be located within three amino acids of the signal peptide peptidase site, as seen in figure 43.

Unlike the FAP motif in chromist TPs, the FVAP motif is infrequently located directly at the N-terminus of dinoflagellate TPs (in 26% of TPs). Thus, the cleavage site predicted by SignalP might only roughly correlate to the actual signal peptidase cleavage site in dinoflagellates. If this were the case, then these FVAP motifs may indeed be conserved at the transition between signal and transit peptides of dinoflagellate BTSs. If SignalP however

is correctly predicting the cleavage site, then the positioning of the motif may have a degree of flexibility relative to the N-terminus of the TP.

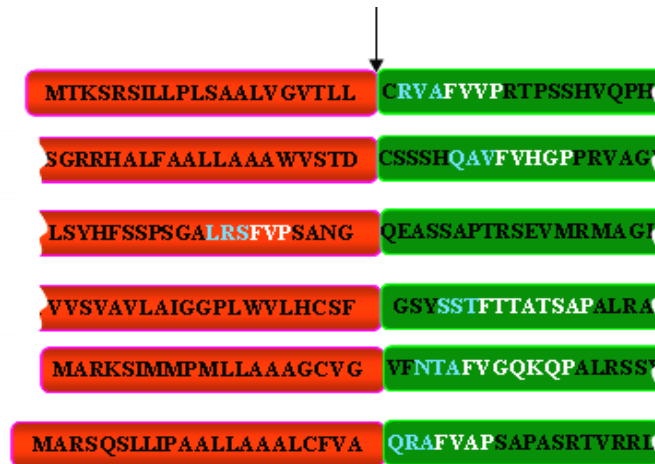


**Figure 43. Signal Peptide Peptidase Cleavage Site in Dinoflagellate BTS as per SignalP.**  
**Arrow:** signal peptide peptidase cleavage site as per SignalP, **Red:** Signal Peptide, **Green:** TP, **White:** FVAP motif, **Blue:** last three amino acids of signal peptide, if FVAP motif marks the actual peptidase cleavage site.

Analysis of *C. horridum* ESTs supports the conclusion that dinoflagellate TPs generally have a positively charged N-terminus and a negatively charged C-terminus. In prior examinations of dinoflagellate TP compositions, this trend has gone unnoticed, possibly due to a relatively small data set (Patron and Waller 2007). In the present study, sampling was broadened to include over three times as many sequences from a broader range of dinoflagellates. The overall picture of dinoflagellate TP composition then differs from published results. Most dinoflagellate TPs are more negatively charged than described in Patron and Waller 2007. Furthermore, the net charge of dinoflagellate TPs is also lower in comparison with TPs from many other chromists and alveolates, which may indicate a difference in the interaction between dinoflagellate TPs and their homologous protein transport machinery.

The posttranslational orientation of proteins in the ER membrane, in plastid-destined vesicles, and in the outermost plastid membrane after vesicle fusion was determined based on whether TPs contained putative membrane-spanning domains. In such hydrophobicity-based predictions, orientations of class I proteins like RbcL differed from class II proteins like Prk, whereas class I proteins and class III proteins like PsbO were extremely similar in their predicted orientations. Thus, class III proteins like PsbO were determined to have

hydrophobicity profiles indicative of a previously undescribed membrane-spanning domain located in the thylakoid targeting domain (TTD). Such hydrophobic membrane-spanning domains located in the TPs of plastid-targeted proteins are thought to be stop-transfer domains (STDs) (Nassoury et al. 2003; Slavikova et al. 2005; van Dooren et al. 2001). Based on the orientation of class I and III preproteins in membranes during transport to the plastid, the mature coding sequence of such preproteins has a cytosolic location during and after transport to the plastid surface. Contrary to published results on dinoflagellate and *Euglena gracilis* TPs (Durnford and Gray 2006), *C. horridum* does not have a high level of plastid-destined TPs containing STDs.

*C. horridum* transit peptides were found to contain a slight degree of charge separation, as shown in figure 19. Upon comparison of dinoflagellate TPs with those of diatoms and plants, this feature was found to be most prominent in dinoflagellate sequences and only present to a lesser degree in diatoms and plants. Besides STDs and charge separation, there is a notably higher level of hydroxylated amino acids in land plants and diatoms than in dinoflagellate TPs.

In respect to TP hydroxylated amino acid content, *C. horridum* is very comparable to *E. gracilis* and nucleus-encoded *Guillardia theta* TPs (Durnford and Gray 2006; Patron and Waller 2007; Ralph et al. 2004) yet very different from the published value for dinoflagellates and apicomplexans (Patron and Waller 2007; Ralph et al. 2004) and identical to the value for the dinoflagellate value found in this study, as seen in table 6.

Source	Land Plant	<i>Euglena gracilis</i>	Diatom	<i>Guillardia theta</i> , nuclear	<i>Guillardia theta</i> , nucleomorph	<i>Ceratium horridum</i>	Dinoflagellate	Apicomplexa
This study	24%	-	29%	-	-	19%	19%	-
Patron & Waller 2007	26%	20%	28%	-	-	-	15%	12%
Ralph et al. 2004	28%	-	-	21%	10%	-	-	14%

**Table 6. Hydroxylated Amino Acids Content of Plastid Transit Peptides in Various Organisms.**

The lack of hydroxylated amino acids in dinoflagellate transit peptides may potentially indicate that they are fundamentally different from plant TPs, in which hydroxylated residues are necessary for efficient translocation into plant chloroplasts (Soll

and Schleiff 2004). Hydroxylated amino acids seem to be replaced by non-polar neutral residues in dinoflagellates, which may reflect the occurrence of STDs in class I and III dinoflagellate TPs. In comparison to plants, organisms containing complex plastids do not need to phosphorylate hydroxylated residues in order to discriminate plastid TPs from mitochondrial TPs (Ralph et al. 2004), possibly because transport to complex plastids is mediated by the endomembrane system where mitochondrial TPs are not present (Waller et al. 2000). Diatoms curiously pose the exception to this line of logic, as they have a level of hydroxylated residues in their TPs that is comparable to plant TPs.

Apicoplast TPs from the genus *Plasmodium* on the other hand have a much lower relative serine/threonine content (ca. 9.5%) than dinoflagellate TPs (Ralph et al. 2004). All other discussed non-plant organisms have at least twice this level in nuclear-encoded TPs, so the content of hydroxylated amino acids is diminished but not necessarily irrelevant in TPs for complex plastids. Therefore, in dinoflagellates and other non-plant organisms (except in *Plasmodium* species), the content of hydroxylated amino acids in TPs may still play a role in protein transport that is not necessarily identical to their role in plant TPs.

### **4.2 Heterologous *in vivo* Import Assays using Dinoflagellate Targeting Signals**

Heretofore, the overwhelming majority of hypotheses about dinoflagellate protein transport have actually been inferences from chromists and alveolates. To test insights obtained from extensive *in silico* analyses of dinoflagellate TPs, experiments were undertaken to confirm and append previous *in vitro* and *in situ* results. Because there is no transfection protocol for dinoflagellates as yet, *in vivo* heterologous transfection is the best method presently available for shedding light on further aspects of protein transport into plastids.

#### 4.2.1 *In vivo* transfection of *Pisum sativum* with *Amphidinium carterae* PsbO and Prk Transit Peptides

*In vivo* and *in vitro* import assays in plants heterologously transfected with transit peptides from organisms containing primary and secondary plastids have been performed previously to determine the viability of heterologous TPs. *In vivo* import assays using TPs from *Guillardia theta* preproteins encoded on the nucleomorph genome (originally the nucleus of a red alga with a primary endosymbiont) have been shown to be viable in *Arabidopsis thaliana* protoplasts (Hjorth et al. 2005). Moreover, a TP from the free-living red alga *Porphyra yezoensis* was also functional in *in vitro* import into isolated chloroplasts (Chaal and Green 2005). PsbO TPs from the euglenophyte *Euglena gracilis*, the dinoflagellate *Heterocapsa triquetra*, and the raphidophyte *Heterosigma akashiwo* have all been determined to be viable for *in vitro* import into isolated pea chloroplasts (Chaal and Green 2005; Inagaki et al. 2000). Furthermore, TPs from nucleus-encoded *Phaeodactylum tricornutum* and *G. theta* proteins were also shown to have mediated import into isolated pea chloroplasts *in vitro* (Lang et al. 1998; Wastl and Maier 2000). From these results, it was deduced that the translocation machineries of the plastid envelope may be analogous in all plastids examined in this fashion and that TPs are arguably so similar that they may mediate transport into most if not all photosynthetic plastids.

In order to supplement existing *in vitro* data, *in vivo* import studies were conducted using topogenic signals from dinoflagellates in *P. sativum* and *P. tricornutum*, which should provide a more accurate determination of whether dinoflagellate presequences can interact with a heterologous translocation machinery in its native milieu. Transfection of plants with chromist and dinoflagellate TPs were expected to be able to mediate import via the homologs of their own Omp85/TOC complexes (Bhattacharya et al. 2007; Bullmann et al. 2010).

The results depicted in figures 23 do not confirm this expectation, as neither PsbO nor Prk constructs allowed for eGFP colocalization with pea chloroplast autofluorescence. These *in vivo* results clearly differ from previous *in vitro* results. No tested variation of any *Amphidinium carterae* or *Ceratium horridum* TPs were able to mediate transport into pea chloroplasts *in vivo* (see figures 23 and appendix). For this reason, cryptophyte and diatom TPs were added as a positive control. These were also unable to confer eGFP with the

capacity for chloroplast import, thus demonstrating that previous results from *in vitro* import assays into isolated chloroplasts may not be accurate. This contradiction of *in vivo* and *in vitro* results has been addressed in homologous experiments in plants, which led to the conclusion that *in vitro* assays lack native cytosolic factors that confer import stringency (Schleiff et al. 2002).

Because chromalveolate transit peptides were not compatible with the plant translocation machinery, their TPs are seemingly clade-specific. This suggests that TPs do not have an intrinsic ability to mediate plastid import, which was previously inferred from heterologous *in vitro* import assays into isolated chloroplasts (Chaal and Green 2005; Inagaki et al. 2000; Lang et al. 1998).

### 4.2.2 Heterologous *in vivo* Transfections of *Phaeodactylum tricornutum*

Homologous bipartite signals from *P. tricornutum* can be used to target eGFP to four subcellular destinations that are readily recognized with CLSM and associated with plastid transport: the ER, the periplastidial compartment (PPC), the intermembrane space (IMS) between the 3<sup>rd</sup> and 4<sup>th</sup> outermost plastid membranes, and the stroma (Bullmann et al. 2010; Gruber et al. 2007). Heterologous BTSs from nuclear-encoded *G. theta* proteins have mediated transport to all of these destinations except the IMS plastid compartment (Gould et al. 2006b), thus demonstrating that BTSs of chromists can be similar enough as to be interchangeable. Like the BTSs of *P. tricornutum* and *G. theta*, *A. carterae* BTSs are divided into signal and transit peptides. The targeting capacity of dinoflagellate BTSs in *P. tricornutum* could have potentially been incompatible with the diatom's protein transport machinery not only due to differences discussed in section 4.1.3 but also because signals within the BTS could have contained information that was specific to the three-membraned dinoflagellate plastids and that could have interfered with transport across the diatom's four plastid membranes.

### 4.2.2.1 Heterologous *in vivo* Transfections of *Phaeodactylum tricornerutum* with *Amphidinium carterae* Signal Peptides

Although signal peptides (SPs) are often interchangeable in heterologous systems (Bhaya and Grossman 1991; Gould et al. 2006a; Howard and Schmidt 1995; Wastl and Maier 2000), a test of the viability of *A. carterae* PsbO and Prk SPs in *P. tricornerutum* was undertaken as a control for further experiments with BTSs. As seen in figure 25, PsbO and Prk signal peptides were found to be sufficient for transport into the ER.

Surprisingly, the SPs also were sufficient for transport into the diatom's PPC. From this, it can be inferred either that this was a byproduct of overexpression or that the SP was not cleaved from eGFP in the ER, in which case the SP mediated transport into the PPC. It can thus be argued that dinoflagellate SPs contain enough features of a TP as to allow for transport across the periplastidial membrane (PPM). Overexpression of the SP constructs could have inundated the ER with so much fusion protein that the PPC localization may be an artifact. If the SPs mitigated PPC import, then it may have done so merely by containing the minimal characteristics of a PPC TP, e.g. positive net charge and hydrophobicity. If this were to be the case, then it might indicate that the PPM-resident translocation machinery is not highly stringent.

### 4.2.2.2 Heterologous *in vivo* Transfections of *Phaeodactylum tricornerutum* with *Amphidinium carterae* BTSs

As seen in figures 27, PsbO BTSs were able to mediate transfer into the plastid stroma, whereas the Prk BTSs could only do so to a lesser degree. This implies that dinoflagellate plastid-targeting signals are, at most, only partially attenuated to the dinoflagellate transport machinery, although dinoflagellate presequences were previously suggested to be modified to accommodate their three-membraned plastids (Nassoury et al. 2003). Theoretically, this postulated attenuation could have resulted in difficulties in mediating transport into the four-membraned *P. tricornerutum* plastid with heterologous dinoflagellate topogenic signals. Based on the results shown here, this postulate is partially applicable: ptPsbO1 and both Prk constructs did not facilitate full plastid import. Nonetheless, like in transfections of *P. tricornerutum* using heterologous BTSs from the fellow



chromist *Guillardia theta* (Gould et al. 2006a; Gould et al. 2006b), dinoflagellate topogenic sequences were shown to function in the diatom.

The ER localization observed with ptPsbO1 indicates that the hydrophobic TTD of PsbO may very well act as an STD *in vivo*. Because STDs have yet to be reported in chromist TPs, the *P. tricornutum* translocation machinery could have been unable to transport the putatively membrane-integrated ptPsbO1 fusion protein. Without the hydrophobic domain, the PsbO presequence was able to mediate transport into the plastid stroma, so the fusion protein probably remained stuck in the ER membrane as a result of being integrated into the membrane via the STD. Although the TTD could be hindering transport in another unknown fashion, *in silico* predictions indicate that a membrane helix is present in the TTD, so the ER localization of ptPsbO1 and not of ptPsbO2 seen in figures 27 is the first good *in vivo* indication that dinoflagellate TTDs can also act as STDs. Inasmuch as the *A. carterae* ptPsbO1 presequence was not able to facilitate transport into the *P. tricornutum* plastid, the sequence seems to be attenuated to the dinoflagellate transport machinery. Due to the prevalence of STDs in dinoflagellate plastid-targeting signals (Durnford and Gray 2006; Patron et al. 2005), it can be deduced that the dinoflagellate protein transport machinery and not the heterologous diatom machinery has the capacity of dealing with STD-containing class I and III proteins.

In line with the discussion of PPC localization mediated by *A. carterae* SPs in section 4.2.2.1, one of the following conclusions may be applicable in explaining the translocation into the PPC facilitated by the Prk BTS: 1) the heterologous dinoflagellate Prk signal peptide was not cleaved in the ER but nevertheless conferred transport across the PPM or 2) the SP was cleaved in the ER lumen and the TP successfully facilitated transport across the PPM. Significant homology of the protease cleavage site in both diatoms and dinoflagellates would be required to truncate the SP at the correct position and thus expose the TP. Although it is possible that the Prk SP mediated transport into the PPC, no partial ER localization resulted from ptPrk1 and ptPrk2 and a partial plastid localization occurred, in contrast to spPrk and spPsbO (figures 26 and 28). It can hence be concluded that the Prk SP was cleaved and the Prk TP was fully compatible with the translocation machinery of the PPM but only partially compatible with the machinery at the third outermost membrane. This would again indicate that discrimination at the PPM was less stringent than at the third outermost plastid membrane.

Despite the net negative charge TPs in constructs ptPsbO2 and ptPrk1, they were sufficient to mediate full and partial transport across the diatom PPM, respectively. This differs from the in ER and PPC eGFP localizations acquired in *P. tricornutum* from homologous TPs that were mutated to contain a net neutral or negative charge instead of a Wt net positive charge (Felsner et al. submitted). Because positive charge was located N-terminally in the *A. carterae* TPs, it is plausible that the position of positive charge was more important than TP net charge in mediating plastid import, as suggested previously (Foth et al. 2003; Tonkin et al. 2008a).

Changes in composition and net charge of *A. carterae* PsbO and Prk transit peptides introduced by truncation had no influence on import into the *P. tricornutum* plastid, as seen in figure 28 for constructs ptPsbO3 and ptPrk2. Conversely, the N-terminal composition of Prk, albeit more similar to that of a typical diatom TP, was at best partially sufficient for translocation. By identifying charge segregation in dinoflagellate TPs, it was inferred that the N-terminal region could potentially mimic the TPs of diatoms and plants due to its overall positive charge and higher serine/threonine content. Because important features tend to be located in the N-termini of TPs (Patron and Waller 2007), truncation of the Prk BTS could potentially have facilitated an improved plastid localization in *P. tricornutum* or in *P. sativum*. Furthermore, the first ~20 amino acids of the heterologous TPs were apparently decisive in conferring plastid import.

Despite apparently not having influenced transport in heterologous systems, the abundance of the negatively charged regions among dinoflagellate TPs implicates the C-terminus as possibly containing dinoflagellate-specific targeting information that was superfluous in the diatom. In conclusion, import into *P. tricornutum* plastids with heterologous TPs was not improved by eliminating regions of net negative charge. Based on these results, it can thus be argued that a TP containing positive charge and conforming to general TP composition was not of primary importance in mitigating import across the plastid envelope, contrary to conclusions reached for apicoplast TPs in *Plasmodium falciparum* (Tonkin et al. 2006a).

### 4.2.3 Implications of *in vivo* Transfections

Dinoflagellate Prk sequences are known to be homologs transferred from the green lineage and most related to the sequence from *Euglena gracilis* (Petersen et al. 2006). A transit peptide from *E. gracilis* has been shown to be sufficient for import into isolated chloroplasts *in vitro* (Inagaki et al. 2000), so although it could have been expected that the dinoflagellate Prk transit peptide could emulate a plant TP *in vivo*, it did not. Because the diatom and the plant translocation machineries of the plastid envelope were partially or totally unable to recognize the *A. carterae* Prk TP, respectively, dinoflagellate transit peptides do not necessarily have the capacity to fully interact with the such translocation systems, as previously suggested (Patron and Waller 2007).

Whereas transit peptides among chromists can be uniform enough to be interchangeable (Gould et al. 2006b), results from *in vivo* transfections seen in figures 22, 23, 26 and 28 suggest that critical changes in TP architecture must have occurred in chromists and dinoflagellates after they acquired red algal endosymbionts and that both of these superphyla differ markedly from plants. This in turn may implicate the “green” transfer of chromist and alveolate Prk as being older than that of the “red” PsbO (Ishida and Green 2002; Petersen et al. 2006), as neither chromist nor dinoflagellate Prk topogenic signals are compatible with the chloroplast import machinery of pea. This would mean that Prk signals have had more time to become divergent from plant signals, while becoming more attenuated to the dinoflagellate protein transports systems.

Thus, it is the dichotomy between dinoflagellates and chromists that is most apparent from the functionality of the “red” PsbO TP interacting more avidly with the *P. tricornutum* plastid import machinery rather than the “green” Prk. Nonetheless, more similarities are present between diatoms and dinoflagellates in respect to their plastid targeting mechanisms than between dinoflagellates and plants. This may indicate that coevolving transport machineries and transit peptides correspond to phylogenetic divergence.

Furthermore, because dinoflagellate TPs were completely disjunctive in the plant milieu and mostly functional in a diatom milieu, targeting was not solely based on phylogenetic homology of mature sequences. This implies that evolution has more rapidly influenced TPs than mature protein sequences, because the identity of the latter can still be

construed by phylogenetic analyses. This concept is supported by variations in the biochemical makeup of TPs for single dinoflagellate isoforms even while the mature protein comparatively unscathed (section 3.1.4). In summary, because plastid transit peptides seem not to be influenced by the same evolutionary constraints as the mature protein domains that they target, the “green” dinoflagellate Prk may be the result of a more ancient gene transfer than the “red” PsbO.

### **4.3 BFA-Sensitive and BFA-insensitive Protein Transport in *Amphidinium carterae***

Prior to this study, the majority of data on protein transport to the plastids of dinoflagellates was extrapolated from *in silico* data and comparisons with data from organisms like *Euglena gracilis*, diatoms, and apicomplexans in which protein transport is better understood (Apt et al. 2002; Patron and Waller 2007; Patron et al. 2005; Slavikova et al. 2005; Tonkin et al. 2008b). Previous *in situ* experiments to determine features of plastid protein transport in dinoflagellates were limited to immunohybridizations of electron microscopic preparations (Nassoury et al. 2003; Nassoury et al. 2005).

Sucrose gradient fractionation and <sup>35</sup>S-labeling of *A. carterae* was methodically established, in order to track protein transport to the dinoflagellate plastid. A number of different vesicle inhibitors would have been suitable for tracking protein transport, but due to its widespread prior use in a large assortment of organisms, Brefeldin A (BFA) was considered to be the most viable candidate for halting vesicle transport specifically from the Golgi apparatus, as it inhibits COPI vesicle transport between the Golgi apparatus and the ER (Nebenfuhr et al. 2002).

BFA treatment at sublethal dosages resulted in complete inhibition of the secretory pathway, as signified by the ER localization of the autoradiograph signals from Cellulase IPs (figures 35 – 37). Addition of Brefeldin A (BFA) to the cells caused no shift in the mobility of the Golgi apparatus in the sucrose gradients, as seen by the signal from proteins containing a Golgi-specific N-acetylglucosamination (figure 34), which is known to localize to the cell surface and trans-face of the Golgi apparatus (Iida and Page 1989; Roberts et al. 2006). As

seen in figure 34, proteins in the plastid and debris fractions are also labeled by WGA, indicating a post-translational modification of plastid proteins at these subcellular locations.

Further effects of BFA on endomembrane compartments were noted upon scrutiny of electron micrographs. A fusion of multiple endomembrane compartments seems to have been invoked by BFA, as signified by the increase in interconnected vesicles that seemingly cannot bud. Furthermore, the number of large endomembrane vesicles increased in number but changed in character: small, circular vesicles of the endomembrane system were replaced with large, ovular vesicles with a vesicle-studded periphery, possibly indicating that the endomembrane system had collapsed into a single multi-lobed fusion of endomembrane compartments. The marked increase of electron dense material in the endomembrane system may have been the result of transport-inhibited proteins aggregating there.

$\alpha$ -PsbO immunogold signals from BFA-treated cells (see figure 40) were spread throughout the cell but remained proximal to the periphery of the endomembrane system. Signals were thus not limited to the center of the cell near the pyrenoid where the Golgi apparatus and ER are typically located in *A. carterae* (figure 38 and 39) as well as *Lingulodinium polyedra* (Schmitter 1971). This endomembrane ultrastructure determined by electron microscopy is dissimilar to that described previously for the BFA treatment of *L. polyedra*. The most prominent feature of BFA treated *L. polyedra* was the formation of the so-called BFA body, which was shown to harbor an amassment of electron dense material, containing a large amount of immunogold labeling was observed using an  $\alpha$ -Rubisco antibody (Nassoury et al. 2005). This BFA body could not be induced in *A. carterae* with the BFA concentrations used in this study.

Because the epitopes for  $\alpha$ -RbcL and  $\alpha$ -PsbO antibodies are within the mature portion of (pre)proteins, the mature protein was labeled by immunogold localizations. Signals observed at the periphery of the endomembrane system in electron micrographs, which is consistent with these proteins containing STDs. This is another confirmation of the *in silico* predictions of STDs in PsbO (section 3.2) and RbcL (Patron et al. 2005).

Whereas RbcL's transport is unaffected by dosages of BFA below half of the lethal dosage, transport of the control protein Cellulase as well as PsbO and Prk are BFA-sensitive at all utilized concentrations. The fact that RbcL is relatively BFA-insensitive at a concentration that supersedes previous BFA inhibition experiments by a factor of 8 (Nassoury et al. 2005) indicates that it is transported via a different pathway than PsbO and

Prk. In apicomplexa, BFA-insensitivity is indicative of plastid-protein-containing vesicles originating from the ER and not the Golgi apparatus (DeRocher et al. 2005). Whereas most if not all apicoplast proteins are thought BFA-insensitive, the findings seen in figures 41 and 42 show that only RbcL was insensitive to BFA inhibition in this dinoflagellate.

Based on these results, at least two endomembrane transport pathways seem to exist side by side in *A. carterae*, one of which utilizes the Golgi apparatus and one of which does not. Perhaps the most elegant explanation for this difference between BFA-insensitive RbcL transport and BFA-sensitive PsbO and Prk transport is that plastid protein transport in dinoflagellates may be dependent on a protein's class. Since RbcL is a class I protein, proteins of this class may be transported by and large in ER-derived vesicles, whereas class II and class III proteins may be mostly transported to the plastid in Golgi-derived vesicles, as seen in figure 44. In conclusion, regardless of how it came about, transport of the class I protein RbcL to the plastid is mediated by a BFA-insensitive pathway, which was previously undescribed in dinoflagellates but similar to the ER-mediated apicomplexan plastid protein transport machinery (Tonkin et al. 2008b).

Plastid protein shuttling in Golgi-derived and ER-derived vesicles in a single organism is novel, previously undescribed premise for protein transport to complex plastids. The hypothetical model proposed for protein transport to dinoflagellate plastids (van Dooren et al. 2001) should thus be revised accordingly to include plastid protein transport via BFA-insensitive vesicles originating from the ER, as seen in figure 44. Dinoflagellates hence seem to have at least two pathways for protein transport to the plastid: 1) class I proteins via the ER and 2) class II and class III via the Golgi apparatus.

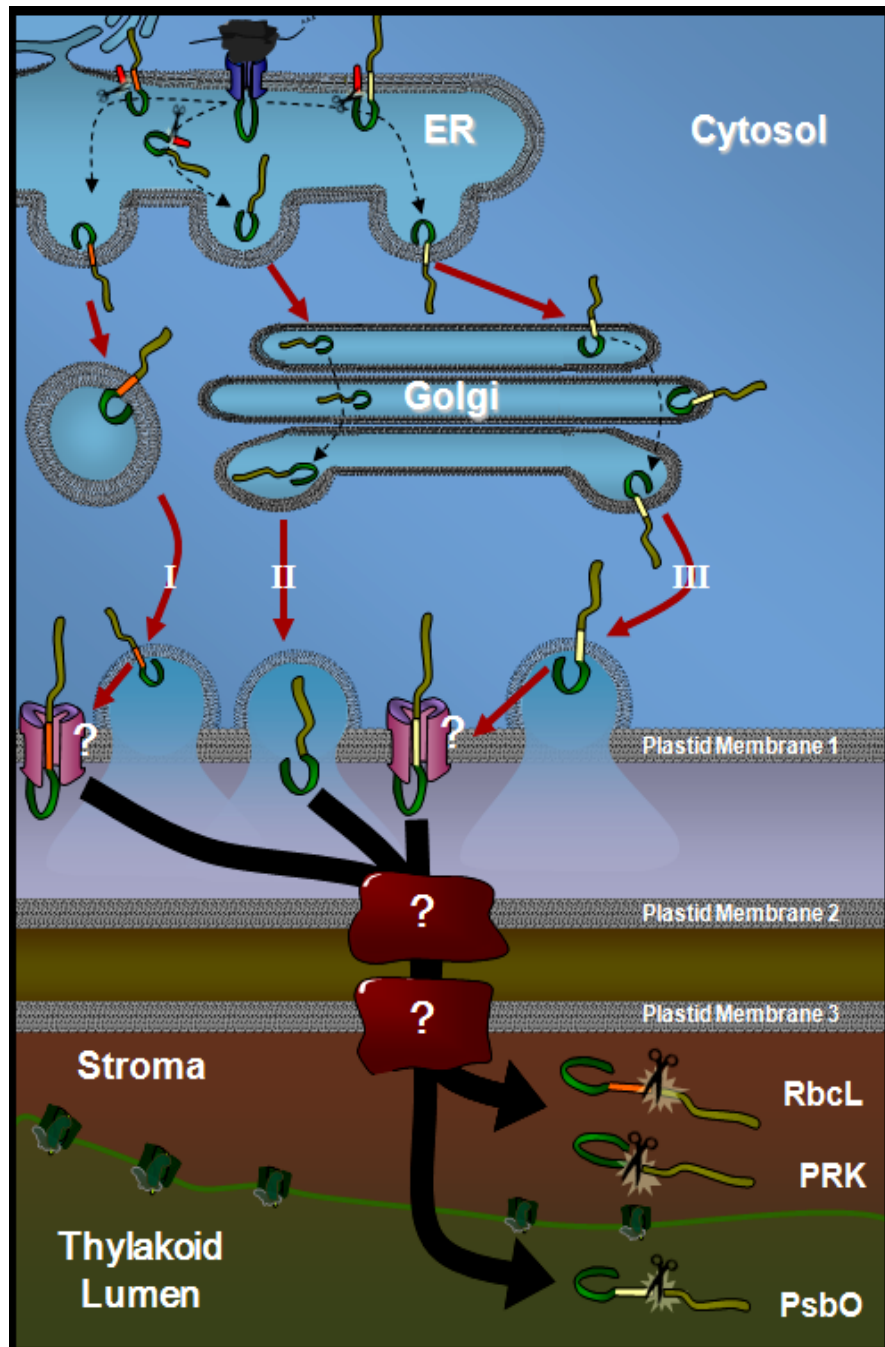


**Figure 44. Model of Protein Transport to the Plastids of Peridinin Dinoflagellate via the Endomembrane System.** Nascent proteins are cotranslationally imported into ER lumen: **Red:** signal peptide, **Green:** TP, **Orange:** stop-transfer domain (STD), **Yellow:** Thylakoid-targeting domain, i.e. STD, **Tan:** Mature protein. **?:** Unknown plastid membrane translocators. **Class I:** Proteins like RbcL are transported to the plastids by way of a BFA insensitive pathway via vesicles from the ER like the situation in apicomplexa (Tonkin et al. 2008b). **Class II:** Class II proteins (without STDs) like Prk are transported by way of the ER to Golgi and then to the plastids. **Class III:** Class III proteins with STDs like PsbO are transported via the ER to the Golgi and then to the plastids. Proteins with STDs must then be removed from the membrane by interaction with channels and/or chaperones for further transport (van Dooren et al. 2001). **1<sup>st</sup>, 2<sup>nd</sup>, and 3<sup>rd</sup>:** refer to the three plastid membranes from outermost to innermost.

## 4.4 Conclusions

Nothing is known about the mechanisms of protein import across dinoflagellate plastid membranes after vesicle fusion with the outer plastid membrane of peridinin dinoflagellates. The hypothetical model that has been suggested for describing protein transport across the three plastid membranes of peridinin dinoflagellates and euglenoids is based on inferences from other organisms containing complex plastids. In this model, protein transport differs from other models, which describe the comparatively well-characterized protein transport across the four membranes of apicomplexan and chromist plastids. According to this hypothetical model, an unknown hypothetical translocator complex is speculated to be recruited around the membrane-spanning domains of class I and III proteins, e.g. RbcL and PsbO, whereafter protein import across the first membrane ensues (Sulli et al. 1999; van Dooren et al. 2001), as seen in figure 44. In this hypothetical model, the translocation machinery of the second and third outermost plastid membranes are subsequently recruited by the hypothetical translocator complex, enabling translocation across the second and third membrane. This model implicitly suggests that utterly different translocation mechanisms exists in peridinin dinoflagellates for translocating membrane-spanning proteins across the outer plastid membrane than is known from chromists and possibly apicomplexans.

Beyond hypotheses based loosely on data from non-dinoflagellates and *in silico* data from peridinin dinoflagellates, no elucidations have been presented that shed light on the cell biological conundrum caused by the dinoflagellate's three plastid membranes as such. As seen in figure 45, there are a number of scenarios that would describe the situation in dinoflagellates, but none of them uphold the general rule of cytosolic compartment division, which dictates that a cytosolic compartment is invariably divided from a non-cytosolic compartment by a biological membrane.

After fusion of protein-laden vesicles with the outermost plastid membrane of peridinin dinoflagellate, the cellular compartmentalization rule dictates that proteins enter a non-cytosolic intermembrane space (IMS). Vesicle shuttling is a process that is retrograde as well as anterograde, so vesicle shuttling must also occur between the plastid and the Golgi and/or ER to replenish membrane lipids, as known in plants and *Plasmodium falciparum* (Benning 2009; Waller and McFadden 2005). In these organisms, the outermost IMS is



considered to be a non-cytosolic compartment. Thus, because vesicles shuttle from a non-cytosolic space, the outer IMS of dinoflagellate plastids is probably also a non-cytosolic space, as seen in figure 45a and 45c.

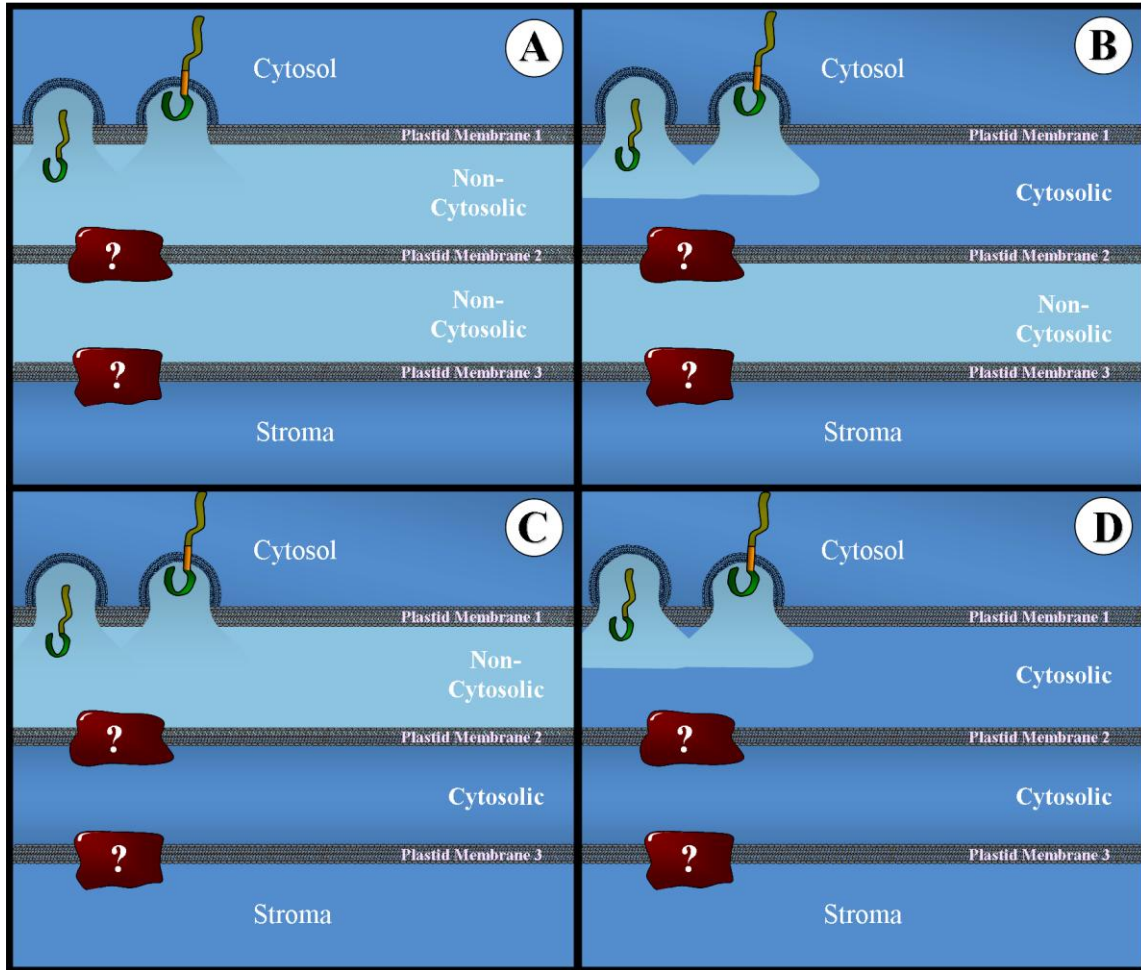


**Figure 45. Possible Cytosolic and Non-Cytosolic Identities of Intermembrane Compartments in the Plastids of Peridinin Dinoflagellates.** Possible identities for outermost and innermost IMSs between dinoflagellate plastid membranes violate the compartmentalization rule, which dictates that biological membranes separate cytosolic spaces from non-cytosolic spaces. **A & C:** Vesicles fuse with the outermost membrane, releasing their non-cytosolic contents into a non-cytosolic outer IMS. **B and D:** Non-cytosolic vesicle lumens fuse with a cytosolic space, whereby the inner IMS could be either cytosolic or non-cytosolic.

It has been suggested that vesicle transport occurs between the membranes of the plant chloroplast in order to replenish lipids of the inner envelope membrane and thylakoid membranes (Vothknecht and Soll 2005). If vesicle transport were occurring from the outer IMS to the stroma, then transport from a cytosolic space to a cytosolic space must be occurring, as the latter is the derivative cytosol of the cyanobacterium. Since the outer IMS

should be similar to the non-cytosolic ER or Golgi lumen, this scenario would therefore actually entail transport from a non-cytosolic compartment to cytosolic compartment. This would eventually transform the stroma into a non-cytosolic plasma, and would thus cease to be the plastid stroma, which therefore renders this scenario implausible.

The conundrum deepens upon considering which translocators can exist in the second outermost membrane, as no translocators are known to translocate from a cytosolic compartment to another cytosolic compartment (figure 45c and 45d). A protein transport complex from a cytosolic compartment to another cytosolic compartment is known: the nuclear pore. This however is embedded in a double-membraned compartment that contains a non-cytosolic space, which is not equivalent with the third plastid membrane. This scenario of a cytosolic identity of the inner IMS is therefore not likely, based on present knowledge. Of the four possibilities, the only tenable scenario remaining implicates the outer and the inner IMSs as being non-cytosolic (figure 45A).

Parallels have been drawn between the origins of peridinin dinoflagellate and apicomplexan plastids, since they are thought to have the same phylogenetic origins (Cavalier-Smith 1999; Janouskovec et al. 2010). General consensus stipulates that dinoflagellates either lost the periplastidial membrane (PPM) or the perialgal vacuole, while retaining the inner two membranes of the former primary plastid. The elimination of the PPM is conducive with the outermost IMS having a non-cytosolic identity as discussed above and suggested previously for apicoplasts (Tonkin et al. 2008b). Furthermore, translocators from a non-cytosolic space to another non-cytosolic space are known to exist: outer membrane protein translocators in Gram negative bacteria translocate proteins from their non-cytosolic periplasmic space to another non-cytosolic space, namely the surrounding medium. Based on these conclusions, of the scenarios displayed in figure 45, it seems most likely that both the outer and the inner IMSs are non-cytosolic with protein transport between the two compartments being mediated by a translocon derived from a Gram negative bacterial homolog (figure 45a).

The fact that dinoflagellate nuclear genes are known to be most homologous to chromists and alveolates (89.5% and 79.4% in dinoflagellates and *C. horridum*, respectively) implies little about the origin of dinoflagellate plastids, because nuclear genes phylogenies do not always correspond to endosymbiont phylogenies (Imanian et al. 2010; Moustafa et al. 2009). This is consistent not only with a peridinin dinoflagellate plastid originating from

secondary endosymbiosis but is also consistent with a primary endosymbiotic event. Both of these possibilities correlate to the plastid membrane identities discussed above.

In the case of primary endosymbiotic origins, the primary plastid is still encased in the perialgal (former phagotrophic) vacuole. Because dinoflagellates constitute the only group that is known to readily supplant their established secondary plastids (Keeling 2009; Yoon et al. 2005), they are the most likely candidates to have replaced their secondary plastid with a primary endosymbiont. The occurrence of primary endosymbiotic events has furthermore been shown to be ongoing (Ikeda-Ohtsubo and Brune 2009; Nowack et al. 2008; Precht et al. 2004), hence this hypothesis is not a baseless premise.

In this hypothesis, the primary plastid would be encased in a perialgal vacuole with which anterograde protein-containing vesicles from the ER and Golgi fuse and retrograde vesicles bud, and lipid recycling would occur in much the same way as for any endomembrane compartment or organelle (Benning 2009; Bonifacino and Rojas 2006; Cavalier-Smith 1999). In this scenario, protein translocation across the second membrane could occur via a protein translocation complex that originated from the endocytosed cyanobacterium, e.g. a general secretion pathway (Gsp) complex, an outer membrane protein (Omp85) assembly factor, or a Type I secretion outer membrane (TolC) protein described for Gram negative bacterial outer membranes (Su et al. 2007). One requirement for such a scenario is that the translocator itself be flipped in its topology such that the proteins are no longer exported out of the endosymbiont, instead being imported into the plastid. This same process is implicit for protein import with Omp85 homologs in plants and other chromalveolates.

Thus in summary, at least two hypotheses can be posited based on the theoretical model of protein import into peridinin dinoflagellate plastids with current knowledge of topogenic signals and of protein transport mediated by ER and Golgi vesicles: 1) the outer IMS is most probably non-cytosolic, and 2) only translocators of the outer membrane of Gram negative bacteria are known to mediate transport from a non-cytosolic compartment to another non-cytosolic compartment, as suggested here to be the case for the outer and inner IMSs of dinoflagellate plastids. Based on these premises, the first dinoflagellate plastid membrane could be the remnant of the host's eukaryotic phagosome membrane, whereas the second and third membranes may be either the plastid envelope from a secondary endosymbiont or the outer and inner membranes of a primary endosymbiont. Two

## Discussion

---

circumstances could have possibly led to this situation based on this theoretical evolutionary heritage of dinoflagellate plastid membranes: 1) the PPM of a secondary red algal endosymbiont was eliminated during the course of peridinin dinoflagellate evolution or 2) the peridinin dinoflagellate plastid arose via a primary endosymbiotic event upon which the secondary endosymbiont was replaced, and the endosymbiont is still encased in a derivative of the phagosomal membrane.

## 5 SUMMARY AND OUTLOOK

Analysis of novel cDNA sequences from *Ceratium horridum* resulted in a previously unnoticed characteristic of peridinin dinoflagellate TPs: positive and negative charges are separated in the N-terminus and C-terminus, respectively. C-terminal negative charge of exemplary TPs from *Amphidinium carterae* did not influence targeting in heterologous *in vivo* experiments, so this feature may be important only for dinoflagellate plastid targeting systems. Homologous transfection of a dinoflagellate with eGFP fusion proteins would greatly assist in determining whether the C-terminal negative TP charge is important for homologous plastid protein targeting.

Dinoflagellate TPs were shown here to be able to at least partially facilitate transport into the plastid stroma and inhibited by an STD in *P. tricornutum*. Chromist and dinoflagellate TPs were observed to be unable to facilitate transport into a plant chloroplast, which contradicts the premise that TPs are universally interchangeable and suggests that clade-specific differences in not only TP makeup but also in plastid TP recognition and possibly translocation machineries of dinoflagellates, plants, and diatoms. Future experiments may identify the dinoflagellate machineries and provide evidence for evolutionary identities of dinoflagellate plastid membranes.

Using Brefeldin A, a novel Golgi-independent route for the transport of the class I protein RbcL. In future experiments, transfection and mutational analysis of could be used to determine sequence-specific features differentiating the ER-mediated from Golgi-mediated pathway to the plastids. Multiple vesicle inhibitors could be employed to determine features of plastid protein transport. Tunicamycin and 2-PMPA could be used to determine whether protein transport depends on post-translational modifications. From which Golgi face plastid-bound vesicles originate can be possibly determined with monensin or megalomicin, which inhibit vesicle trafficking between the cis- and trans-Golgi cisterns. Chlorpromazine could be used to block vesicle trafficking from the trans-Golgi network (Hunt and Marshall-Carlson 1986; Wang et al. 1993), as sub-nanomolar concentrations cause visible cell death in *A. carterae* within minutes. Furthermore, N-ethylmaleimide is also a promising candidate in determining whether vesicle fusion with plastids is SNARE-independent as suggested for *Euglena gracilis* (Slavikova et al. 2005).

## 6 MATERIALS AND METHODS

### 6.1 Materials

#### 6.1.1 Instruments

##### Centrifuges:

Centrifuge 5417R und 5417C	Eppendorf-Netheler-Hinz, Hamburg
GP Centrifuge	Beckman Coulter, Fullerton (USA)
Labofuge 400R	Heraeus Instruments, Hanau
Sepatech Biofuge 17RS	Heraeus Instruments, Hanau
Centrikon T-1080	Kontron Instruments, Neufahrn
TH-641 Rotor for Centrikon T-1080	Sorvall, Braunschweig
Polyallomer Tubes 11x60 mm, thin-walled	BeraneK, Weinheim
Table centrifuge Mini Spin plus	Eppendorf-Netheler-Hinz GmbH, Hamburg
Cooled Centrifuge 5810R	Eppendorf-Netheler-Hinz GmbH, Hamburg

##### PCR-Thermocycler:

MasterCycler Gradient/ Personal	Eppendorf-Netheler-Hinz GmbH, Hamburg
---------------------------------	---------------------------------------

##### Microscopes:

Transmission Electron Microscope EM902	Zeiss, Oberkochen
Transmission Electron Microscope EM2100	Jeol, Eching
Confocal Laser Scan Microscope TCS SP2	Leica, Wetzlar
Light Field Microscope	Zeiss, Oberkochen

##### Sequencing Apparatuses:

LI-COR 4200	MWG, Ebersberg
ABI Prism 377	Applied Biosystems (USA)

##### Power Sources, Electrophoresis, and Blotting Apparatuses

Pharmacia LKB GPS 200/400	Pharmacia/Amersham, Munich
Electrophoresis Power Supply EPS 200/301/601	Pharmacia/Amersham, Munich
DNA Electrophoresis Chambers	Werkstatt, Uni-Marburg FB17
Geldoc1000	Peqlab, Erlangen
SDS Gel Chambers	Werkstatt, Uni-Marburg FB17
Poraplot NCP Nitrocellulose Membrane	Macherey-Nagel, Düren
Amicon Ultra Centrifugal Filter Device	Millipore, Hannover

## Materials and Methods

---

Semidry Transfer Unit TE 77  
Whatman 3MM

GE Healthcare, Munich  
Schleicher & Schuell, Dassel

### Photographic Materials:

X-ray Film Exposition Cassette  
Fuji Medical X-ray Film, 30x40 cm Photo  
X-ray Film Developer  
X-ray Film Fixer Reagent

Appligene, Heidelberg  
Fuji Film, Düsseldorf  
Kodak, Rochester (USA)  
Kodak, Rochester (USA)

### Biolistic transformation:

Biolistic PDS-1000/He Particle Delivery System  
Spherical gold particles Ø 1.5 to 3 µm  
M 10 (Ø 0.7 µm) Tungsten-Partikel  
Rapature Disks 1350 psi  
Rapature Disks 900 psi  
Macrocarrier  
Hepta stopping screens  
Climate chamber MLR-350

Biorad, Munich  
Sigma-Aldrich, Deisenhofen  
Biorad, Munich  
Biorad, Munich  
Biorad, Munich  
Biorad, Munich  
Biorad, Munich  
Sanyo, Bad Nenndorf

### Accessories for Detecting Radioactivity:

Multi-Purpose Scintillation Counter LS 6500 Beckman Coulter, Krefeld  
Fluorescence Scanner Storm 860 Molecular Dynamics, Freiburg

### Other:

Thermomixer® Dry Block Heating Shaker  
NanoDrop ND – 1000  
BioRAD GelDoc  
Exposition cassettes

Eppendorf-Netheler-Hinz GmbH, Hamburg  
PEQLAB, Erlangen  
BioRad, Munich  
Appligene, Heidelberg  
GE Healthcare, Munich  
Hecht-Assistant, Sondheim  
GE Healthcare, Munich  
Filter Spectronics Corp.  
GE Healthcare, Munich  
Phillips, Münster  
Bachofer, Reutlingen  
IK, Staufen  
Sartorius Laboratory, Göttingen  
Stuart, Staffordshire (UK)

Laborator 3D rocker  
Spectralphotometer Ultrospec II  
UV-Table Spectroline® M730 Longlife™  
Spectral Photometer Ultrospec 2000  
Microwave Oven  
Hybridization Oven 400-HY E  
Magnetic Stirrer IKAMAG RCT  
Fine Scales  
Roller-Mixer SRT1

### 6.1.2 Chemicals

Chemicals used for his thesis were analysis grade. Chemicals were stored and used according to the manufacturer's instructions.

<b>Chemical</b>	<b>Manufacturer</b>
2-Mercaptoethanol	Serva, Heidelberg
5-Brom-4-chlor-3-inodyl- $\beta$ -galactoside	Roth, Karlsruhe
Acetone, CHROMASOLV	Sigma-Aldrich, Munich
Acetone	Roth, Karlsruhe
Agar Agar	Roth, Karlsruhe
Agarose NEEDO	Roth, Karlsruhe
Ammoniumpersulfat (APS)	Sigma-Aldrich, Munich
Ampicillin Trihydrat (Amp)	Sigma-Aldrich, Munich
Bacto-Yeast extract	Roth, Karlsruhe
Bacto-Trypton	Roth, Karlsruhe
Bisiminotris methane Bis-Tris	Roth, Karlsruhe
Blocking Reagent (5% Milchpulverlsg)	Roche, Mannheim
Boric acid (HBr)	Roth, Karlsruhe
Bromphenolblue	Biorad, Munich
Calcium chloride (CaCl <sub>2</sub> )	Roth, Karlsruhe
Cetyltrimethylammonium bromide (CTAB)	Sigma-Aldrich, Munich
Chloroform	Merck, Darmstadt
Diethylpyrocarbonate (DEPC)	Roth, Karlsruhe
Dimethylsulfoxide (DMSO)	Sigma-Aldrich, Munich
Dinatrium hydrogen phosphate (Na <sub>2</sub> HPO <sub>4</sub> )	Roth, Karlsruhe
Dithiothreitol (DTT)	Roth, Karlsruhe
Ethylendiamintetraacetic acid (EDTA)	Roth, Karlsruhe
Ethanol (EtOH)	Roth, Karlsruhe
Ethidium bromide (EtBr)	Sigma-Aldrich, Munich
2 mL 70% Glutaraldehyde Ampules	Polysciences, Eppelheim
Glycerin	Roth, Karlsruhe
Glycine	Roth, Karlsruhe
Urea	Roth, Karlsruhe
Hydrochloric acid (HCl)	Roth, Karlsruhe
Isopropanol	Roth, Karlsruhe
Isopropyl- $\beta$ -D-thiogalactoside (IPTG)	Roth, Karlsruhe
Luminol	Roth, Karlsruhe
Magnesium chloride (MgCl <sub>2</sub> )	Roth, Karlsruhe
Methanol (MeOH)	Roth, Karlsruhe
Mineral oil	Sigma-Aldrich, Munich
Phenol, TE-gepuffert	Roth, Karlsruhe
Potassium acetate (KAc)	Roth, Karlsruhe
Protein A Sepharose beads	ThermoScientific, Braunschweig
Rotiphorese®-Gel 30	Roth, Karlsruhe
Skim milk powder	Fluka, Karlsruhe
Sodium acetate (NaAc)	Roth, Karlsruhe
Sodium chloride (NaCl)	Roth, Karlsruhe
Sodium dodecylsulfate (SDS)	Roth, Karlsruhe
Sodium nitrate (NaNO <sub>3</sub> )	Merck, Mannheim
Sodium hydroxide (NaOH)	Roth, Karlsruhe
Spermidine	Sigma-Aldrich, Munich



## Materials and Methods

---

Trichloroacetic acid (TCA)	Roth, Karlsruhe
Trihydroxymethylaminoethane (Tris)	Roth, Karlsruhe
Trimethylethylene diamine (TEMED)	Sigma-Aldrich, Munich
Triton X-100 (TX-100)	Roth, Karlsruhe
Trizol® Reagent	Invitrogen, Karlsruhe
Tropic marin Sea Salt	Dr. Biener GmbH, Wartenberg
Tween 20	Sigma-Aldrich, Munich
Zeocin	Duchefa, Haarlem, Netherlands

### Radioactive chemicals

For the *in vivo* radioactive labeling of proteins,  $^{35}\text{S}$ -sulfate,  $^{35}\text{S}$ -methionine, and  $^{35}\text{S}$ -Metmix (10 mCi Hartmann Analytical GmbH per L) were used.

### Buffers & Solutions

All standard buffers were prepared as described in Sambrook et al. (1989), unless otherwise indicated.

### Molecular Biological Enzymes and Kits

All restriction nucleases were purchased from MBI Fermentas (St. Leon-Rot).

DNA kinase	MBI-Fermentas, St. Leon-Rot
CloneJet™ PCR Cloning Kit	MBI-Fermentas, St. Leon-Rot
DYEnamic ET terminator Cycle Sequencing Kit	GE Healthcare, Munich
JETsorb DNA Extraction Kit	Genomed, St. Lois, USA
Phusion High-Fidelity PCR Kit	Finnzymes, Espoo
QIAGEN Plasmid Purification Midi/ Maxi Kit	Qiagen, Hilden
Qiagen PCR purification kit	Qiagen, Hilden
Rapid DNA Ligation Kit	MBI-Fermentas
Superscript® III Reverse Transcriptase	Invitrogen, Karlsruhe
Superscript® II Reverse Transcriptase	Invitrogen, Karlsruhe
Taq DNA-Polymerase	Biotech, Madrid
GeneRacer™ Kit	Invitrogen, Karlsruhe
DYEnamic ET Terminator Cycle Sequencing Kit	GE-Healthcare, Munich

### Oligonucleotides

All oligonucleotides were either ordered at MWG Biotech (Ebersberg) or Sigma-Aldrich (Munich).

#### Name Sequence 5' - 3' (Restriction sites underlined)

##### Sequencing oligonucleotides:

M13r	CAGGAAACAGCTATGACC
M13u	TGTAAAACGACGGCCAGT

T7 TAATACGACTCACTATAGGGC  
 pJet fw GCACAAGTGTTAAAGCAGTT  
 pJet rv CTCTCAAGATTTTCAGGCTGTAT  
 pPhaT1 fw AAGAGTGCTCGTGTGCTTCG  
 pPhaT1 rv GCGGCACAAATGGGCATCCTTGCTC

Ceratium horridum Primers for EST database:

PolyT\_not GGGGCCC[21xT]VNN  
 SL\_apa primer GGGCCCCCGTAGCCATTTTGGCTCAAG

Ceratium horridum Primers for Constructs involving Isolated Chloroplasts/Thylakoids:

PsbO\_Sig\_apa GGGGCCC<sup>CGCCTGGGGCACAACCAGTAC</sup>  
 PsbO\_No\_TTD\_apa GGGGCCC<sup>ATCCGTCAAAGTTTCAGGTGA</sup>  
 PsbO\_Code\_apa2 GGGGCCC<sup>ATCACAGCTGAACAGTTCAGC</sup>  
 PsbO\_Code\_bam GGG<sup>ATCCATCACAGCTGAACAGTTCAGC</sup>  
 Psbo\_signal\_eco GGA<sup>ATTCATGGAGGGTGTAAGCATGCGC</sup>  
 Psbo\_transit\_eco

GGA<sup>ATTCATGTTCGTTGCTACCCCTGCATCT</sup>

TCA

Ch\_TTD GGA<sup>ATTCATGCGCAGAGGAGTTCTCAGGGG</sup>

Primers used to acquire the *A. carterae* full-length sequence:

AC\_Prk\_3'seq1 GTGGTSGAGATGGACGGTGAGAT  
 AC\_Prk\_3'seq2 GACATGGACAACATGGAGGCGCAG  
 AC\_Prk\_A-3' GAYGACTACCACACMAAYGACCG  
 AC\_Prk\_A-5' CGGTCRTTKGTGTGGTAGTCRTC  
 AC\_Prk\_C-3' AAGTCCACSTTYCTGCGCCGSATC  
 AC\_Prk\_C-5' GATSCGGCGCAGRAASGTGGACTT

AC\_psbo\_atg1\_xho  
 CCCTCGAGATGAGCAAAGCCATGCGCGGTTTGGTGGCCTTT

**pAVA constructs**

*Amphidinium carterae*

AC\_sig\_pscI AAACATGTTGCGCGGTTTGGTGGCCTTT  
 AC\_trans\_pscI AAACATGTTTGTGCAGCTGCCGTCGCAG  
 AC\_trans\_end\_pscI AAACATGTATCGAACCCAAGATCCAGCAT  
 AC\_code\_pscI AAACATGTTGTTGGCCAAGCCAGAACCCTT  
 AC\_kurz2\_pscI AAACATGTTTTGGCCGCGGAGACTGGTTCC  
 AC\_Prk\_SP\_psc AAACATGTTTGC<sup>CCGATCGCAGTCAGGG</sup>  
 AC\_Prk\_TP\_psc2 AAACATGTT<sup>CGTAGCACCGCGCCTGCCA</sup>  
 AC\_Prk\_Trunc2\_nco GCC<sup>ATGGCACCATAGCGGGCAATGAA</sup>  
 AC\_Prk\_COD3psc AAACATGT<sup>CCGCGCAACACCAATAATCAC</sup>

*Pisum sativum*

Pea\_OTP<sub>end</sub>\_nco CCCCATGGAGTAACCTTAGCTCCATAGTG  
 Pea\_OTP<sub>nco</sub> CCCCATGGACAGCCTCACTTCAAGCA

*Ceratium horridum*

PsbO\_start\_psc AAACATGTTT<sup>GAGGGTGTAAGCATGCGC</sup>

## Materials and Methods

---

PsbO_TP_psc	AA <u>ACATGTT</u> CGTTGCTACCCCTGCATCTTCA
C	
PsbO_TTS_psc	AA <u>ACATGTT</u> GATTGCACGCACAGGACTGC
Psbo_BTS_esp	CC <u>GTCTCAAT</u> CCCAAACAGCACAAAGGATCC
CG	
<u><i>Phaeodactylum tricornutum</i></u>	
Pt_AtpC_5'psc	AA <u>ACATGTT</u> CACCACACAGCCAACTTCC
Pt_AtpC_3'psc	AA <u>CCATGGC</u> GTTGGCTTTTCCATCCAT
<u><i>Guillardia theta</i></u>	
atpCGFP-for	CC <u>ATGGCCTT</u> CCAGGCTCCGTTCTCTCTTC
TTC	
atpCGFP-rev	CC <u>ATGGT</u> AGGTCCACATGCGCGAGCACGAG
GA	
GapGFP-for	CC <u>ATGGCCTT</u> CAACCCTGGATCCTCCTTTGT
TCC	
GapGFP-rev	CC <u>ATGGCCT</u> GCATGGTGGGGCCGGTCATCTT
AG	
<u><i>Amphidinium carterae</i> pPha constructs</u>	
AC_sig_eco	GGAATTCATGCGCGGTTTGGTGGCCTTT
AC_eco_OSP	GGAATTCATGAGCAAAGCCATGCGCGGTTT
GGTGGCCTTTGCCCTTTGCGGCACCTGCTCTGCGATGGTGAGCAAGGGCGAGGA	
G	
AC_kurzTP_bam	GGGATCCTTGCCGCGGAGACTGGTTCC
AC_trans_end_bam2	GGGATCCGGATCGAACCCAAGATCCAGC
AC_Ocod2_bam	GGGATCCGTTGGCCAAGCCAGAACCCTT
AC_Prk_SP_eco	GGAATTCATGGCCCGATCGCAGTCAGGG
AC_Prkcode_bam	GGGATCCATATTGTAGGAGATCTTCTAG
AC_Prk_Trunc2_bam	GGGATCCAGCACCATAGCGGGCAATGAA
Prk-sp 3'blunt	GGCAACGCCAGCCAACTGCC

### Plasmids

<u>Plasmid</u>	<u>Specification</u>	<u>Supplier</u>
pJET	Ampr, lacZ', P T7, P SP6	Fermentas, St. Leon-Rot
pBluescript II KS	Ampr, lacZ', P T7, P SP6	Fermentas, St. Leon-Rot
pPha-T1	Ampr, Zeor	see Apt et al. 1996
pAVA393	Ampr	see Von Arnim et al. 1998

## Markers

All markers were purchased at MBI Fermentas (St. Leon-Rot). For DNA electrophoresis the GeneRuler™ 1kb DNA Ladder and for protein electrophoresis, the PageRuler™ Prestained Protein Ladder was used.

### 6.1.3 Antibodies

All of the antibodies utilized for this thesis were diluted at the following concentrations for Western Blots (WB), Immunoprecipitations (IP), and Electron Microscopy (EM):

#### Primary Peptide Antibodies from Eurogentec:

α PsbO: Epitope PSYRTGGFLDPKGRG, WB: 1:1000, IP: 1:10, EM: 1:50

α Prk: Epitope LDDYHTNDRAGRKAT, WB: 1:1000, IP: 1:10, EM: 1:50

α Exocellulase: Epitope QQAGSQKQEEHVPLC, WB: 1:500, IP: 1:10

#### Commercially Acquired Primary Peptide Antibodies:

α RbcL (Agrisera, WB: 1:3000, IP: 1:40, EM: 1:1500)

α PsbD (Agrisera, WB: 1:3000)

α Sec61 (US Biological #S0580-02, WB: 1:300, EM: 1:10)

#### Commercially Acquired Lectins:

WGA-HRP (Fluka, WB: 1:1000)

WGA-Gold, 10nm (Gentaur, EM: 1:75)

#### Secondary Antibodies:

α rabbit HRP-coupled (Sigma-Aldrich, WB: 1:10000)

α goat HRP-coupled (Sigma-Aldrich, WB: 1:10000)

α rabbit an 30 nm Goldpartikel gekoppelt (Biocell, EM: 1:140)

#### Bacterial Strains

For standard transformation and amplification of plasmids, the TOP10™ *Escherichia coli* (*E. coli*) strain was used:

*E. coli* TOP10 (Invitrogen, Karlsruhe): F<sup>-</sup>, mcrA, Δ(mrr-hsdRMS-mcrBC), φ80lacZΔM15, ΔlacX74, recA1, araD139 Δ(ara-leu)7697, galU, galK, rpsL, endA1, nupG.

### 6.1.4 Culture media

#### Media for *E. coli*

All LB medium ingredients were purchased at Roth chemicals (Karlsruhe).

## Materials and Methods

---

### LB Medium (1 L):

Bacto-Tryptone	10 g
Bacto-Yeast Extract	5 g
NaCl	10 g

For agar plates 15 g/l agar-agar was added prior to autoclaving. For selection, the following antibiotics were utilized: Ampicillin (50 µg/ml final concentration). For blue-white screening of pBluescript transformants, 60 mg/L β-X-Gal and 1 mM of IPTG was added (final concentration).

### Media for *C. horridum*, *A. carterae*, *G. theta* and *P. tricornutum*

#### f/2 Basic Medium:

Tropic Marine	30 (15 for <i>P. tricornutum</i> )	g/l
Tris/HCl (pH 8)	5	mM
NaNO <sub>3</sub>	0.883	mM
NaH <sub>2</sub> PO <sub>4</sub> x 2H <sub>2</sub> O	0.036	mM

pH 6.3 was adjusted with 5M HCl and the medium autoclaved and the stored at 4°C (pH 7.5 after autoclaving). From vitamin and trace metal solutions, 1 mL/L was added to f/2 basic medium.

#### f/2 Trace Metals:

FeCl <sub>3</sub> x 6 H <sub>2</sub> O	11.65	mM
Na <sub>2</sub> EDTA	11.71	mM
CuSO <sub>4</sub> x 5 H <sub>2</sub> O	0.039	mM
ZnSO <sub>4</sub> x 7 H <sub>2</sub> O	0.077	mM
CoCl <sub>2</sub> x 6 H <sub>2</sub> O	0.042	mM
MnCl <sub>2</sub> x 4 H <sub>2</sub> O	0.91	mM
Na <sub>2</sub> MoO <sub>4</sub> x 2 H <sub>2</sub> O	0.026	mM

Each substance was fully dissolved before the next was added.

#### f/2 Vitamins:

Biotin	0.0020	mM
Cyanocobalamin	0.00037	mM
Thiamine-HCl	0.297	mM

Vitamins were sterile-filtered and aliquots of 10 ml stored at -20°C.

#### ASP-Medium:

NaCl	400	mM
MgCl <sub>2</sub> 6 H <sub>2</sub> O	60	mM
CaCl <sub>2</sub> 2H <sub>2</sub> O	10	mM
KCl	10	mM
NaHCO <sub>3</sub>	2	mM
NaNO <sub>3</sub>	1	mM
NaH <sub>2</sub> PO <sub>4</sub>	0.1	mM

1 ml/L of vitamin solution was added after autoclaving. The pH of the medium was adjusted to 7.3 before autoclaving, which leads to a pH of 7.9 after autoclaving. Cultures were constant illuminated at a light intensity at the culture surface of 100 µwatts/cm<sup>2</sup>.

ASP-Vitamin Solution:

Substance	Concentration
H <sub>3</sub> BO <sub>3</sub>	12 g/L
EDTA	11 g/L
p-aminobenzoic acid	20 g/L
Ca-pantothenate	0.2 g/L
Nicotinic acid	0.2 g/L
Inositol	10 g/L
Na <sub>2</sub> EDTA	4.36 g/l
FeCl <sub>3</sub> 6 H <sub>2</sub> O	3.15 g/l
3.5 mM MnCl <sub>2</sub> 4 H <sub>2</sub> O	689 mg/L
0.8 mM ZnCl <sub>2</sub> 4H <sub>2</sub> O	186 mg/L
Co(NO <sub>3</sub> ) <sub>2</sub> 6H <sub>2</sub> O	12.2 mg/L
Thiamin/Hcl (Vit B <sub>1</sub> )	10 mg/L
Cu(OAc) <sub>2</sub> 2H <sub>2</sub> O	8.6 mg/L
Na <sub>2</sub> MoO <sub>4</sub> x 2 H <sub>2</sub> O	6.3 mg/L
Folic acid	4 mg/L
Cyanocobalamin (Vit B <sub>12</sub> )	20 mg/L
Biotin (Vit H)	20 mg/L

Computer Hardware and Software

Data collected during the course of this doctorate thesis was compiled using a standard commercially available personal computer. Microsoft Office and other standard programs were used to evaluate and present data. Raw sequencing data corrections and aligning was performed using Sequencher (GeneCode, Ann Arbor, MI, USA).

*In silico* analyses were carried out using algorithms and/or information from the following websites:

BioEdit v7.0.5	<a href="http://www.mbio.ncsu.edu/BioEdit/page2.html">http://www.mbio.ncsu.edu/BioEdit/page2.html</a>
BlastN, BlastP, tBlastX	<a href="http://www.ncbi.nlm.nih.gov/cgi-bin/BLAST">http://www.ncbi.nlm.nih.gov/cgi-bin/BLAST</a>
EhuxDBv1.0	<a href="http://genome.jgi-psf.org/Emihu1/Emihu1/">http://genome.jgi-psf.org/Emihu1/Emihu1/</a>
ExpASy	<a href="http://www.expasy.ch/tools/pi_tool.html">http://www.expasy.ch/tools/pi_tool.html</a>
Geneious	<a href="http://www.geneious.com/default.390.plugins.sm">http://www.geneious.com/default.390.plugins.sm</a>
<i>Guillardia theta</i> Genome Resource	<a href="http://www.jgi.doe.gov/sequencing/why/50026.html">http://www.jgi.doe.gov/sequencing/why/50026.html</a>
Local BLAST v2.2.22 from NCBI	<a href="http://blast.ncbi.nlm.nih.gov/Blast.cgi?CMD=Web&amp;PAGE_TYPE=BlastNews#1">http://blast.ncbi.nlm.nih.gov/Blast.cgi?CMD=Web&amp;PAGE_TYPE=BlastNews#1</a>
NCBI	<a href="http://www.ncbi.nlm.nih.gov/">http://www.ncbi.nlm.nih.gov/</a>
PhatrDBv2.0	<a href="http://genome.jgi-psf.org/Phatr2/">http://genome.jgi-psf.org/Phatr2/</a>
PHYLIP V3.69	<a href="http://evolution.genetics.washington.edu/phylip.html">http://evolution.genetics.washington.edu/phylip.html</a>
PHYML V3.0	<a href="http://evolution.genetics.washington.edu/phyml.html">http://evolution.genetics.washington.edu/phyml.html</a>

PlasmoDBv6.1	<a href="http://plasmodb.org/plasmo/">http://plasmodb.org/plasmo/</a>
SOSUIv1.11	<a href="http://bp.nuap.nagoya-u.ac.jp/sosui/">http://bp.nuap.nagoya-u.ac.jp/sosui/</a>
SYM-BLAST	<a href="http://131.204.120.103/srsantos/symbiodinium/blast/blast_cs.html">http://131.204.120.103/srsantos/symbiodinium/blast/blast_cs.html</a>
ThapsDBv3.0	<a href="http://genome.jgi-psf.org/Thaps3/">http://genome.jgi-psf.org/Thaps3/</a>
TMHMM v2.0	<a href="http://www.cbs.dtu.dk/services/TMHMM-2.0/">http://www.cbs.dtu.dk/services/TMHMM-2.0/</a>
WebLogo	<a href="http://weblogo.berkeley.edu/">http://weblogo.berkeley.edu/</a> <a href="http://www.geneious.com/default,28,downloads.sm">http://www.geneious.com/default,28,downloads.sm</a>

## 6.2 Methods

### 6.2.1 Culture Conditions

*Guillardia theta* and *Amphidinium carterae* cultures were inoculated 1:5 from a full-grown culture and grown for 6 days in F/2 medium in a 12:12 light dark cycle. 1 L cultures were grown in 3 L Erlenmeyer flasks. All cultures were harvested by centrifugation at 2,000 g for 5 minutes.

*Ceratium horridum* cultures were cultivated at 100 lux in f/2 artificial sea water medium at 15°C with 12:12 hour light/dark phases. 100 mL cultures were grown in 500 mL Erlenmeyer flasks for 8 weeks and harvested via filtration with 50 µm nylon net. Wet cells were then scooped off the net and deposited in an Eppendorf reaction tube.

### 6.2.2 Culturing and Preparation of Chemical Competent Top10™ *E. coli*

A 2 mL overnight culture of Top 10™ (Invitrogen, Karlsruhe) was used to inoculate 100 mL LB medium, which was spruced up with 10 mM of MgCl<sub>2</sub> and MgSO<sub>4</sub> (end concentration). The culture was incubated at 37°C with shaking for ca 2.5 hr until an OD<sub>600</sub> of ca. 0.6 was reached. Cells were cooled on ice for 20 min, whereupon they were centrifuged at 3000 rpm for 10 min at 4°C. Cells were resuspended in RF1 with a glass pipette, incubated for a further 20 min on ice, and then centrifuged as above. Cells were then resuspended in 5 mL RF2 as above, incubated for 20 min on ice, aliquoted into 100 µL in Eppendorf tubes, and frozen using liquid nitrogen. Chemically competent *E. coli* Top 10 aliquots were stored at -80°C until use.

## Materials and Methods

---

### **RF1:**

Rubidium chloride	100	mM
Magnesium chloride	50	mM
Potassium acetate	30	mM
Calcium chloride dihydrate	10	mM
Glycerin	15%	w/v

RF1 was adjusted to pH 5.8 with 0.2 M acetate and then sterile filtered.

### **RF2:**

Rubidium chloride	10	mM
MOPS	10	mM
Calcium chloride dihydrate	75	mM
Glycerin	15%	w/v

RF2 was adjusted to pH 5.8 with NaOH and then sterile filtered.

### 6.2.3 Sequencing of DNA

DNA Sequencing was performed using DYEnamic ET Terminator Cycle Sequencing Kit employing the chain-termination method (Sanger et al. 1977). A 10  $\mu$ L sequencing reaction consisted of 1  $\mu$ g Plasmid-DNA, 5 pmol sequencing primer, 2  $\mu$ l ABI-Mix, and ddH<sub>2</sub>O. The standard sequencing reaction was initially 3 min of 95 °C denaturing, followed by 30 cycles of denaturing (30 sec, 95 °C), primer annealing (30 sec, 50 °C), and elongation (90 sec, 60 °C). Final elongation was 30 sec at 60 °C. Precipitation of DNA was executed by adding 26  $\mu$ l ddH<sub>2</sub>O and 64  $\mu$ l absolute EtOH to the reaction mix and incubating for 30 min. DNA was centrifuged for 20 min, subsequently washed with 70% EtOH, dried for ca. 5 min at 50°C, and resuspended in ABI loading dye. Electrophoretic separation ensued using the program for the automated ABI377 sequencer. All sequences were analyzed and edited with the Sequencher program.

### 6.2.4 Amplification of Reverse Transcripts and Rapid Amplification of cDNA Ends (RACE) Products

RNA was prepared using Trizol™ using the manufacturer's instructions. After DNase I treatment, cDNA was synthesized from single-stranded mRNA using SuperScript II reverse transcriptases and using the polyT<sub>12</sub> primer, according to the manufacturer's instructions. In the cases of the *Amphidinium carterae* Prk and the *Ceratium horridum* PsbO sequences, Superscript III reverse transcriptase was used at 55°C, as these transcripts were not obtained at 42°C. From polyT cDNA, RT-PCRs were performed. For non-EST PCRs, Phusion polymerase was employed. All PCRs were separated with 1% agarose gels and eluted from gels with JETsorb Extraction-Kit or with Wizard®-SV Gel/PCR Clean-Up System. Restriction of DNA fragments was carried out in accordance with the guidelines from the restriction enzyme manufacturer.



### 6.2.5 Acquisition of the *C. horridum* *psbO* Sequence with RACE

The reverse transcription of *C. horridum* mRNA for *PsbO* employed the primer instead of the polyT\_not primer, using Superscript III generally in accordance with the manufacturer's instructions, except for the fact that the reaction was started directly after the 70°C denaturing step without cooling and took place at 57°C for 30 min. RACE was executed using the Generacer kit in accordance to the manufacturer's instructions.

### 6.2.6 EST Database

For amplification of cDNA for the *C. horridum* database, Biotools Taq polymerase was used. RT-PCR amplification of the resulting template cDNA employed said PolyT\_not and SL\_apa primer, derived from the spliced leader sequence preceding dinoflagellate mRNAs (Zhang et al. 2007). PCR fragments were purified from the PCR with Qiagen PCR purification kit and then subjected to *NotI* and *ApaI* digestion. Fragments  $\geq 500$  bp were purified from agarose gels with Jetsorb for subsequent ligation with *NotI/ApaI* digested pBluescript KS+ using T4 DNA Fast Ligation Kit according to the manufacturer's instructions for transformation in chemically competent Top10 and spread evenly onto an LB Amp50/IPTG/X-Gal plate. Initial blue/white screening of colonies was followed by the determination of the average insert size as being  $\geq 500$  bp in 80% of randomly selected clones, which were ABI sequenced to determine if diversity was present among them. Clones from successful transformations were used to inoculate 96 well plates filled with Amp50/LB/agar. Sequencing of cloned plasmids was performed in Berlin at Agowa GmbH.

### 6.2.7 Acquisition of *A. carterae* cDNA Sequences

All *A. carterae* cDNA was synthesized as described above and amplified with Phusion polymerase in accordance with the manufacturer's instructions, using the primer AC\_psbo\_atg1\_xho, which was derived from the NCBI database for the *PsbO*-encoding EST EU742854, and PolyT\_not to acquire a full length sequence from which all other fragments were amplified with Phusion polymerase. The N-terminal *prk* sequence was acquired from nested PCR Phusion polymerase in accordance with the manufacturer's instructions from cDNA with the following degenerate primers for the 3' end: Prk\_C-5' in the first PCR, Prk\_A-5' in the second PCR. The 5' primer in each PCR was SL\_apa.

### 6.2.8 BLAST Analysis using a Local Database

*C. horridum* EST sequences were analyzed with BLASTX to determine homologies to annotated proteins. For all *C. horridum* ESTs, tBLASTX from SYM-BLAST (Santos lab, Auburn University) was employed to analyze comparison to all other dinoflagellate EST data. BLAST hits with the best e-value were evaluated, to acquire a list of organisms with which *C. horridum* sequences are most homologous. For each of these organisms (or most related model organism, if adequate sequence information for the BLAST hit was lacking), the totality of protein sequences were downloaded in FASTA format. In addition to protein sequences from these organisms, special emphasis was put on chromalveolates in that the following sequences databases were downloaded for further BLAST analyses: unpublished partial genomic sequences from the cryptophyte *Guillardia theta* (JGI), the published proteomes from the diatoms *Phaeodactylum tricornutum* and *Thalassiosira pseudonana* (Armbrust et al. 2004; Bowler et al. 2008), the unpublished proteome from *Emiliana huxleyi* CCMP1516, as well as all NCBI database protein sequences for apicomplexa, oomycetes, cryptophytes, haptophytes, and ciliates.

In order to use be able to compare *C. horridum* EST homologies to those of the 96,036 other dinoflagellate ESTs available as of February 2010, a database of both *C. horridum* and all other dinoflagellate EST sequences were used to make two databases with the downloadable local BLAST program 2.2.22 from NCBI. The proteins downloaded from each organism (or most related model organism with an annotated genome) from *C. horridum* BLAST results as well as chromalveolate sequences were blasted locally with BLASTN against both the *C. horridum* and dinoflagellate EST databases with an e-value cut-off of  $e^{-10}$ , output format 9. Using a macro written for Microsoft Excel (see Appendix), BLAST results were combined by choosing the blast hit for each EST that had the best e-value. In this manner, the best homologies were determined for all dinoflagellate and *C. horridum* ESTs based on the annotated proteomes of organisms with the best homology to *C. horridum* ESTs.

### 6.2.9 Horizontal Gene Transfer Phylogenetic Analyses

Based on the BLAST results for *C. horridum* sequences excluding other dinoflagellate hits (as including them would constitute a search for transfers to the *C. horridum* genome since its speciation), ESTs were chose for horizontal gene transfer (HGT) analysis according to their not being most homologous to a chromalveolate protein sequence, whereby published

HGTs, e.g. Rubisco, were omitted in these analyses. Amino acid sequences were aligned using ClustalW and manually refined under BioEdit. For each data set, a phylogeny was reconstructed under maximum likelihood (ML) using the PHYML V3.0 (Felsenstein 1985; Guindon and Gascuel 2003) using the Whelan and Goldman (WAG) + + I evolutionary model and tree optimization. The alpha values were calculated using 8 rate categories. Stability of monophyletic grouping in ML trees was calculated with PHYML bootstrap (100 replicates) support values (Felsenstein 1985). Further bootstrap values (500 replications) were calculated with the Neighbor-Joining (NJ) method using Jones-Taylor-Thornton + distance matrices (PHYMLIPV3.69). The NJ analysis was done with randomized taxon addition. Bayesian posterior probabilities (BPPs) for nodes in the ML tree were calculated using Geneious pro software v4.8.5 with the MrBayes v3.1.2 plugin, for which the WAG +  $\Gamma$  model was used starting with a random seed for 1,000,000 generations, from which a tree was produced every 1,000 cycles (Huelsenbeck and Ronquist 2001). The initial 20,000 cycles (200 trees) were discarded as the "burn-in." A consensus tree was made with the remaining 800 phylogenies to determine the posterior probabilities at the different nodes. A consensus tree from these three different methods was created using Geneious, whereupon values from each of the three methods were labeled on the final consensus tree. Trees with insignificant differences between chromist and dinoflagellate sequences were disregarded.

### 6.2.10 *In silico* Transit Peptide Analyses

123 nucleus-encoded diatom sequences for proteins with plastid stroma localization were acquired from publications for *Phaeodactylum tricornutum* and *Thalassiosira pseudonana* (Apt et al. 1996; Bullmann et al. 2010; Gould et al. 2007; Gould et al. 2006b; Gruber et al. 2007; Hempel et al. 2009; Kilian and Kroth 2004; Kilian and Kroth 2005; Kroth et al. 2008; Sommer et al. 2007). 227 nucleus-encoded peridinin dinoflagellate sequences for proteins with plastid localization were acquired from EST data at NCBI and those acquired from SL-PCR amplification as described above (Bachvaroff et al. 2004; Hackett et al. 2005; Kuo et al. 2004; Nosenko and Bhattacharya 2007; Nosenko et al. 2006; Patron et al. 2005; Sanchez-Puerta et al. 2007; Slamovits and Keeling 2008; Soares et al. 2009; Tanikawa et al. 2004; Uribe et al. 2008; Waller et al. 2006a; Wang et al. 2008).

134 nucleus-encoded plant sequences for proteins with chloroplast localization were acquired from blast results from the plastid-targeted dinoflagellate sequences; BLAST expect value

cut-off was set at  $e^{-20}$ . Signal peptides of dinoflagellate and diatom sequences were truncated according to SignalP results. Alignments of sequences from the other two clades in this study were used to determine the beginning of the mature protein, which were then truncated. The resulting set of TPs was truncated C-terminally to the average TP length in the clade. These sequences were reduced to amino acids that are ionized at a physiological pH by replacing all other amino acids with a dash at each non-charged position in order to extrapolate a WebLogo depiction. These TPs were then divided into N-terminal half and C-terminal half (based on the length of the average TP) to determine the charged amino acid content of each half.

### 6.2.11 Transient Transfection of *Pisum sativum* Leaves

pAVA393 was used as the transfection vector for *Pisum sativum*. All DNA fragments were amplified with Phusion polymerase were restricted with *NcoI* and ligated into *NcoI*-restricted SAP-dephosphorylated vector and sequenced to verify correct orientation. 60mg spherical gold carrier particles with a diameter of 1.5 to 3  $\mu\text{m}$  (Sigma-Aldrich, Deisenhofen) were suspended in 1 mL 96% ethanol and vortexed for 10 minutes. Particles were then pelleted at 22 000 x g for 1 min. and the supernatant decanted. Particles were then washed with ddH<sub>2</sub>O, pelleted once more, and frozen in sterile 50% glycerol. The concentration of midi preps of constructs was determined photometrically with the Nanodrop (peqlab), using their absorbtion at a wavelength of 260 nm. For each construct, 25 $\mu\text{L}$  gold particles, 4  $\mu\text{g}$  plasmid, 20  $\mu\text{L}$  2.5 M CaCl<sub>2</sub>, and 8  $\mu\text{L}$  100 mM spermidine were pipetted together and vortexed for 3 min. and incubated on ice. The loaded particles were then pelleted as before, washed three times with 1 mL absolute ethanol, and then resuspended in 37  $\mu\text{L}$  absolute ethanol. 6 $\mu\text{L}$  of this was used for transfecting each *P. sativum* leaf with a Biolistic PDS-1000/He Particle Delivery System fitted with 900 psi rupture discs. Peas were soaked in water overnight and planted in vermiculite. After 10-14 days at room temperature in sunlight, the youngest leaves were plucked from seedlings and laid on 1.5% agarose in Petri dishes. Bombarded leaves were then incubated in the dark overnight for analysis using a Leica TCS SP2 confocal microscope the following day.

### 6.2.12 Stable Transfection of *Phaeodactylum tricornutum*

For amplification of *A. carterae psbO* and *prk*, Phusion polymerase was used according to the manufacturer's instructions. The vector pPhaT1-eGFP-6xHis was restricted with *EcoRI* and *BamHI* for in frame insertions of *A. carterae* DNA encoding N-terminal extension fragments of PsbO and Prk. The concentration of midi preps of constructs was determined photometrically with the Nanodrop (peqlab), using their absorbtion at a wavelength of 260 nm. Biorad Biolistic transfection of the diatom *Phaeodactylum tricornutum* was accomplished as previously described (Apt et al. 1996). M 10 ( $\varnothing$  0.7 $\mu$ m) tungsten particles were used as microcarriers and prepared as follows. 60 mg of microcarriers were washed with 1 ml 100 % EtOH (HPLC quality) by vortexing for 3 min, whereupon they were pelleted and washed twice with 1 ml sterile ddH<sub>2</sub>O. Carriers were then resuspended in 1 ml sterile ddH<sub>2</sub>O and decanted into 50  $\mu$ l aliquots. Aliquots were then stored at -20 °C until use. Construct DNA was bound to 50  $\mu$ L microcarriers by adding 5  $\mu$ g construct, 50  $\mu$ l 2.5 M CaCl<sub>2</sub>, and 20  $\mu$ l 0.1 M spermidine. The mixture was then vortexed for 1 min and sedimented for 10 min at room temperature. The supernatant was removed, and the particles were washed with 250  $\mu$ l 100 % EtOH (HPLC quality) and vortexed for 30 sec. After sedimentation, the pellet was resuspended in 50  $\mu$ l fresh 100 % EtOH. Biolistic transfection was performed with the Biorad Biolistic PDS-1000/He Particle Delivery System. Each construct was shot thrice. 10  $\mu$ l of the microcarrier-DNA suspension was pipetted upon the center of the macrocarriers. The macrocarriers were then screwed into place for the shot. Biolistic transfection took place in a vacuum of -25 psi. A pressure of 1350 psi was placed on the rupture disk.

A 7-day-old *P. tricornutum* culture was harvested via centrifugation (5 min, 1500 x g). 10<sup>8</sup> cells per transfection were suspended in 100  $\mu$ l F/2 and spread centrally upon an f/2-plate ( $\varnothing$  8,5 cm). Transfected cells were then exposed to light for 24 h (8000 - 11000 Lux) at 22 °C in the MLR-350 climate chamber. Cells were then removed from the plates with 1 ml f/2 medium and distributed evenly among 3 f/2 plates containing 75  $\mu$ g zeocin/ml, sealed with Parafilm and incubated at culturing conditions until colonies were visible.

## 6.3 Protein Studies

### 6.3.1 Brefeldin A Radioactive Labeling of *Amphidinium carterae* Proteins

*Amphidinium carterae* cells were inoculated on day 0 with 200 mL fully grown culture (per L) at hr 8 of their light phase (12:12) and grown for 5 days in F/2 (30% sea salt) or ASP-Medium. On day 6, the cells are going through mitosis for the last time before stationary phase (Ismael et al. 1999). Due to the fact that differing reports exist as to the circadian nature of RbcL, PsbO, and Prk (Mittag et al. 2005; Nassoury et al. 2005; Uribe et al. 2008; Wang et al. 2005), cells were synchronized such to allow for application of radioactivity to occur one hour before anticipation of the onset of light in the circadian rhythm. 0-7.5 mg BFA/L were added from a BFA stock solution (5 mg/mL DMSO) 1 hr before the onset of the light phase, as to allow BFA to inhibit and radioactivity to be imported and incorporated into proteins that may be expressed at or before the onset of light (Nassoury et al. 2001; Wang et al. 2005). The three different <sup>35</sup>S-labelled radioactive compounds utilized from Hartmann Analytic GmbH (Braunschweig, Germany) to determine the maximal absorption and incorporation into protein were <sup>35</sup>S-sulfate, <sup>35</sup>S-methionine, and <sup>35</sup>S-Metmix (70% Methionine, 25% Cysteine, and 5% other non-radioactive amino acids), based upon prior published results concerning the uptake of these substances in various dinoflagellates (Deane and O'Brien 1981; Wang et al. 2005). The culture was then divided into 3 x 333 mL cultures in 500 mL culture flasks (Sarstedt). 3.3 mCi <sup>35</sup>S/L (Harmann Analytical) was added per culture flask and incubated for 1 hr in the dark, ensued by a 4 hr incubation at 150 lux and 20°C. BFA concentrations used were 2.5 µg/mL, 5 µg/mL, and 7.5 µg/mL as determined by empirical experiments. Cells were harvested, concentrated in 1 mL, and washed three times with F/2 containing BFA in accordance with the BFA incubation and then resuspended in solubilization buffer containing protease inhibitor cocktail (PIC) and the same BFA concentration.

#### **Protease inhibitor cocktail (PIC):**

Antipain	50 µl (2 mg/ml)
Chymostatin	20 µl (5 mg/ml)
Aprotinin	50 µl (2 mg/ml)
Trypsin-Inhibitor	20 µl (5 mg/ml)
NaEDTA	50 µl (2 mg/ml)
Pepstatin	50 µl (2 mg/ml)
Leupeptin	20 µl (5 mg/ml)
Elastatinal	100 µl (1 mg/ml)

To the list of inhibitors, 140  $\mu$ l of Hepes-KOH (pH 7.0) was added, so that each inhibitor had a final concentration of 200  $\mu$ g/ml. PIC was used at a concentration of 50  $\mu$ l/mL.

### 6.3.2 Cell lysis (repeated 3 times):

Cells were pelleted again, the supernatant removed, and pellet lysed by shock freezing with liquid nitrogen. Cells were centrifuged at 500 g for 5 min to pellet intact cells. The pellet was then shock frozen in a liquid nitrogen bath and a steel ball bearing was inserted. The sample was then re-immersed into the liquid nitrogen bath and transported to a bead-beating aperture for cell lysis at 30 Hertz for 2.5 min. The Epi was then re-immersed into the nitrogen bath. The pellet was washed with the supernatant from before bead-beating, pelleted as before, the pellet was shock frozen. This process was repeated 5 times. This extract was cleared of intact cells by centrifugation at 500 g for 5 minutes.

### 6.3.3 Semidiscontinuous Sucrose Gradient

Continuous gradients of 20% to 80% sucrose and of 8.5% to 70% sucrose were attempted to adequately separate cell compartments. Discontinuous gradients attempted were 25% step on a continuous 35% to 55% step, both including and excluding a 70% or 80% step. An 8.5% step on a 25% step on a 40% step on a 55% step was also attempted. Cell lysates were also varied from 0% to 8.5%. For these gradients, TBS, Solubilization A, and HB-T (10 mM Triethanolamine, 1 mM EDTA, 250 mM Saccharose, pH7.4) buffers were attempted.

The following gradient was chosen. Sucrose solutions of 20%, 30%, 50%, 55%, and 80% were dissolved in Solubilization Buffer A. A 0.5 mL sucrose step was pipetted upon a 1.5 mL 80% step. The 30% to 50% continuous gradient was mixed with 20 bubbles in a 10 mL glass pipette containing 3 mL 30% layered upon 2.5 mL 50%. A 1.5 mL 20% sucrose step was carefully pipetted upon the continuous portion of the gradient in the polyallomer centrifuge tube. 1 mL cell extract was carefully pipetted upon the 20% sucrose step. Fractionation then took place by overnight centrifugation at 30 000 rpm in a Sorvall TH-641 rotor in a Centrikon T-1080 ultracentrifuge:



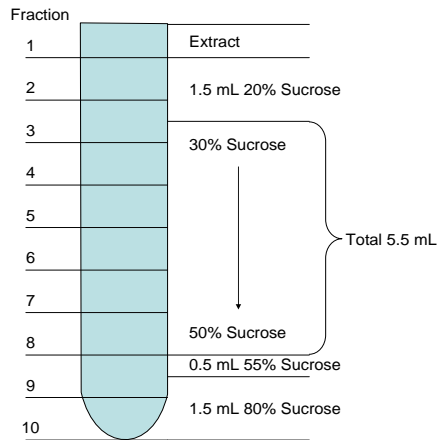


**Figure 46. Pipetting Scheme for Sucrose Fractionation.**

1 mL Fractions were pipetted from top to bottom of the gradient, scintillized (5 $\mu$ L used), and TCA precipitated. The first supernatant from TCA precipitation was scintillized (5 $\mu$ L used) to determine what proportion of the radioactivity was actually incorporated into protein and how much was present in the cell as free methionine, cysteine, or sulfate.

**Solubilization Buffer A:**

50 mM Imidazol/HCl pH7,5  
 50 mM NaCl  
 2 mM 6-Amino-Capronsäure  
 1 mM EDTA

**6.3.4 Fraction Preparation for Immunoprecipitation (IP):**

Samples were TCA precipitated by adding 150  $\mu$ L 70% TCA solution to each 1 mL fraction and incubating on ice for 10 min, whereupon protein was pelleted for 10 min at 20000x g. Protein pellets from each fraction were then washed thrice with ice-cold 80% acetone. The pellet was then dried in the Eppendorf Thermomixer at 70°C for ca. 5 min with 1400 rpm shaking (as to avoid spontaneous boiling). The dried pellets were then resuspended in 100 $\mu$ L Resuspension Buffer (RB), boiled for 10 min with shaking, and dissolved completely with a pestle. This solution was then diluted to 1 mL with IP buffer and heated to 70°C for 10 min with shaking, allowed to cool, scintillized (5 $\mu$ L used per 1 mL scintillation reagent), and then applied to prepared IP beads.

**RB:**

50 mM Tris/HCl, pH7.5  
 1 mM EDTA  
 1% (w/v) SDS

**IP Buffer:**

0.5% (w/v) Tween 20  
 50 mM Tris/HCl pH 7.5  
 150 mM NaCl  
 0.1 mM EDTA



### 6.3.5 Sepharose A Bead Preparation and Immunoprecipitation

100  $\mu$ l Sepharose beads were aliquoted, pelleted 10 sec, 6000x g, and washed thrice with 1 mL PBS. Beads were then resuspended in 100  $\mu$ L IP buffer containing 5  $\mu$ g specific primary antibody in Eppendorf tubes, which were incubated in a 50 mL Falcon tube at 4°C overnight. Beads were washed three times with 1 mL IP buffer. Extracts and beads were incubated overnight in Eppendorf tubes in Falcon tubes under constant agitation with a roller mixer. IP beads were washed three times with 1 mL TBS-T and then eluted by application of 50  $\mu$ L 2x Laemli SDS sample buffer and incubated at 95°C for 5-10 min. Fractions were then electrophoretically separated with 12.5% SDS-polyacrylamide gels (Laemmli 1970).

### 6.3.6 Semi-Dry Western Blot

In order to immobilize proteins for detection, proteins were transferred from the SDS gel to a nitrocellulose membrane. 6 pleats of Whatman paper, the SDS gel containing the proteins, as well as the nitrocellulose membrane were inundated with Transfer Buffer. Between the anode and the cathode, 3 pleats of Whatman paper were laid above and below the gel and nitrocellulose membrane. Proteins were immobilized by applying 1 mA/cm<sup>2</sup> and a maximum of 50 V for 1 hr to the sandwiched gel, whereupon proteins migrate away from the negatively charge and adhere to the positively charged membrane, where they are exposed sufficiently for immunodetection or 4 day incubation for autoradiography development with a StormJet scanner.

#### **Transfer Buffer:**

25 mM Tris/HCl pH 8.4  
192 mM Glycin  
20% (v/v) Methanol

### 6.3.7 Immunodetection of Proteins

Western blotted nitrocellulose membranes were saturated with protein by incubating in blocking reagent (5% [w/v] skim milk powder in TBS-T for antibody reactions and 5% [w/v] glutamate powder in TBS-T for WGA-HRP) for 1 h at room temperature. Primary antibodies were then added to the reagent for overnight incubation at 4°C. Western blots were then washed thrice with TBS-T and incubated for 1 hr with the horse radish peroxidase-coupled secondary antibody (1:10000) in blocking reagent. Blots were washed thrice with TBS-T, the last of which was incubated on the roller mixer for 30 min. Detection took place by

incubating drip-dry blots for 2 min in 5 mL ECL solution. The membrane was then drip-dried and applied to Seran wrap (Dupont, USA), which was then applied to an X-ray film in an X-ray film cassette. X-ray film incubation was dependent on signal intensity, varying as much as 5 sec to overnight. Films were developed with Kodak developer solution, washed shortly with water, fixed in Kodak fixation solution, and washed in water once more before air-drying.

### **ECL Solution**

400  $\mu$ l 250 mM Luminol in DMSO  
178  $\mu$ l 90 mM Coomarcic acid in DMSO  
4 ml 1 M Tris/HCl, pH 8.5  
Ad 20 ml  $dH_2O$   
1:1000 30% (v/v)  $H_2O_2$  (added directly before use)

A commercially available global antibody was obtained for the large subunit of Rubisco (RbcL). Antibodies were synthesized against epitopes for Prk and PsbO sequence in functional domains of the mature protein that are conserved in all dinoflagellate PsbO and Prk sequences. An antibody for the protein Cellulase was likewise synthesized as a marker protein for the plasma membrane (Kwok and Wong 2010). With Western blot analyses, PsbO, RbcL, Cellulase, and Prk were shown to detect ~30kDa, ~55kDa, ~60kDa, and ~35kDa proteins, respectively, which were within the expected parameters for these proteins based on cDNA sequences.

### 6.3.8 Stripping Western Blots

Western blots allowed for multiple immunodetections using a single blot. In order to accomplish this, antibodies were stripped from their epitopes by incubation in 25 mL Stripping Reagent at 70°C for 1 hr. The blot was then washed with tap water and blocked again with Blocking Reagent and immunodetection reinitiated with another primary antibody, as above.

### **Stripping Reagent:**

300 mM Tris/HCl, pH 6.7  
2% (w/v) SDS  
0.7% (v/v) 2-Mercaptoethanol

## 6.4 Electron Microscopy

Cells were grown as described above for radioactive labeling. BFA was added at a concentration of 2.5  $\mu\text{g}/\text{mL}$  for electron microscopic examination of the effects of BFA on *Amphidinium carterae* ultrastructure.

### 6.4.1 Freeze Substitution

*A. carterae* cells were harvest via centrifugation. Freeze substitution was executed by applying cells to a copper wire loop and quickly freezing the cells manually in liquid propanol. Cells were then stored in liquid nitrogen until substitution. 0.5% EM grade glutaraldehyde from 70% ampule dissolved in 100% Acetone was used to fix cells at  $-90^{\circ}\text{C}$  over the course of 3 days. The temperature was then raised gradually to  $-60^{\circ}\text{C}$  for 8 hrs and then  $-30^{\circ}\text{C}$  for another 8 hrs. Samples were then washed three times with acetone. Cells were then incubated on ice in two hr steps of LR White-to-acetone dilutions of 1:2, 1:1, and 2:1, which served to fully and gradually impregnate the cells with polymer. Undiluted LR White was then polymerized in indirect sunlight until hardened (4 days), which was finished with UV radiation overnight at  $4^{\circ}\text{C}$ . LR White blocks containing freeze-substituted BFA-treated and untreated cells were cut into ultrathin slices with a diamond knife (Dupont, USA) on the microtome. Slices were then mounted on copper nets and were either labeled with immunogold or contrasted with a saturated lead citrate solution followed by a saturated uranyl acetate solution and then 1% osmium tetroxide in 0.1 M phosphate buffer, pH 7.4 for direct visualization via EM.

### 6.4.2 Immunogold Labeling

Electron micrographs were produced to determine the subcellular localization of proteins using primary antibodies detected with secondary antibodies coupled to 30nm gold particles. Slices mounted on copper nets were incubated for 15 min in TBS containing 1% BSA. After drying, slices were incubated in TBS containing primary antibody for 4 hrs (or in the case of RbcL overnight at  $4^{\circ}\text{C}$  in a moisture chamber), whereupon they were washed thrice with TBS-T and thrice with ddH<sub>2</sub>O. Gold-coupled secondary antibody was then applied at 1 to 140 for 45 min. After washing thrice with ddH<sub>2</sub>O, slices were contrasted with a saturated lead citrate solution, washed thrice with ddH<sub>2</sub>O, stained with a saturated uranyl acetate

solution, then thrice with ddH<sub>2</sub>O and dried. Slices were then stored dry at 16°C until viewing with electron microscope.

## 7 APPENDIX

### 7.1 Microsoft Excel Macro

For section 3.1.2, the following macro was written for Microsoft Excel for use in deleting redundant homologies BLAST hits from the NCBI local BLAST program v2.2.22:

```

Sub blast()
'
' blast Makro
' Makro am 17.02.2010 von Andrew aufgezeichnet
'
' Tastenkombination: Strg+ü
'
Columns("C:J").Select
Selection.Delete Shift:=xlToLeft
Columns("D:D").Select
Selection.Delete Shift:=xlToLeft
Cells.Select
Selection.Sort Key1:=Range("C1"), Order1:=xlAscending, Header:=xlGuess,
-
OrderCustom:=1, MatchCase:=False, Orientation:=xlTopToBottom, _
DataOption1:=xlSortNormal
Range("D1").Select
ActiveCell.FormulaR1C1 = "=IF(RC[-1]<0.000000001,RC[-3],\"\")"
Range("D1").Select
Selection.AutoFill Destination:=Columns("D:D")
Range("E1").Select
ActiveCell.FormulaR1C1 = "=IF(RC[-2]<0.000000001,RC[-3],\"\")"
Range("E1").Select
Selection.AutoFill Destination:=Columns("E:E")
Columns("E:E").Select
Range("F1").Select
ActiveCell.FormulaR1C1 = "=IF(RC[-3]<0.000000001,RC[-3],\"\")"
Range("F1").Select
Selection.AutoFill Destination:=Columns("F:F")
Columns("F:F").Select
Columns("D:F").Select
Selection.Copy
Selection.PasteSpecial Paste:=xlPasteValues, Operation:=xlNone,
SkipBlanks _
:=False, Transpose:=False
Columns("A:C").Select
Application.CutCopyMode = False
Selection.Delete Shift:=xlToLeft
Cells.Select
Selection.Sort Key1:=Range("B1"), Order1:=xlAscending, Header:=xlGuess,
-
OrderCustom:=1, MatchCase:=False, Orientation:=xlTopToBottom, _
DataOption1:=xlSortNormal
Selection.Sort Key1:=Range("B1"), Order1:=xlDescending, Header:=xlGuess,
-
OrderCustom:=1, MatchCase:=False, Orientation:=xlTopToBottom, _
DataOption1:=xlSortNormal
Selection.Sort Key1:=Range("B1"), Order1:=xlAscending, Header:=xlGuess,
-
OrderCustom:=1, MatchCase:=False, Orientation:=xlTopToBottom, _
DataOption1:=xlSortNormal

```

```

Range("D2").Select
ActiveCell.FormulaR1C1 = "=IF(RC[-2]=R[-1]C[-2],"",RC[-3])"
Range("E2").Select
ActiveCell.FormulaR1C1 = "=IF(RC[-3]=R[-1]C[-3],"",RC[-3])"
Range("F2").Select
ActiveCell.FormulaR1C1 = "=IF(RC[-4]=R[-1]C[-4],"",RC[-3])"
Range("D2:F2").Select
Selection.AutoFill Destination:=Range("D2:F65536"), Type:=xlFillDefault
Range("D2:F65536").Select
Columns("D:F").Select
Range("D65486").Activate
Selection.Copy
Selection.PasteSpecial Paste:=xlPasteValues, Operation:=xlNone,
SkipBlanks _
:=False, Transpose:=False
Columns("A:C").Select
Range("A65486").Activate
Application.CutCopyMode = False
Selection.Delete Shift:=xlToLeft
Cells.Select
Range("A65486").Activate
Selection.Sort Key1:=Range("C1"), Order1:=xlAscending, Header:=xlGuess,
_
OrderCustom:=1, MatchCase:=False, Orientation:=xlTopToBottom, _
DataOption1:=xlSortNormal
Range("E34").Select
End Sub

```

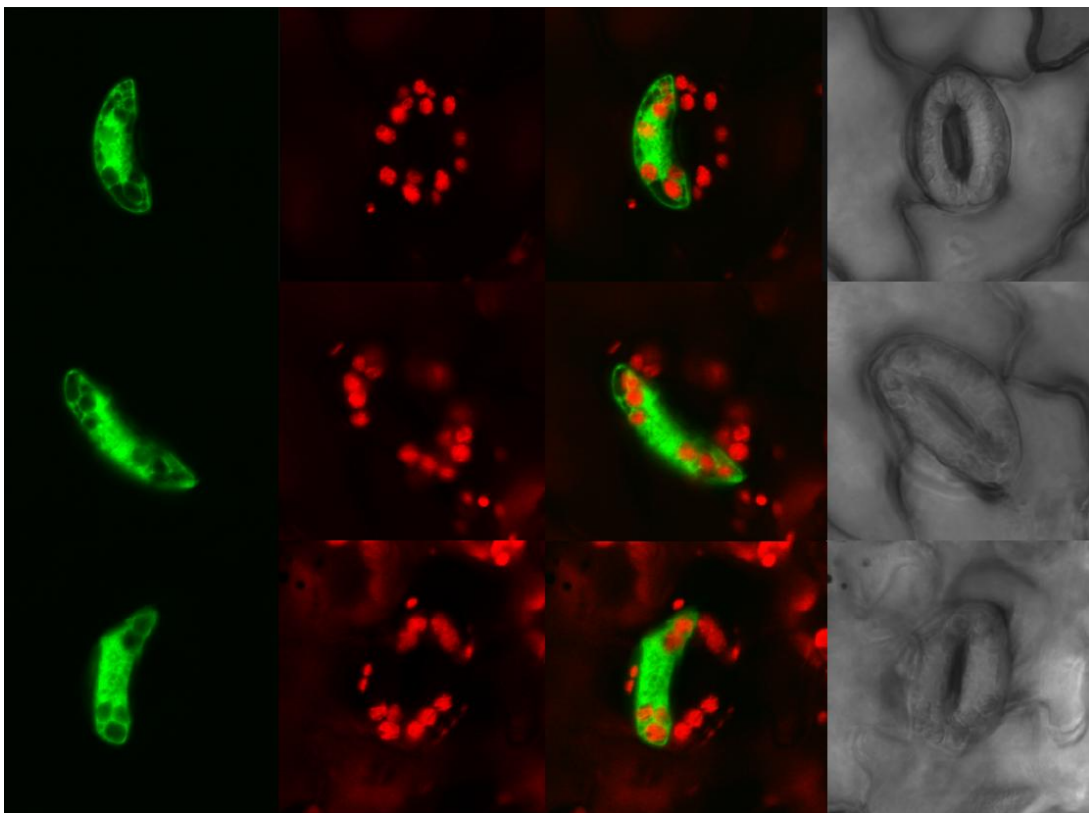
## 7.2 Standard deviations (SD) Relative Amino Acid Abundances in Plant and Diatom TPs.

These standard deviations were used in the discussion of figure 17.

<b>Amino Acid Type</b>	<b>Basic</b>	<b>Acidic</b>	<b>Hydroxylated</b>	<b>Polar neutral</b>	<b>Non-polar Neutral</b>
<b>Dinoflagellate SD</b>	5%	3%	5%	5%	6%
<b>Plants SD</b>	3%	3%	6%	5%	9%
<b>Diatoms SD</b>	3%	5%	2%	5%	8%

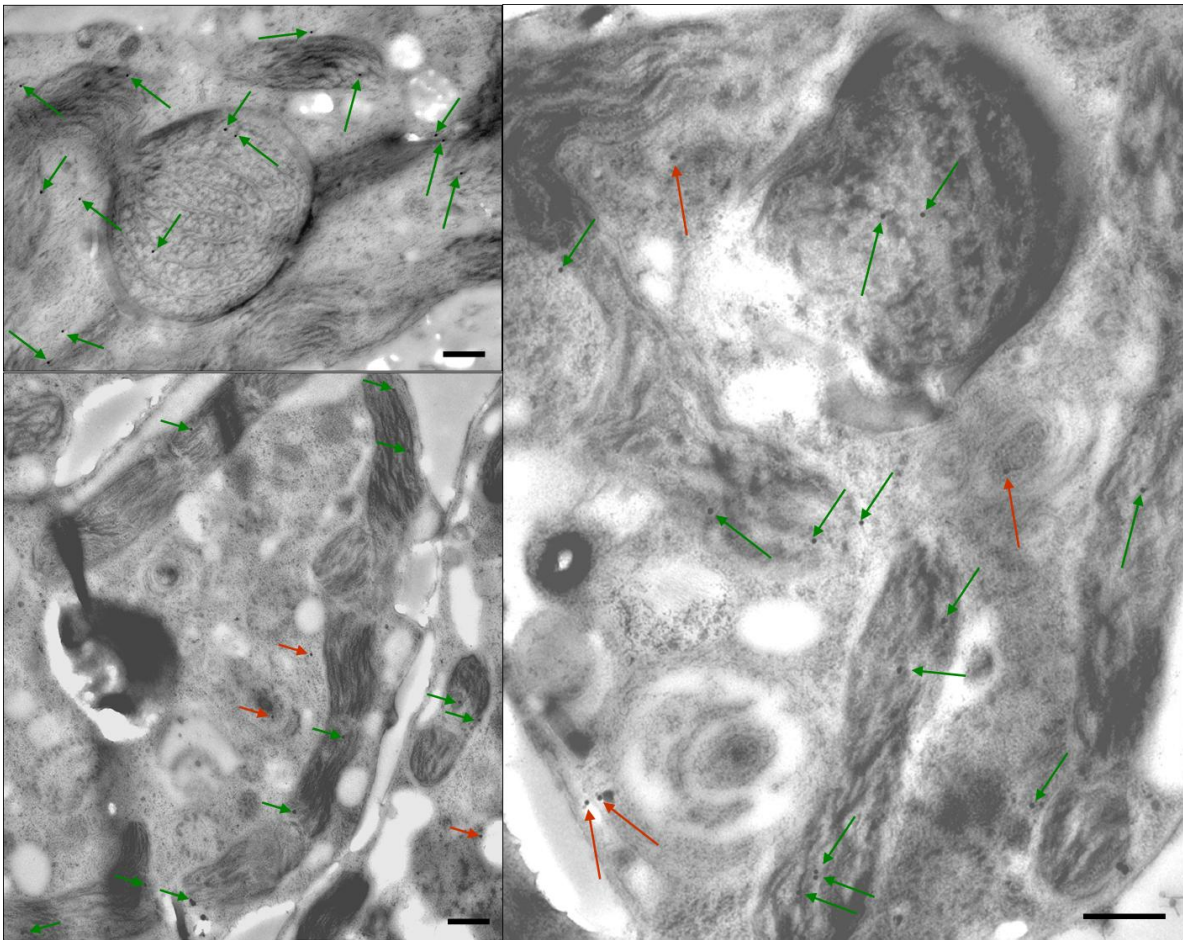
### 7.3 Heterologous Transfection of *Pisum sativum* with eGFP Fused N-terminally to Truncated TPs from *Ceratium horridum* PsbO and Prk N-terminal Extensions.

These results are an addendum to section 3.2.1. **Top:** eGFP fluorescence from eGFP fused N-terminally to the full-length PsbO TP. **Middle:** eGFP fluorescence from eGFP fused N-terminally to the PsbO TP without the hydrophobic thylakoid targeting domain. **Bottom:** eGFP fluorescence from eGFP fused N-terminally to the full-length Prk TP. **From left to right:** eGFP fluorescence, chloroplast autofluorescence, merge, DIC. **Green:** eGFP fluorescence, **Red:** Autofluorescence.



7.4 1:50  $\alpha$ -PsbO Immunogold Labeling of Untreated *Amphidinium carterae* Cells Fixed via Freeze Substitution.

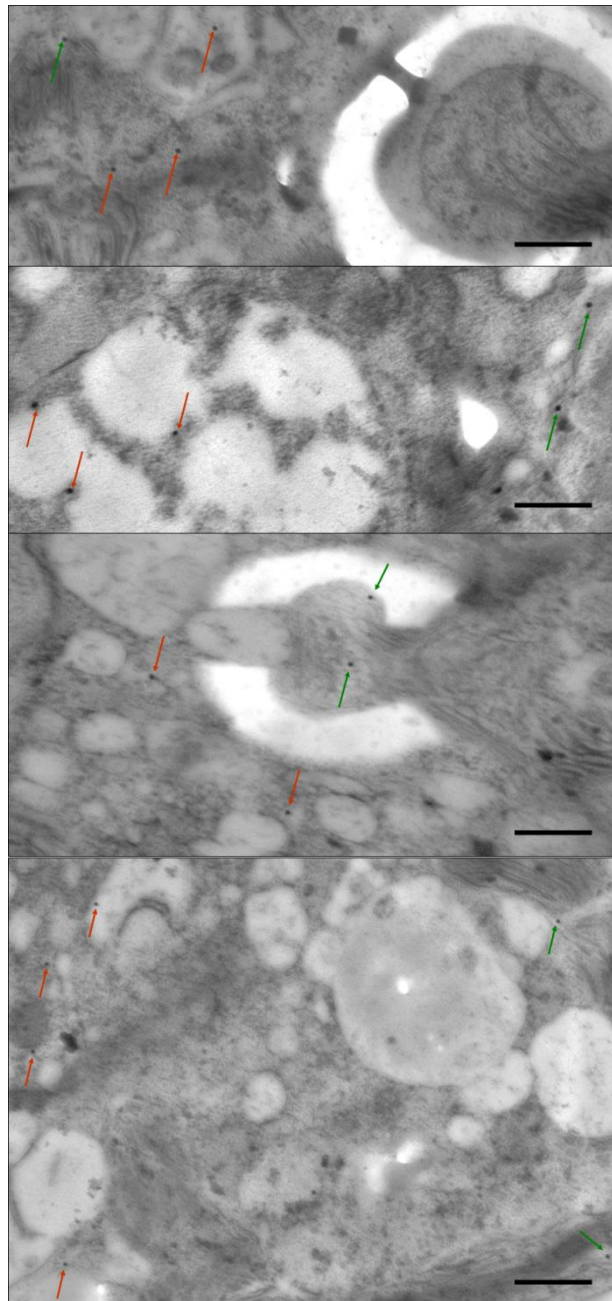
This is a supplement to figure 39. **Green Arrows:** indicate signal arising from the plastids. **Red Arrows:** indicate signal arising from the endomembrane system. **Bar:** 500 nm.





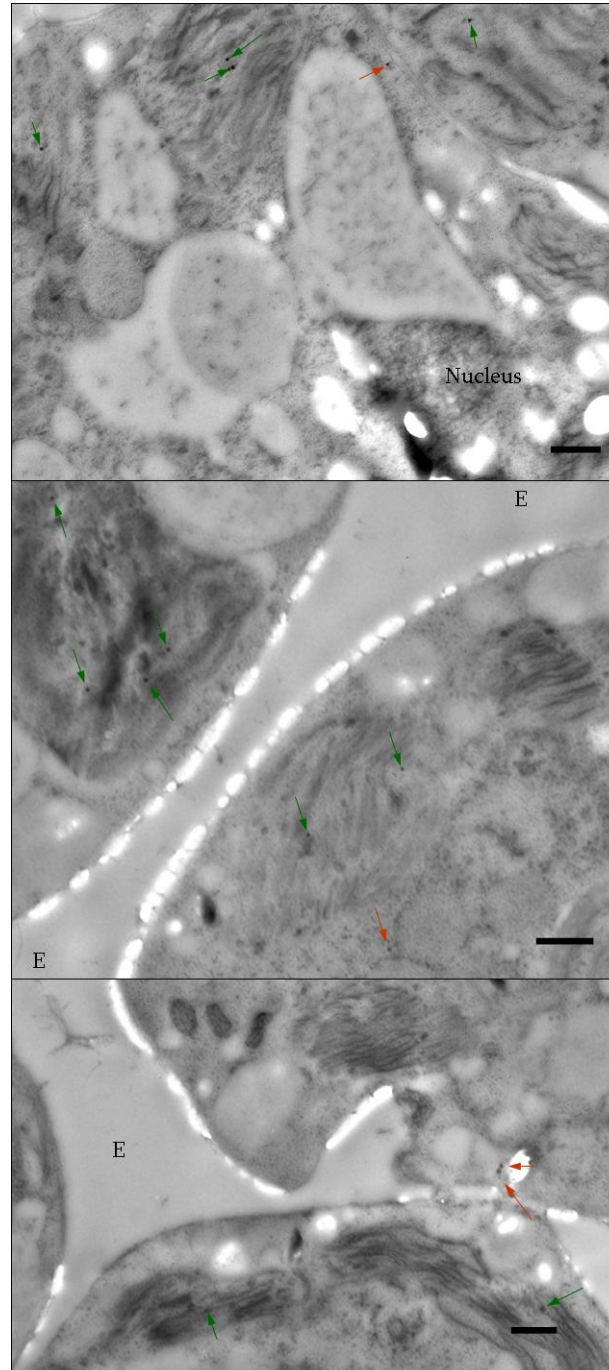
7.5 1:50  $\alpha$ -PsbO Immunogold Labeling of *Amphidinium carterae* Cells  
treated with 2.5  $\mu$ g BFA/mL and Fixed via Freeze Substitution.

This is a supplement to figure 40. **Green Arrows:** indicate signal arising from the plastids. **Red Arrows:** indicate signal arising from the periphery of fused endomembrane system. **Bar:** 500 nm.



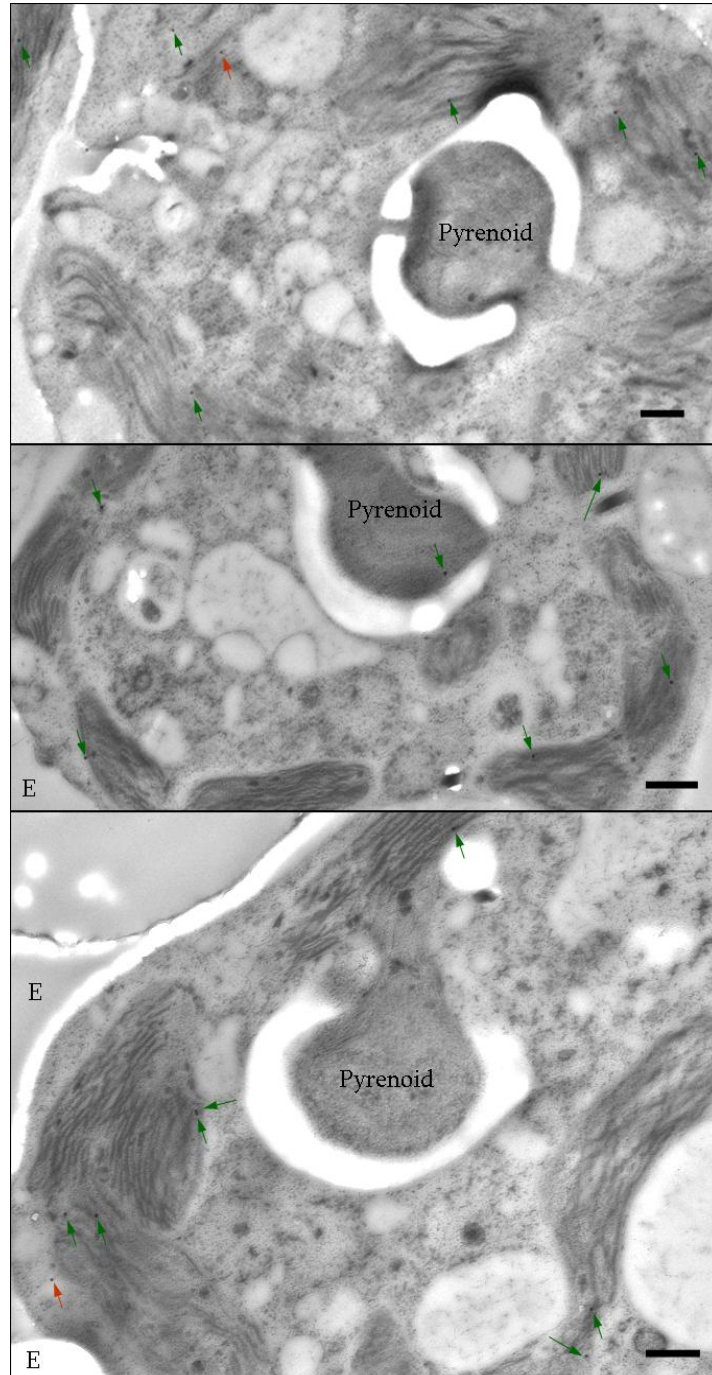
7.6 1:2200  $\alpha$ -RbcL Immunogold Labeling of *Amphidinium carterae*  
Untreated Cells Fixed via Freeze Substitution.

This is a supplement to figure 41. **Green Arrows:** indicate signal arising from the plastids. **Red Arrows:** indicate signal arising from the periphery of fused endomembrane system. **E:** external to cell. **Bar:** 500 nm.



7.7 1:2200  $\alpha$ -RbcL Immunogold Labeling of *Amphidinium carterae* Cells treated with 2.5  $\mu$ g BFA/mL and Fixed via Freeze Substitution.

This is a supplement to figure 42. **Green Arrows:** indicate signal arising from the plastids. **Red Arrows:** indicate signal arising from the periphery of fused endomembrane system. **E:** external to cell. **Bar:** 500 nm.



## 8 References

- Adl, S. M., A. G. Simpson, et al. (2005). "The New Higher Level Classification of Eukaryotes with Emphasis on the Taxonomy of Protists." J Eukaryot Microbiol **52**(5): 399-451.
- Agrawal, S., G. G. van Dooren, et al. (2009). "Genetic Evidence That an Endosymbiont-Derived Endoplasmic Reticulum-Associated Protein Degradation (Erad) System Functions in Import of Apicoplast Proteins." J Biol Chem **284**(48): 33683-91.
- Allen, J. F. (2003). "Why Chloroplasts and Mitochondria Contain Genomes." Comp Funct Genomics **4**(1): 31-6.
- Allen, J. F. (2005). "Photosynthesis: The Processing of Redox Signals in Chloroplasts." Curr Biol **15**(22): R929-32.
- Apt, K. E., P. G. Kroth-Pancic, et al. (1996). "Stable Nuclear Transformation of the Diatom *Phaeodactylum Tricornutum*." Mol Gen Genet **252**(5): 572-9.
- Apt, K. E., L. Zaslavkaia, et al. (2002). "In Vivo Characterization of Diatom Multipartite Plastid Targeting Signals." J Cell Sci **115**(Pt 21): 4061-9.
- Archibald, J. M. (2009). "The Puzzle of Plastid Evolution." Curr Biol **19**(2): R81-8.
- Archibald, J. M. and C. E. Lane (2009). "Going, Going, Not Quite Gone: Nucleomorphs as a Case Study in Nuclear Genome Reduction." J Hered **100**(5): 582-90.
- Armbrust, E. V. (2009). "The Life of Diatoms in the World's Oceans." Nature **459**(7244): 185-92.
- Armbrust, E. V., J. A. Berges, et al. (2004). "The Genome of the Diatom *Thalassiosira Pseudonana*: Ecology, Evolution, and Metabolism." Science **306**(5693): 79-86.
- Bachvaroff, T. R., G. T. Concepcion, et al. (2004). "Dinoflagellate Expressed Sequence Tag Data Indicate Massive Transfer of Chloroplast Genes to the Nuclear Genome." Protist **155**(1): 65-78.
- Bachvaroff, T. R., M. V. Sanchez-Puerta, et al. (2006). "Rate Variation as a Function of Gene Origin in Plastid-Derived Genes of Peridinin-Containing Dinoflagellates." J Mol Evol **62**(1): 42-52.
- Bachvaroff, T. R., M. V. Sanchez Puerta, et al. (2005). "Chlorophyll C-Containing Plastid Relationships Based on Analyses of a Multigene Data Set with All Four Chromalveolate Lineages." Mol Biol Evol **22**(9): 1772-82.
- Baldauf, S. L., A. J. Roger, et al. (2000). "A Kingdom-Level Phylogeny of Eukaryotes Based on Combined Protein Data." Science **290**(5493): 972-7.
- Barbrook, A. C. and C. J. Howe (2000). "Minicircular Plastid DNA in the Dinoflagellate *Amphidinium Operculatum*." Mol Gen Genet **263**(1): 152-8.

## References

---

- Barbrook, A. C., S. Visram, et al. (2006). "Molecular Diversity of Dinoflagellate Symbionts of Cnidaria: The Psba Minicircle of Symbiodinium." Protist **157**(2): 159-71.
- Baurain, D., H. Brinkmann, et al. (2010). "Phylogenomic Evidence for Separate Acquisition of Plastids in Cryptophytes, Haptophytes and Stramenopiles." Mol Biol Evol.
- Benning, C. (2009). "Mechanisms of Lipid Transport Involved in Organelle Biogenesis in Plant Cells." Annu Rev Cell Dev Biol **25**: 71-91.
- Bhattacharya, D., J. M. Archibald, et al. (2007). "How Do Endosymbionts Become Organelles? Understanding Early Events in Plastid Evolution." Bioessays **29**(12): 1239-46.
- Bhaud, Y., D. Guillebault, et al. (2000). "Morphology and Behaviour of Dinoflagellate Chromosomes During the Cell Cycle and Mitosis." J Cell Sci **113** ( Pt 7): 1231-9.
- Bhaya, D. and A. Grossman (1991). "Targeting Proteins to Diatom Plastids Involves Transport through an Endoplasmic Reticulum." Mol Gen Genet **229**(3): 400-4.
- Bodyl, A., P. Mackiewicz, et al. (2009a). "Early Steps in Plastid Evolution: Current Ideas and Controversies." Bioessays **31**(11): 1219-32.
- Bodyl, A., J. W. Stiller, et al. (2009b). "Chromalveolate Plastids: Direct Descent or Multiple Endosymbioses?" Trends Ecol Evol **24**(3): 119-21; author reply 121-2.
- Bolte, K., L. Bullmann, et al. (2009). "Protein Targeting into Secondary Plastids." J Eukaryot Microbiol **56**(1): 9-15.
- Bonifacino, J. S. and R. Rojas (2006). "Retrograde Transport from Endosomes to the Trans-Golgi Network." Nat Rev Mol Cell Biol **7**(8): 568-79.
- Bowler, C., A. E. Allen, et al. (2008). "The Phaeodactylum Genome Reveals the Evolutionary History of Diatom Genomes." Nature **456**(7219): 239-44.
- Bravo, I., R. I. Figuero, et al. (2010). "The Intricacies of Dinoflagellate Pellicle Cysts: The Example of Alexandrium Minutum Cysts from a Bloom-Recurrent Area (Bay of Baiona, Nw Spain)." Deep Sea Research Part II: Topical Studies in Oceanography **57**(3-4): 166-174.
- Bruce, B. D. (2001). "The Paradox of Plastid Transit Peptides: Conservation of Function Despite Divergence in Primary Structure." Biochim Biophys Acta **1541**(1-2): 2-21.
- Buick, R. (2008). "When Did Oxygenic Photosynthesis Evolve?" Philos Trans R Soc Lond B Biol Sci **363**(1504): 2731-43.
- Bullmann, L., R. Haarmann, et al. (2010). "Filling the Gap, Evolutionarily Conserved Omp85 in Plastids of Chromalveolates." J Biol Chem **285**(9): 6848-56.
- Burki, F., K. Shalchian-Tabrizi, et al. (2007). "Phylogenomics Reshuffles the Eukaryotic Supergroups." PLoS One **2**(8): e790.

## References

---

- Cavalier-Smith, T. (1987a). "The Origin of Eukaryotic and Archaeobacterial Cells." Ann N Y Acad Sci **503**: 17-54.
- Cavalier-Smith, T. (1987b). "The Simultaneous Symbiotic Origin of Mitochondria, Chloroplasts, and Microbodies." Ann N Y Acad Sci **503**: 55-71.
- Cavalier-Smith, T. (1991). "Cell Diversification in Heterotrophic Flagellates." The Biology of Free-living Heterotrophic Flagellates.(Oxford (UK):Clarendon Press): 113–131.
- Cavalier-Smith, T. (1998). "A Revised Six-Kingdom System of Life." Biol Rev Camb Philos Soc **73**(3): 203-66.
- Cavalier-Smith, T. (1999). "Principles of Protein and Lipid Targeting in Secondary Symbiogenesis: Euglenoid, Dinoflagellate, and Sporozoan Plastid Origins and the Eukaryote Family Tree." J Eukaryot Microbiol **46**(4): 347-66.
- Cavalier-Smith, T. (2002). "The Phagotrophic Origin of Eukaryotes and Phylogenetic Classification of Protozoa." Int J Syst Evol Microbiol **52**(Pt 2): 297-354.
- Cavalier-Smith, T. (2003). "Genomic Reduction and Evolution of Novel Genetic Membranes and Protein-Targeting Machinery in Eukaryote-Eukaryote Chimaeras (Meta-Algae)." Philos Trans R Soc Lond B Biol Sci **358**(1429): 109-33; discussion 133-4.
- Cavalier-Smith, T. (2006). "Origin of Mitochondria by Intracellular Enslavement of a Photosynthetic Purple Bacterium." Proc Biol Sci **273**(1596): 1943-52.
- Chaal, B. K. and B. R. Green (2005). "Protein Import Pathways in 'Complex' Chloroplasts Derived from Secondary Endosymbiosis Involving a Red Algal Ancestor." Plant Mol Biol **57**(3): 333-42.
- Chaal, B. K., K. Ishida, et al. (2003). "A Thylakoidal Processing Peptidase from the Heterokont Alga *Heterosigma Akashiwo*." Plant Mol Biol **52**(2): 463-72.
- Chen, C. and H. Chou (2001). "Ichthyotoxicity Studies of Milkfish *Chanos Chanos* Fingerlings Exposed to a Harmful Dinoflagellate *Alexandrium Minutum*." J Exp Mar Bio Ecol **262**(2): 211-219.
- Cramm-Behrens, C. I., M. Dienst, et al. (2008). "Apical Cargo Traverses Endosomal Compartments on the Passage to the Cell Surface." Traffic **9**(12): 2206-20.
- Daley, D. O. and J. Whelan (2005). "Why Genes Persist in Organelle Genomes." Genome Biol **6**(5): 110.
- de Duve, C. (2007). "The Origin of Eukaryotes: A Reappraisal." Nat Rev Genet **8**(5): 395-403.
- Deane, E. M. and R. W. O'Brien (1981). "Uptake of Sulphate, Taurine, Cysteine and Methionine by Symbiotic and Free-Living Dinoflagellates." Archives of Microbiology **128**: 311-319.
- Delwiche, C. F. (1999). "Tracing the Thread of Plastid Diversity through the Tapestry of Life." Am Nat **154**(S4): S164-S177.

## References

---

- Delwiche, C. F. and J. D. Palmer (1996). "Rampant Horizontal Transfer and Duplication of Rubisco Genes in Eubacteria and Plastids." Mol Biol Evol **13**(6): 873-82.
- DeRocher, A., B. Gilbert, et al. (2005). "Dissection of Brefeldin a-Sensitive and -Insensitive Steps in Apicoplast Protein Targeting." J Cell Sci **118**(Pt 3): 565-74.
- Dodge, J. and C. Gruet (1987). "Dinoflagellate Ultrastructure and Complex Organelles. ." The biology of dinoflagellates.: Boston (MA): Blackwell. pp. 92–142.
- Douglas, S., S. Zauner, et al. (2001). "The Highly Reduced Genome of an Enslaved Algal Nucleus." Nature **410**(6832): 1091-6.
- Durnford, D. G. and M. W. Gray (2006). "Analysis of Euglena Gracilis Plastid-Targeted Proteins Reveals Different Classes of Transit Sequences." Eukaryot Cell **5**(12): 2079-91.
- Elias, M. and J. M. Archibald (2009). "Sizing up the Genomic Footprint of Endosymbiosis." Bioessays **31**(12): 1273-9.
- Emanuelsson, O., H. Nielsen, et al. (1999). "Chlorop, a Neural Network-Based Method for Predicting Chloroplast Transit Peptides and Their Cleavage Sites." Protein Sci **8**(5): 978-84.
- Embley, T. M. and W. Martin (2006). "Eukaryotic Evolution, Changes and Challenges." Nature **440**(7084): 623-30.
- Falcon, L. I., S. Magallon, et al. (2010). "Dating the Cyanobacterial Ancestor of the Chloroplast." ISME J.
- Falkowski, P. G., M. E. Katz, et al. (2004). "The Evolution of Modern Eukaryotic Phytoplankton." Science **305**(5682): 354-60.
- Fast, N. M., L. Xue, et al. (2002). "Re-Examining Alveolate Evolution Using Multiple Protein Molecular Phylogenies." J Eukaryot Microbiol **49**(1): 30-7.
- Felsenstein, J. (1985). "Confidence Limits on Phylogenies: An Approach Using the Bootstrap." Evolution **39**: 783-791.
- Felsner, G., M. S. Sommer, et al. (submitted). "The Physical and Functional Borders of Transit Peptide-Like Sequences in Secondary Endosymbionts." BMC Plant Biology.
- Foth, B. J., S. A. Ralph, et al. (2003). "Dissecting Apicoplast Targeting in the Malaria Parasite Plasmodium Falciparum." Science **299**(5607): 705-8.
- Funes, S., E. Davidson, et al. (2002). "A Green Algal Apicoplast Ancestor." Science **298**(5601): 2155.
- Gaskins, E., S. Gilk, et al. (2004). "Identification of the Membrane Receptor of a Class Xiv Myosin in Toxoplasma Gondii." J Cell Biol **165**(3): 383-93.



## References

---

- Gibbs, S. P. (1979). "The Route of Entry of Cytoplasmically Synthesized Proteins into Chloroplasts of Algae Possessing Chloroplast Er." J Cell Sci **35**: 253-66.
- Gilson, P. R., V. Su, et al. (2006). "Complete Nucleotide Sequence of the Chlorarachniophyte Nucleomorph: Nature's Smallest Nucleus." Proc Natl Acad Sci U S A **103**(25): 9566-71.
- Gomez, S. M., K. Y. Bil, et al. (2003). "Transit Peptide Cleavage Sites of Integral Thylakoid Membrane Proteins." Mol Cell Proteomics **2**(10): 1068-85.
- Gould, S. B., E. Fan, et al. (2007). "Translocation of a Phycoerythrin Alpha Subunit across Five Biological Membranes." J Biol Chem **282**(41): 30295-302.
- Gould, S. B., M. S. Sommer, et al. (2006a). "Protein Targeting into the Complex Plastid of Cryptophytes." J Mol Evol **62**(6): 674-81.
- Gould, S. B., M. S. Sommer, et al. (2006b). "Nucleus-to-Nucleus Gene Transfer and Protein Retargeting into a Remnant Cytoplasm of Cryptophytes and Diatoms." Mol Biol Evol **23**(12): 2413-22.
- Gould, S. B., R. F. Waller, et al. (2008). "Plastid Evolution." Annu Rev Plant Biol **59**: 491-517.
- Gray, M. W., G. Burger, et al. (2001). "The Origin and Early Evolution of Mitochondria." Genome Biol **2**(6): REVIEWS1018.
- Gross, J. and D. Bhattacharya (2009). "Mitochondrial and Plastid Evolution in Eukaryotes: An Outsiders' Perspective." Nat Rev Genet **10**(7): 495-505.
- Gruber, A., S. Vugrinec, et al. (2007). "Protein Targeting into Complex Diatom Plastids: Functional Characterisation of a Specific Targeting Motif." Plant Mol Biol **64**(5): 519-30.
- Guindon, S. and O. Gascuel (2003). "A Simple, Fast, and Accurate Algorithm to Estimate Large Phylogenies by Maximum Likelihood." Syst Biol **52**(5): 696-704.
- Hackett, J. D., D. M. Anderson, et al. (2004a). "Dinoflagellates: A Remarkable Evolutionary Experiment." American Journal of Botany **91**: 1523-1534.
- Hackett, J. D., T. E. Scheetz, et al. (2005). "Insights into a Dinoflagellate Genome through Expressed Sequence Tag Analysis." BMC Genomics **6**(1): 80.
- Hackett, J. D., H. S. Yoon, et al. (2004b). "Migration of the Plastid Genome to the Nucleus in a Peridinin Dinoflagellate." Curr Biol **14**(3): 213-8.
- Harper, J. D., J. Thuet, et al. (2009). "Proteins Related to Green Algal Striated Fiber Assemblin Are Present in Stramenopiles and Alveolates." Protoplasma **236**(1-4): 97-101.
- Harper, J. T., E. Waanders, et al. (2005). "On the Monophyly of Chromalveolates Using a Six-Protein Phylogeny of Eukaryotes." Int J Syst Evol Microbiol **55**(Pt 1): 487-96.
- Hempel, F., A. Bozarth, et al. (2007). "Transport of Nuclear-Encoded Proteins into Secondarily Evolved Plastids." Biol Chem **388**(9): 899-906.



## References

---

- Hempel, F., L. Bullmann, et al. (2009). "Erad-Derived Preprotein Transport across the Second Outermost Plastid Membrane of Diatoms." Mol Biol Evol **26**(8): 1781-90.
- Hiller, R. G. (2001). "'Empty' Minicircles and Petb/Atpa and Psbd/Psbe (Cytb559 Alpha) Genes in Tandem in Amphidinium Carterae Plastid DNA." FEBS Lett **505**(3): 449-52.
- Hjorth, E., K. Hadfi, et al. (2005). "Unique Genetic Compartmentalization of the Suf System in Cryptophytes and Characterization of a Sufd Mutant in Arabidopsis Thaliana." FEBS Lett **579**(5): 1129-35.
- Hoppenrath, M. and B. S. Leander (2009). "Molecular Phylogeny of Parvilucifera Procentri (Alveolata, Myzozoa): Insights into Perkinsid Character Evolution." J Eukaryot Microbiol **56**(3): 251-6.
- Howard, R. F. and C. M. Schmidt (1995). "The Secretary Pathway of Plasmodium Falciparum Regulates Transport of P82/Rap1 to the Rhoptries." Mol Biochem Parasitol **74**(1): 43-54.
- Huang, J., N. Mullapudi, et al. (2004). "A First Glimpse into the Pattern and Scale of Gene Transfer in Apicomplexa." Int J Parasitol **34**(3): 265-74.
- Huelsenbeck, J. P. and F. Ronquist (2001). "MrBayes: Bayesian Inference of Phylogenetic Trees." Bioinformatics **17**(8): 754-5.
- Hummel, E., A. Osterrieder, et al. (2010). "Inhibition of Golgi Function Causes Plastid Starch Accumulation." J Exp Bot.
- Hunt, R. C. and L. Marshall-Carlson (1986). "Internalization and Recycling of Transferrin and Its Receptor. Effect of Trifluoperazine on Recycling in Human Erythroleukemic Cells." J Biol Chem **261**(8): 3681-6.
- Iida, H. and E. Page (1989). "Localization of Wheat-Germ Agglutinin-Binding Sites in the Golgi Complex of Cultured Rat Atrial Myocytes." Cell Tissue Res **257**(2): 325-31.
- Ikeda-Ohtsubo, W. and A. Brune (2009). "Cospeciation of Termite Gut Flagellates and Their Bacterial Endosymbionts: Trichonympha Species and 'Candidatus Endomicrobium Trichonymphae'." Mol Ecol **18**(2): 332-42.
- Imanian, B., J. F. Pombert, et al. (2010). "The Complete Plastid Genomes of the Two 'Dinotoms' Durinskia Baltica and Kryptoperidinium Foliaceum." PLoS One **5**(5): e10711.
- Inagaki, J., Y. Fujita, et al. (2000). "Protein Translocation within Chloroplast Is Similar in Euglena and Higher Plants." Biochem Biophys Res Commun **277**(2): 436-42.
- Ishida, K. and B. R. Green (2002). "Second- and Third-Hand Chloroplasts in Dinoflagellates: Phylogeny of Oxygen-Evolving Enhancer 1 (Psbo) Protein Reveals Replacement of a Nuclear-Encoded Plastid Gene by That of a Haptophyte Tertiary Endosymbiont." PNAS **99**(14): 9294-9299.

## References

---

- Ismael, A., Y. Halim, et al. (1999). "Optimum Growth Conditions for Amphidinium Carterae Hulburt from Eutrophic Waters in Alexandria (Egypt) and Its Toxicity to the Brine Shrimp *Artemia Salina*." Grana **38**(2): 179-185.
- Janouskovec, J., A. Horak, et al. (2010). "A Common Red Algal Origin of the Apicomplexan, Dinoflagellate, and Heterokont Plastids." Proc Natl Acad Sci U S A.
- Jarvis, P. (2008). "Targeting of Nucleus-Encoded Proteins to Chloroplasts in Plants." New Phytol **179**(2): 257-85.
- Johnson, M. D., D. Oldach, et al. (2007). "Retention of Transcriptionally Active Cryptophyte Nuclei by the Ciliate *Myrionecta Rubra*." Nature **445**(7126): 426-8.
- Joseph, S. J., J. A. Fernandez-Robledo, et al. (2010). "The Alveolate *Perkinsus Marinus*: Biological Insights from Est Gene Discovery." BMC Genomics **11**(1): 228.
- Keeling, P. (2004). "A Brief History of Plastids and Their Hosts." Protist **155**(1): 3-7.
- Keeling, P. J. (2009). "Chromalveolates and the Evolution of Plastids by Secondary Endosymbiosis." J Eukaryot Microbiol **56**(1): 1-8.
- Keeling, P. J., G. Burger, et al. (2005). "The Tree of Eukaryotes." Trends Ecol Evol **20**(12): 670-6.
- Keeling, P. J. and J. D. Palmer (2008). "Horizontal Gene Transfer in Eukaryotic Evolution." Nat Rev Genet **9**(8): 605-18.
- Kellmann, R., A. Stuken, et al. (2010). "Biosynthesis and Molecular Genetics of Polyketides in Marine Dinoflagellates." Mar Drugs **8**(4): 1011-48.
- Kilian, O. and P. G. Kroth (2004). "Presequence Acquisition During Secondary Endocytobiosis and the Possible Role of Introns." J Mol Evol **58**(6): 712-21.
- Kilian, O. and P. G. Kroth (2005). "Identification and Characterization of a New Conserved Motif within the Presequence of Proteins Targeted into Complex Diatom Plastids." Plant J **41**(2): 175-83.
- Kita, M., O. Ohno, et al. (2010). "Bioactive Secondary Metabolites from Symbiotic Marine Dinoflagellates: Symbiodinolide and Durinskiols." Chem Rec.
- Kitajima, A., S. Asatsuma, et al. (2009). "The Rice Alpha-Amylase Glycoprotein Is Targeted from the Golgi Apparatus through the Secretory Pathway to the Plastids." Plant Cell **21**(9): 2844-58.
- Kobayashi, J. and T. Kubota (2007). "Bioactive Macrolides and Polyketides from Marine Dinoflagellates of the Genus *Amphidinium*." J Nat Prod **70**(3): 451-60.
- Kofoid, C. A. (1908). "Exuviation, Autotomy and Regeneration in *Ceratium*." Univ. Calif. Publ. Zool. **4**(345-386).

## References

---

- Kroth, P. G., A. Chiovitti, et al. (2008). "A Model for Carbohydrate Metabolism in the Diatom *Phaeodactylum Tricornutum* Deduced from Comparative Whole Genome Analysis." *PLoS One* **3**(1): e1426.
- Kugita, M., A. Kaneko, et al. (2003). "The Complete Nucleotide Sequence of the Hornwort (*Anthoceros Formosae*) Chloroplast Genome: Insight into the Earliest Land Plants." *Nucleic Acids Res* **31**(2): 716-21.
- Kuo, J., M. C. Chen, et al. (2004). "Comparative Gene Expression in the Symbiotic and Aposymbiotic *Aiptasia Pulchella* by Expressed Sequence Tag Analysis." *Biochem Biophys Res Commun* **318**(1): 176-86.
- Kwok, A. C. and J. T. Wong (2010). "The Activity of a Wall-Bound Cellulase Is Required for and Is Coupled to Cell Cycle Progression in the Dinoflagellate *Cryptothecodinium Cohnii*." *Plant Cell*.
- Kyte, J. and R. F. Doolittle (1982). "A Simple Method for Displaying the Hydrophobic Character of a Protein." *J Mol Biol* **157**(1): 105-32.
- Laatsch, T., S. Zauner, et al. (2004). "Plastid-Derived Single Gene Minicircles of the Dinoflagellate *Ceratium Horridum* Are Localized in the Nucleus." *Mol Biol Evol* **21**(7): 1318-22.
- Laemmli, U. K. (1970). "Cleavage of Structural Proteins During the Assembly of the Head of Bacteriophage T4." *Nature* **227**(5259): 680-5.
- Lajeunesse, T. C., R. Smith, et al. (2010). "Host-Symbiont Recombination Versus Natural Selection in the Response of Coral-Dinoflagellate Symbioses to Environmental Disturbance." *Proc Biol Sci*.
- Lang, M., K. E. Apt, et al. (1998). "Protein Transport Into "Complex" Diatom Plastids Utilizes Two Different Targeting Signals." *J Biol Chem* **273**(47): 30973-8.
- Lidie, K. B. and F. M. van Dolah (2007). "Spliced Leader Rna-Mediated Trans-Splicing in a Dinoflagellate, *Karenia Brevis*." *J Eukaryot Microbiol* **54**(5): 427-35.
- Lill, R. and U. Muhlenhoff (2008). "Maturation of Iron-Sulfur Proteins in Eukaryotes: Mechanisms, Connected Processes, and Diseases." *Annu Rev Biochem* **77**: 669-700.
- Little, A. F., M. J. van Oppen, et al. (2004). "Flexibility in Algal Endosymbioses Shapes Growth in Reef Corals." *Science* **304**(5676): 1492-4.
- Longhurst, A., S. Sathyendranath, et al. (1995). "An Estimate of Global Primary Production in the Ocean from Satellite Radiometer Data." *Journal of Plankton Research* **17**(6): 1245-1271.
- Lukes, J., B. S. Leander, et al. (2009). "Cascades of Convergent Evolution: The Corresponding Evolutionary Histories of Euglenozoans and Dinoflagellates." *Proc Natl Acad Sci U S A* **106 Suppl 1**: 9963-70.

## References

---

- Maberly, S. C., C. Courcelle, et al. (2009). "Phylogenetically-Based Variation in the Regulation of the Calvin Cycle Enzymes, Phosphoribulokinase and Glyceraldehyde-3-Phosphate Dehydrogenase, in Algae." J Exp Bot **61**(3): 735-45.
- Margulis, L. (1996). "Archaeal-Eubacterial Mergers in the Origin of Eukarya: Phylogenetic Classification of Life." Proc Natl Acad Sci U S A **93**(3): 1071-6.
- Martin, W. and R. G. Herrmann (1998). "Gene Transfer from Organelles to the Nucleus: How Much, What Happens, and Why?" Plant Physiol **118**(1): 9-17.
- Martin, W., T. Rujan, et al. (2002). "Evolutionary Analysis of Arabidopsis, Cyanobacterial, and Chloroplast Genomes Reveals Plastid Phylogeny and Thousands of Cyanobacterial Genes in the Nucleus." Proc Natl Acad Sci U S A **99**(19): 12246-51.
- McEwan, M., R. Humayun, et al. (2008). "Nuclear Genome Sequence Survey of the Dinoflagellate *Heterocapsa Triquetra*." J Eukaryot Microbiol **55**(6): 530-5.
- Mereschkowsky, C. (1905). "Über Natur Und Ursprung Der Chromatophoren Im Pflanzenreiche." Bio. Zentralbl. **25**(593-604).
- Mittag, M., S. Kiaulehn, et al. (2005). "The Circadian Clock in *Chlamydomonas Reinhardtii*. What Is It For? What Is It Similar To?" Plant Physiol **137**(2): 399-409.
- Morden, C. W. and A. R. Sherwood (2002). "Continued Evolutionary Surprises among Dinoflagellates." Proc Natl Acad Sci U S A **99**(18): 11558-60.
- Moustafa, A., B. Beszteri, et al. (2009). "Genomic Footprints of a Cryptic Plastid Endosymbiosis in Diatoms." Science **324**(5935): 1724-6.
- Murata, N., N.-A. Kume, et al. (1979). "Preparation of Girdle Lamella-Containing Chloroplasts from the Diatom *Phaeodactylum Tricornutum*." Plant & Cell Physiol. **20**(6): 1047-1053.
- Nash, E. A., A. C. Barbrook, et al. (2007). "Organization of the Mitochondrial Genome in the Dinoflagellate *Amphidinium Carterae*." Mol Biol Evol **24**(7): 1528-36.
- Nassoury, N., M. Cappadocia, et al. (2003). "Plastid Ultrastructure Defines the Protein Import Pathway in Dinoflagellates." J Cell Sci **116**(Pt 14): 2867-74.
- Nassoury, N., L. Fritz, et al. (2001). "Circadian Changes in Ribulose-1,5-Bisphosphate Carboxylase/Oxygenase Distribution inside Individual Chloroplasts Can Account for the Rhythm in Dinoflagellate Carbon Fixation." Plant Cell **13**(4): 923-34.
- Nassoury, N., Y. Wang, et al. (2005). "Brefeldin A Inhibits Circadian Remodeling of Chloroplast Structure in the Dinoflagellate *Gonyaulax*." Traffic **6**(7): 548-61.
- Nayak, B. B. and I. Karunasagar (1997). "Influence of Bacteria on Groth and Hemolysin Production by the Marine Dinoflagellate *Amphidinium Carterae*." Marine Biology **130**: 35-39.
- Nebenfuhr, A., C. Ritzenthaler, et al. (2002). "Brefeldin A: Deciphering an Enigmatic Inhibitor of Secretion." Plant Physiol **130**(3): 1102-8.

## References

---

- Nelson, M. J., Y. Dang, et al. (2007). "Identification and Transcription of Transfer Rna Genes in Dinoflagellate Plastid Minicircles." Gene **392**(1-2): 291-8.
- Nosenko, T. and D. Bhattacharya (2007). "Horizontal Gene Transfer in Chromalveolates." BMC Evol Biol **7**: 173.
- Nosenko, T., K. L. Lidie, et al. (2006). "Chimeric Plastid Proteome in the Florida "Red Tide" Dinoflagellate *Karenia Brevis*." Mol Biol Evol **23**(11): 2026-38.
- Nowack, E. C., M. Melkonian, et al. (2008). "Chromatophore Genome Sequence of *Paulinella* Sheds Light on Acquisition of Photosynthesis by Eukaryotes." Curr Biol **18**(6): 410-8.
- Obornik, M., J. Janouskovec, et al. (2009). "Evolution of the Apicoplast and Its Hosts: From Heterotrophy to Autotrophy and Back Again." Int J Parasitol **39**(1): 1-12.
- Okamoto, N., C. Chantangsi, et al. (2009). "Molecular Phylogeny and Description of the Novel Katablepharid *Roombia Truncata* Gen. Et Sp. Nov., and Establishment of the *Hacrobia* Taxon Nov." PLoS One **4**(9): e7080.
- Patron, N. J. and R. F. Waller (2007). "Transit Peptide Diversity and Divergence: A Global Analysis of Plastid Targeting Signals." Bioessays **29**(10): 1048-58.
- Patron, N. J., R. F. Waller, et al. (2005). "Complex Protein Targeting to Dinoflagellate Plastids." J Mol Biol **348**(4): 1015-24.
- Peters, N. (1929). "Orts- Und Geisselbewegung Bei Marinen Dinoflagellaten." Protistenk. **67**: 291-321.
- Petersen, J., R. Teich, et al. (2006). "A "Green" Phosphoribulokinase in Complex Algae with Red Plastids: Evidence for a Single Secondary Endosymbiosis Leading to Haptophytes, Cryptophytes, Heterokonts, and Dinoflagellates." J Mol Evol **62**(2): 143-57.
- Prechtel, J., C. Kneip, et al. (2004). "Intracellular Spheroid Bodies of *Rhopalodia Gibba* Have Nitrogen-Fixing Apparatus of Cyanobacterial Origin." Mol Biol Evol **21**(8): 1477-81.
- Ralph, S. A., B. J. Foth, et al. (2004). "Evolutionary Pressures on Apicoplast Transit Peptides." Mol Biol Evol **21**(12): 2183-94.
- Reichman, J. R., T. P. Wilcox, et al. (2003). "Pcp Gene Family in *Symbiodinium* from Hippopus Hippopus: Low Levels of Concerted Evolution, Isoform Diversity, and Spectral Tuning of Chromophores." Mol Biol Evol **20**(12): 2143-54.
- Reyes-Prieto, A., A. Moustafa, et al. (2008). "Multiple Genes of Apparent Algal Origin Suggest Ciliates May Once Have Been Photosynthetic." Curr Biol **18**(13): 956-62.
- Richardson, A. O. and J. D. Palmer (2007). "Horizontal Gene Transfer in Plants." J Exp Bot **58**(1): 1-9.

## References

---

- Roberts, E. C., M. V. Zubkov, et al. (2006). "Cell Surface Lectin-Binding Glycoconjugates on Marine Planktonic Protists." FEMS Microbiol Lett **265**(2): 202-7.
- Rogers, M. B., P. R. Gilson, et al. (2007). "The Complete Chloroplast Genome of the Chlorarachniophyte *Bigeloviella Natans*: Evidence for Independent Origins of Chlorarachniophyte and Euglenid Secondary Endosymbionts." Mol Biol Evol **24**(1): 54-62.
- Rosati, G. and L. Modeo (2003). "Extrusomes in Ciliates: Diversification, Distribution, and Phylogenetic Implications." J Eukaryot Microbiol **50**(6): 383-402.
- Rosenberg, E., A. Kushmaro, et al. (2009). "The Role of Microorganisms in Coral Bleaching." ISME J **3**(2): 139-46.
- Saldarriaga, J. F., M. L. McEwan, et al. (2003). "Multiple Protein Phylogenies Show That *Oxyrrhis Marina* and *Perkinsus Marinus* Are Early Branches of the Dinoflagellate Lineage." Int J Syst Evol Microbiol **53**(Pt 1): 355-65.
- Saldarriaga, J. F., F. J. Taylor, et al. (2004). "Molecular Data and the Evolutionary History of Dinoflagellates." European Journal of Protistology **40**(1): 85-111.
- Sanchez-Puerta, M. V., J. C. Lippmeier, et al. (2007). "Plastid Genes in a Non-Photosynthetic Dinoflagellate." Protist **158**(1): 105-17.
- Sanchez Puerta, M. V. and C. F. Delwiche (2008). "A Hypothesis for Plastid Evolution in Chromalveolates." Journal of Phycology **44**: 1097-1107.
- Sanger, F., S. Nicklen, et al. (1977). "DNA Sequencing with Chain-Terminating Inhibitors." Proc Natl Acad Sci U S A **74**(12): 5463-7.
- Sato, S. and R. J. Wilson (2005). "The Plastid of *Plasmodium* Spp.: A Target for Inhibitors." Curr Top Microbiol Immunol **295**: 251-73.
- Schleiff, E., M. Motzkus, et al. (2002). "Chloroplast Protein Import Inhibition by a Soluble Factor from Wheat Germ Lysate." Plant Mol Biol **50**(2): 177-85.
- Schmitter, R. E. (1971). "The Fine Structure of *Gonyaulax Polyedra*, a Bioluminescent Marine Dinoflagellate." J Cell Sci **9**(1): 147-73.
- Schopf, J. W. (1993). "Microfossils of the Early Archean Apex Chert: New Evidence of the Antiquity of Life." Science **260**: 640-6.
- Sibley, L. D. (2004). "Intracellular Parasite Invasion Strategies." Science **304**(5668): 248-53.
- Simpson, A. G. and A. J. Roger (2002). "Eukaryotic Evolution: Getting to the Root of the Problem." Curr Biol **12**(20): R691-3.
- Slamovits, C. H. and P. J. Keeling (2008). "Plastid-Derived Genes in the Nonphotosynthetic Alveolate *Oxyrrhis Marina*." Mol Biol Evol **25**(7): 1297-306.

## References

---

- Slamovits, C. H., J. F. Saldarriaga, et al. (2007). "The Highly Reduced and Fragmented Mitochondrial Genome of the Early-Branching Dinoflagellate *Oxyrrhis Marina* Shares Characteristics with Both Apicomplexan and Dinoflagellate Mitochondrial Genomes." J Mol Biol **372**(2): 356-68.
- Slavikova, S., R. Vacula, et al. (2005). "Homologous and Heterologous Reconstitution of Golgi to Chloroplast Transport and Protein Import into the Complex Chloroplasts of *Euglena*." J Cell Sci **118**(Pt 8): 1651-61.
- Soares, M. B., M. de Fatima Bonaldo, et al. (2009). "Expressed Sequence Tags: Normalization and Subtraction of Cdna Libraries Expressed Sequence Tags\ Normalization and Subtraction of Cdna Libraries." Methods Mol Biol **533**: 109-22.
- Soldati, D., B. J. Foth, et al. (2004). "Molecular and Functional Aspects of Parasite Invasion." Trends Parasitol **20**(12): 567-74.
- Soll, J. and E. Schleiff (2004). "Protein Import into Chloroplasts." Nat Rev Mol Cell Biol **5**(3): 198-208.
- Sommer, M. S., S. B. Gould, et al. (2007). "Der1-Mediated Preprotein Import into the Periplastid Compartment of Chromalveolates?" Mol Biol Evol **24**(4): 918-28.
- Steiner, J. M. and W. Löffelhardt (2002). "Protein Import into Cyanelles." Trends Plant Sci **7**(2): 72-7.
- Steiner, J. M., F. Yusa, et al. (2005). "Homologous Protein Import Machineries in Chloroplasts and Cyanelles." Plant J **44**(4): 646-52.
- Stelter, K., N. M. El-Sayed, et al. (2007). "The Expression of a Plant-Type Ferredoxin Redox System Provides Molecular Evidence for a Plastid in the Early Dinoflagellate *Perkinsus Marinus*." Protist **158**(1): 119-30.
- Stoebe, B. and U. G. Maier (2002). "One, Two, Three: Nature's Tool Box for Building Plastids." Protoplasma **219**(3-4): 123-30.
- Strittmatter, P., J. Soll, et al. (2010). "The Chloroplast Protein Import Machinery: A Review." Methods Mol Biol **619**: 307-21.
- Su, E. C., H. S. Chiu, et al. (2007). "Protein Subcellular Localization Prediction Based on Compartment-Specific Features and Structure Conservation." BMC Bioinformatics **8**: 330.
- Sulli, C., Z. Fang, et al. (1999). "Topology of *Euglena* Chloroplast Protein Precursors within Endoplasmic Reticulum to Golgi to Chloroplast Transport Vesicles." J Biol Chem **274**(1): 457-63.
- Sulli, C. and S. D. Schwartzbach (1995). "The Polyprotein Precursor to the *Euglena* Light-Harvesting Chlorophyll a/B-Binding Protein Is Transported to the Golgi Apparatus Prior to Chloroplast Import and Polyprotein Processing." J Biol Chem **270**(22): 13084-90.

## References

---

- Tanikawa, N., H. Akimoto, et al. (2004). "Expressed Sequence Tag Analysis of the Dinoflagellate *Lingulodinium Polyedrum* During Dark Phase." Photochem Photobiol **80**: 31-5.
- Tonkin, C. J., B. J. Foth, et al. (2008a). "Evolution of Malaria Parasite Plastid Targeting Sequences." Proc Natl Acad Sci U S A **105**(12): 4781-5.
- Tonkin, C. J., M. Kalanon, et al. (2008b). "Protein Targeting to the Malaria Parasite Plastid." Traffic **9**(2): 166-75.
- Tonkin, C. J., D. S. Roos, et al. (2006a). "N-Terminal Positively Charged Amino Acids, but Not Their Exact Position, Are Important for Apicoplast Transit Peptide Fidelity in *Toxoplasma Gondii*." Mol Biochem Parasitol **150**(2): 192-200.
- Tonkin, C. J., N. S. Struck, et al. (2006b). "Evidence for Golgi-Independent Transport from the Early Secretory Pathway to the Plastid in Malaria Parasites." Mol Microbiol **61**(3): 614-30.
- Toulza, E., M. S. Shin, et al. (2010). "Gene Expression in Proliferating Cells of the Dinoflagellate *Alexandrium Catenella* (Dinophyceae)." Appl Environ Microbiol.
- Ueda, M., M. Fujimoto, et al. (2006). "Evidence for Transit Peptide Acquisition through Duplication and Subsequent Frameshift Mutation of a Preexisting Protein Gene in Rice." Mol Biol Evol **23**(12): 2405-12.
- Uribe, P., D. Fuentes, et al. (2008). "Preparation and Analysis of an Expressed Sequence Tag Library from the Toxic Dinoflagellate *Alexandrium Catenella*." Mar Biotechnol (NY) **10**(6): 692-700.
- Van de Peer, Y. and R. De Wachter (1997). "Evolutionary Relationships among the Eukaryotic Crown Taxa Taking into Account Site-to-Site Rate Variation in 18s Rna." J Mol Evol **45**(6): 619-30.
- van Dooren, G. G., S. D. Schwartzbach, et al. (2001). "Translocation of Proteins across the Multiple Membranes of Complex Plastids." Biochim Biophys Acta **1541**(1-2): 34-53.
- Vothknecht, U. C. and J. Soll (2005). "Chloroplast Membrane Transport: Interplay of Prokaryotic and Eukaryotic Traits." Gene **354**: 99-109.
- Wagner, G. J. and G. Hrazdina (1984). "Endoplasmic Reticulum as a Site of Phenylpropanoid and Flavonoid Metabolism in *Hippeastrum*." Plant Physiol **74**(4): 901-906.
- Waller, R. F., P. J. Keeling, et al. (1998). "Nuclear-Encoded Proteins Target to the Plastid in *Toxoplasma Gondii* and *Plasmodium Falciparum*." Proc Natl Acad Sci U S A **95**(21): 12352-7.
- Waller, R. F. and G. I. McFadden (2005). "The Apicoplast: A Review of the Derived Plastid of Apicomplexan Parasites." Curr Issues Mol Biol **7**(1): 57-79.
- Waller, R. F., N. J. Patron, et al. (2006a). "Phylogenetic History of Plastid-Targeted Proteins in the Peridinin-Containing Dinoflagellate *Heterocapsa Triquetra*." Int J Syst Evol Microbiol **56**(Pt 6): 1439-47.



## References

---

- Waller, R. F., M. B. Reed, et al. (2000). "Protein Trafficking to the Plastid of *Plasmodium Falciparum* Is Via the Secretory Pathway." EMBO J **19**(8): 1794-802.
- Waller, R. F., C. H. Slamovits, et al. (2006b). "Lateral Gene Transfer of a Multigene Region from Cyanobacteria to Dinoflagellates Resulting in a Novel Plastid-Targeted Fusion Protein." Mol Biol Evol **23**(7): 1437-43.
- Wang, L. H., K. G. Rothberg, et al. (1993). "Mis-Assembly of Clathrin Lattices on Endosomes Reveals a Regulatory Switch for Coated Pit Formation." J Cell Biol **123**(5): 1107-17.
- Wang, Y., L. Jensen, et al. (2005). "Synthesis and Degradation of Dinoflagellate Plastid-Encoded Psba Proteins Are Light-Regulated, Not Circadian-Regulated." Proc Natl Acad Sci U S A **102**(8): 2844-9.
- Wang, Y., S. Joly, et al. (2008). "Phylogeny of Dinoflagellate Plastid Genes Recently Transferred to the Nucleus Supports a Common Ancestry with Red Algal Plastid Genes." J Mol Evol **66**(2): 175-84.
- Wastl, J. and U. G. Maier (2000). "Transport of Proteins into Cryptomonads Complex Plastids." J Biol Chem **275**(30): 23194-8.
- Weber, A. P., M. Linka, et al. (2006). "Single, Ancient Origin of a Plastid Metabolite Translocator Family in Plantae from an Endomembrane-Derived Ancestor." Eukaryot Cell **5**(3): 609-12.
- Yoon, H. S., J. D. Hackett, et al. (2002). "A Single Origin of the Peridinin- and Fucoxanthin-Containing Plastids in Dinoflagellates through Tertiary Endosymbiosis." Proc Natl Acad Sci U S A **99**(18): 11724-9.
- Yoon, H. S., J. D. Hackett, et al. (2004). "A Molecular Timeline for the Origin of Photosynthetic Eukaryotes." Mol Biol Evol **21**(5): 809-18.
- Yoon, H. S., J. D. Hackett, et al. (2005). "Tertiary Endosymbiosis Driven Genome Evolution in Dinoflagellate Algae." Mol Biol Evol **22**(5): 1299-308.
- Yoon, H. S., T. Nakayama, et al. (2009). "A Single Origin of the Photosynthetic Organelle in Different *Paulinella* Lineages." BMC Evol Biol **9**: 98.
- Yutin, N., M. Y. Wolf, et al. (2009). "The Origins of Phagocytosis and Eukaryogenesis." Biol Direct **4**: 9.
- Zerges, W. and J. D. Rochaix (1998). "Low Density Membranes Are Associated with Rna-Binding Proteins and Thylakoids in the Chloroplast of *Chlamydomonas Reinhardtii*." J Cell Biol **140**(1): 101-10.
- Zhang, H., D. A. Campbell, et al. (2009). "Dinoflagellate Spliced Leader Rna Genes Display a Variety of Sequences and Genomic Arrangements." Mol Biol Evol **26**(8): 1757-71.
- Zhang, H., Y. Hou, et al. (2007). "Spliced Leader Rna Trans-Splicing in Dinoflagellates." Proc Natl Acad Sci U S A **104**(11): 4618-23.

## References

---

Zhang, Z., B. R. Green, et al. (1999). "Single Gene Circles in Dinoflagellate Chloroplast Genomes."  
Nature **400**(6740): 155-9.

## 9 Acknowledgements

"It was the best of times, it was the worst of times, it was the age of wisdom, it was the age of foolishness, it was the epoch of belief, it was the epoch of incredulity, it was the season of Light, it was the season of Darkness, it was the spring of hope, it was the winter of despair, we had everything before us, we had nothing before us, we were all going direct to heaven, we were all doing direct the other way." --Charles Dickens, A Tale of Two Cities

I utterly treasured the elation of research, and really never tired of the most banal of successes. I have always enjoyed theoretical conversations and have always thought of myself as being a boon to those who wish to discuss the theoretical aspects of evolution and biochemistry. Despite having always kept the fire of ardor alit, the tinge of disappointment was never far away. Disgust and despair were constantly my cerebral enemies, during the duration of any experiment that went awry, and as any scientist will tell you, the successes are usually dwarfed by experiments that did not turn out. Altogether it was a time of soaring thoughts, modest success, laced with relentless doubt.

I would like to thank my wife for having the patience to help me through the trying ordeal of my doctorate thesis. Thanks also to my kids, Emma and Luke have always been able to distract me from the frustrations of failed clonings, so I am thankful to them...they are always able to put a smile on my face. Thanks also are due to my parents-in-law, who helped our family get through tough times.

Special thanks go out to Dr. Kathrin Bolte for having helped me in lab, for the dedicated work on the electron microscope, and for always having been willing to lend an ear and a piece of advice, like no one else was able to.

I would like to thank Uwe Maier for having given me the opportunity to be in the the Intra- and Intercellular Transport and Communication Graduate College. Thanks to Stefan Zauner for having advised me on this thesis. Without their involvement, my doctorate would never have reached fruition.

Thanks to Dr. Erhard Möschel and Marriane Johannsen for the discussions touching on Nor'deutschland to Denver to electron microscopy to dinoflagellates to the hot barracks of the Bundeswehr in the fifties.

Thanks to Heidi Thierfelder for her constant willingness to lend a hand and an ear. Thanks to Lucette Claudet for her friendliness and dedication to detail...and for her patience when I came with an urgent order at 3:45 p.m. on Friday when she was packing her bag to go home.

Thanks to my diploma student Susanne Lieske and Bachelor's student Christine Weber for the assistance. Thanks to Jan Wilhelm and Christopher Grosche for assistance with experiments and stimulating conversation.

Thanks to all the students of AG Maier for the help in lab and the good times.

## 10 Curriculum vitae

### **Personal Data:**

Name	Andrew Bozarth
Born	October 21, 1980
In	Columbia, MD, USA
Wife (as of April 12, 2007)	Katja Miriam Bozarth (maiden name: Junker)
Children	Emma Jean Bozarth, born 5/23/2007 Lucas Liam Bozarth, born 12/26/2008

### **Education**

September, 1994 – June, 1998	Secondary education at Elizabethtown Area High School
September, 1997 – June, 1998	Exchange Student at Professor Hofmann Gymnasium Kölleda
June, 1998	High School Diploma
August, 1998 – May, 2002	Biology and German Bachelor Studies at Elizabethtown College
May, 2002	Biology B.Sc. and German B.A.
September, 2000 – July, 2001	Exchange Student at Philipps University of Marburg
October, 2002 – February, 2003	Human Biology Studies at Philipps University of Marburg
April, 2003 – March, 2006	Biology Studies at Philipps-University of Marburg in the subjects of Microbiology, Biochemistry and Developmental Biology
March, 2006	German Diploma in Microbiology at Philipps University of Marburg “Examination of a Common Nicotinate Metabolism in Proteobacteria”

### **Ph. D. Studies**

April, 2006 – July, 2010	Philipps University of Marburg Biology Department, Cell Biology Ph.D. thesis in the lab of Prof. Dr. Uwe G. Maier “Investigation of Dinoflagellate Plastid Protein Transport using Heterologous and Homologous <i>in vivo</i> Systems”
--------------------------	---

## 11 Erklärung

Ich versichere, dass ich meine Dissertation

**„Investigation of Dinoflagellate Plastid Protein Transport  
using Heterologous and Homologous *in vivo* Systems“**

selbständig, ohne unerlaubte Hilfe angefertigt und mich dabei keiner anderen als der von mir ausdrücklich bezeichneten Quellen und Hilfen bedient habe. Die Dissertation wurde in der jetzigen oder einer ähnlichen Form noch bei keiner anderen Hochschule eingereicht und hat noch keinen sonstigen Prüfungszwecken gedient.

Marburg, den 7. Juni 2010

Andrew Scott Bozarth